UNIVERSIDADE ESTADUAL DE CAMPINAS (UNICAMP)
FACULDADE DE CIÊNCIAS MÉDICAS (FCM)
PROGRAMA DE PÓS-GRADUAÇÃO EM CLÍNICA MÉDICA

Maurício Martins Baldissin

AUTOIMMUNE ENCEPHALITIS: CLINICAL CORRELATION WITH ^{18}F-FDG PET/CT

Encefalite Autoimune: Correlação Clínica com **^{18}F-FDG PET/CT**

CAMPINAS
2026

Maurício Martins Baldissin

AUTOIMMUNE ENCEPHALITIS: CLINICAL CORRELATION WITH ^{18}F-FDG PET/CT

Encefalite Autoimune: Correlação Clínica com ^{18}F-FDG PET/CT

Thesis presented to the Faculty of Medical Sciences (FCM) of the University of Campinas (UNICAMP) as part of the requirements for obtaining the title of Doctor in Sciences in the area of Clinical Medicine.

Tese apresentada à Faculdade de Ciências Médicas (FCM) da Universidade Estadual de Campinas (UNICAMP) como parte dos requisitos exigidos para a obtenção do título de Doutor em Ciências, na área de Clínica Médica.

ORIENTADORA: Profa. Dra. Bárbara Juarez Amorim
COORIENTADORA: Dra. Edna Marina de Souza

ESTE TRABALHO CORRESPONDE À VERSÃO FINAL DA TESE DEFENDIDA.

Ficha catalográfica
Universidade Estadual de Campinas (UNICAMP)
Biblioteca da Faculdade de Ciências Médicas
Maristella Soares dos Santos - CRB 8402

B193a

Baldissin, Maurício Martins, 1966-
Autoimmune encephalitis : clinical correlation with 18F-FDG PET/CT / Maurício Martins Baldissin. – Campinas, SP : [s.n.], 2026.

Orientador: Bárbara Juarez Amorim.
Coorientador: Edna Marina de Souza.
Tese (doutorado) – Universidade Estadual de Campinas (UNICAMP), Faculdade de Ciências Médicas.

1. Doenças autoimunes do sistema nervoso. 2. Anticorpos. 3. Medicina nuclear. 4. PET/CT. 5. Fluordesoxiglucose F18. I. Amorim, Bárbara Juarez, 1974-. II. Souza, Edna Marina de, 1982-. III. Universidade Estadual de Campinas (UNICAMP). Faculdade de Ciências Médicas. IV. Título.

Informações complementares

Título em outro idioma: Encefalite autoimune : correlação clínica com 18F-FDG PET/CT
Palavras-chave em inglês:
Autoimmune diseases of the nervous system
Antibodies
Nuclear medicine
PET/CT
Fluorodeoxyglucose F18
Área de concentração: Clínica Médica
Titulação: Doutor em Ciências
Banca examinadora:
Bárbara Juarez Amorim [Orientador]
Marina Koutsodontis Machado Alvim
Allan de Oliveira Santos
Edmir Américo Lourenço
Lauro Wichert Ana
Data de defesa: 27-02-2026
Programa de Pós-Graduação: Clínica Médica

Objetivos de Desenvolvimento Sustentável (ODS)
ODS: 3. Saúde e bem-estar

Identificação e informações acadêmicas do(a) aluno(a)
- ORCID do autor: https://orcid.org/0000-0002-9585-074X
- Currículo Lattes do autor: http://lattes.cnpq.br/2768059809624628

FOLHA DE APROVAÇÃO

Maurício Martins Baldissin

Tese apresentada ao Programa de Pós-Graduação em Clínica Médica, defendida na data de 27/02/2026.

Composição da Comissão Examinadora:

Profa. Dra. Barbara Juarez Amorim
Faculdade de Ciências Médicas (FCM) / Unicamp / Campinas

Profa. Dra. Marina Koutsodontis Machado Alvim
Faculdade de Ciências Médicas (FCM) / Unicamp / Campinas

Prof. Dr. Allan de Oliveira Santos
Faculdade de Ciências médicas (FCM) / Unicamp / Campinas

Prof. Dr. Edmir Américo Lourenço
Faculdade de Medicina de Jundiaí / Jundiaí

Prof. Dr. Lauro Wichert Ana
Faculdade de Medicina de Ribeirão Preto – USP / Ribeirão Preto

DEDICATION

For their strong and loving presence in my life, I dedicate this work
to my father, José Décio Baldissin (in memoriam);
to my mother, Maria Cecília Martins Baldissin;
to my sister, Maria Teresa Martins Baldissin;
to my daughters, Luísa Grigoletto Baldissin and
Sofia Grigoletto Baldissin;
and to Júlio Dias Gaspar.

ACKNOWLEDGEMENTS

I express my profound gratitude to Professor Barbara Juarez Amorim, PhD, for illuminating our path with her competence, generosity, and inestimable care; to Professor Edna Marina de Souza, PhD, a tireless companion throughout countless hours of work, who shared with me both the joys and challenges during the construction of this thesis.

I extend my thanks to Professors Edmir Lourenço, PhD, Fernando Cendes, PhD, Nancy Watanabe, PhD, and Elba C. S. C. Etchebehere, PhD, who, at different times and in distinct ways, supported, encouraged, and enriched the production of this study.

I especially include my gratitude to the team at the Neurodiagnose Clinic in Jundiaí, whose history of over 30 years has been built with competence, dedication, and a fraternal spirit — with the constant support of Elijoice Seles Alves dos Santos and the Medical-Anthroposophic Study Group.

Finally, I thank the School of Medical Sciences at Unicamp, the Jundiaí Medical School (Faculdade de Medicina de Jundiaí), and the Medizinische Sektion der Freien Hochschule für Geisteswissenschaft am Goetheanum (Medical Section of the School of Spiritual Science at the Goetheanum), institutions that helped make the development of this research possible and contributed decisively to broadening the horizons of my work as a physician, professor, and researcher in the field of neuroscience.

EPIGRAPH

"Only when we carry the study of the physical human being so far that through it we discover the spiritual, do we have the foundation for a true medicine."
Rudolf Steiner and Ita Wegman, 1925.

RESUMO

Introdução: A encefalite autoimune (EA) é uma doença neurológica inflamatória cujo diagnóstico continua sendo um desafio. Este estudo avalia o papel do PET/CT com ^{18}F-FDG na identificação de alterações metabólicas cerebrais em pacientes com EA.

Objetivos: Analisar as apresentações clínicas e os achados do PET/CT com ^{18}F-FDG em pacientes com EA, comparando as alterações metabólicas associadas a anticorpos de superfície e intracelulares, além de avaliar a prevalência de neoplasias subjacentes.

Métodos: Avaliamos retrospectivamente 37 pacientes com diagnóstico clínico de EA submetidos a PET/CT com ^{18}F-FDG dedicado ao cérebro entre 2013 e 2023. As imagens foram avaliadas por meio de análises visual e quantitativa (software Scenium®). Os pacientes foram categorizados por tipo de anticorpo (superfície, intracelular, negativo ou não testado) para comparação estatística.

Resultados: Todos os 37 pacientes apresentaram alterações metabólicas cerebrais na análise visual de seu primeiro PET/CT com ^{18}F-FDG. Verificou-se um predomínio de áreas hipermetabólicas (62,5%) sobre as hipometabólicas (37,5%). O anticorpo mais frequentemente detectado foi o anti-NMDA (24,2%). Observou-se uma diferença metabólica significativa entre os grupos de anticorpos de superfície e intracelulares. Os anticorpos intracelulares associaram-se a uma maior intensidade de hipometabolismo em comparação com os de superfície, refletindo um mecanismo celular potencialmente mais destrutivo. O PET/CT de corpo inteiro identificou neoplasias em apenas 5,4% (n=2) dos casos.

Conclusões: O PET/CT com ^{18}F-FDG demonstrou-se uma ferramenta valiosa para a detecção de alterações metabólicas cerebrais na encefalite autoimune (EA), sendo o hipermetabolismo nas fases iniciais um achado que reforça seu potencial como marcador preditivo desta doença. O método distingue as assinaturas metabólicas associadas a biomarcadores imunológicos neuronais de superfície e intracelulares, estes últimos caracterizados por hipometabolismo mais extenso e pronunciado. Apesar da baixa prevalência de neoplasias no grupo estudado, o PET/CT com ^{18}F-FDG demonstra utilidade complementar no rastreio de neoplasias em pacientes com EA.

Palavras-chave: Doenças Autoimunes do Sistema Nervoso, Anticorpos, Medicina Nuclear, PET/CT, Fluordesoxiglucose F18.

ABSTRACT

Background: Autoimmune encephalitis (AE) is an inflammatory neurological disorder that has a challenging diagnosis. This study evaluates the role of ^{18}F-FDG PET/CT in identifying metabolic brain alterations in AE patients.

Objectives: To analyze clinical presentations and ^{18}F-PET/CT findings in patients with AE, comparing metabolic changes associated with surface and intracellular antibodies, and assessing the prevalence of underlying neoplasms.

Methods: We retrospectively evaluated 37 patients clinically diagnosed with AE who underwent whole-body and brain-dedicated ^{18}F-FDG PET/CT between 2013 and 2023. Images were assessed through visual and quantitative (Scenium® software) analyses. Patients were categorized by antibody type (surface, intracellular, negative, or untested) for statistical comparison.

Results: All 37 patients exhibited brain metabolic alterations on visual analysis of their initial ^{18}F-FDG PET/CT. There was a predominance of hypermetabolic areas (62.5%) over hypometabolic ones (37.5%). The most frequent antibody detected was anti-NMDA (24.2%). A significant metabolic difference was observed between surface and intracellular antibody groups. Intracellular antibodies were associated with a higher intensity of hypometabolism, compared to surface antibodies, reflecting a potentially more destructive mechanism. Whole-body PET/CT identified neoplasms in only 5.4% (n=2) of the cohort.

Conclusions: ^{18}F-FDG PET/CT has proven to be a valuable tool for detecting cerebral metabolic abnormalities in autoimmune encephalitis (AE), with hypermetabolism in the early stages representing a finding that reinforces its potential as a predictive marker of the disease. The method distinguishes metabolic signatures associated with neuronal surface and intracellular immunological biomarkers, the latter characterized by more extensive and pronounced hypometabolism. Despite the low prevalence of neoplasms in the studied group, ^{18}F-FDG PET/CT demonstrates complementary utility in oncological screening in patients with AE.

Keywords: Autoimmune Diseases of the Nervous System, Antibodies, Nuclear Medicine, PET/CT, Fluorodeoxyglucose F18.

FIGURES

TABLES

ABBREVIATIONS AND ACRONYMS

ADCC: Antibody-Dependent Cellular Cytotoxicity.
AE: Autoimmune Encephalitis
Amphiphysin: 128-kDa protein expressed on presynaptic nerve terminals
ANOVA: Analysis of Variance
Aquaporin-4: osmoreceptor which regulates body water balance and mediates water flow within the central nervous system
BG: Basal Ganglia
C: Central Region
CE: Cerebellum
CI: Cingulate Gyrus
CNS: Central Nervous System
CO: Colonoscopy
CSF: Cerebrospinal Fluid
CT: Computed Tomography
EEG: Electroencephalogram
EN: Endoscopy
F: Frontal Lobe
^{18}F (or F-18): Fluorine Eighteen (radioactive fluorine, positron-emitter)
^{18}F-FDG: Fluorodeoxyglucose labeled with ^{18}F
^{18}F-Flortaucipir: radioconjugate composed of the paired helical filament tau binding agent flortaucipir, a benzimidazole pyrimidine derivative, labeled with F-18.
^{18}F-GE-179: radiopharmaceutical labeled with F-18 that selectively binds to the open/active state of the NMDA receptor ion channel, displacing the binding of (3)H-tenocyclidine from the intrachannel binding site.
FDG: Fluorodeoxyglucose
FDG-PET/CT: Positron Emission Tomography with Fluorodeoxyglucose as radiopharmaceutical
GAD: Glutamic Acid Decarboxylase
GAP: Anteroposterior Gradient
Hu: System nervous proteins, expressed in the nuclei of neurons
kg: Kilogram
LE: Limbic Encephalitis
LGI1: Leucine-rich, glioma inactivated 1 protein
MBq: MegaBequerel
MRI: Magnetic Resonance Imaging
MT: Mesial Temporal Lobe
NMDA: N-Metil-D-Aspartate
O: Occipital Lobe
P: Parietal Lobe
PET: Positron Emission Tomography
PET/CT: Positron Emission Tomography combined with Computed Tomography
PET/MRI: Positron Emission Tomography combined with Magnetic Resonance Imaging
PNS: Paraneoplastic Syndrome
PR: Precuneus
SD: Standard Deviation
SMV: Standard Mean Value
ST: striatum
T: Temporal Lobe
TSPO: Translocator Protein 18 kDa
U/mL: Units per milliliter
US: Ultrasound
Yo: Purkinje cell cytoplasmic type 1 (PCA1) antibodies

SUMMARY

INTRODUCTION AND CONTEXTUALIZATION

Autoimmune encephalitis (AE) is a debilitating neurological disorder characterized by inflammation of brain tissue. It is the most common cause of non-infectious acute encephalitis, described for the first time in 1888, when patients with neurological symptoms but without brain pathology were reported (1) The postmortem investigation of patients with behavioral alterations related to acute encephalitis dates from 1960s, revealing inflammation mainly in limbic region (hippocampus and amygdala), being the condition named limbic encephalitis (LE) (2), later associated with malignancy (3) and specific antibodies targeting intracellular neuronal antigens (4-8). These onconeural auto-antibodies are also associated with other paraneoplastic syndromes, characterized by relentless progression and poor treatment response, as they result from rapid and permanent neuronal loss (9, 10).

Over the past 20 years, novel forms of encephalitis associated with antibodies to neuronal surface or synaptic proteins have been described, generally with favorable outcome and good response to immunotherapy, even when associated with tumor, as they result from reversible neuronal dysfunction. Depending on associated antibody, AE can produce different clinical presentation and imaging findings (10, 11). The diagnosis of AE is still a challenge. The clinical manifestations of AE may include behavioral, metabolic, inflammatory, infectious, due to a diversity of neurological damage (10). According to the publication of Graus et al., the background of investigation is based on guidelines already defined (6), including clinical attention with laboratory tests (including blood, urine, cerebrospinal fluid - CSF), and magnetic resonance imaging (MRI) (12), being the Brazilian protocol based on these one (13). Nowadays, many types of antibodies have been associated with the disease.

For adults, the Brazilian diagnostic criteria for AE includes: subacute onset (rapid progression in fewer than three months) of working memory deficits (short-term memory loss), altered mental status (decreased level of consciousness, lethargy or personality changes), or psychiatric symptoms, as well as at least one of the following: new focal central nervous system (CNS) findings, seizures not explained by a previously-known seizure disorder, CSF pleocytosis or MRI suggestive of encephalitis, considering the reasonable exclusion of alternative causes. In case of children, the diagnostic of AE is based on the following three criteria: onset of neurologic and/or psychiatric symptoms over less than 3 months in a previously-healthy child. Two of the following manifestations: altered mental status/level of consciousness, or EEG with slowing or epileptiform activity (focal or generalized), focal

neurologic deficits, cognitive difficulties, acute developmental regression, movement disorder (except tics), psychiatric symptoms, or seizures not explained by a previously-known seizure disorder or other condition, also added to a reasonable exclusion of alternative causes, including other causes of CNS inflammation (13).

Positron emission tomography (PET) performed with fluorodeoxyglucose labeled with fluorine-18 (^{18}F-FDG) is an imaging technique able to identify glucose metabolic changes in several pathological conditions. When combined with computed tomography (PET/CT) or even with magnetic resonance imaging (PET/MRI), it is possible to fuse the physiological images from PET to the anatomical images (14). However, there is not a defined pattern of metabolism in PET/CT with ^{18}F-FDG (FDG-PET/CT) in AE, despite this condition being recently more explored with this technique, highlighting this relevance mainly when the antibodies test is inconclusive or unavailable (15, 16).

In AE, pathogenic antibodies are broadly categorized into two principal groups based on their molecular targets, which critically determine disease mechanisms and clinical presentations. Surface antibodies target extracellular epitopes on neuronal surface proteins, such as the N-Methyl-D-Aspartate (NMDA) receptor, leucine-rich glioma inactivated 1 (LGI1), or Aquaporin-4 (17). These antibodies are directly pathogenic; they cause reversible synaptic dysfunction by modulating receptor internalization, trafficking, or blocking ligand binding, often leading to neuropsychiatric symptoms, seizures, movement disorders, and memory deficits (18-20). In contrast, intracellular antibodies (also known as onconeural antibodies), such as those against Hu, Yo, Glutamic Acid Decarboxylase (GAD), and Amphyphisin, primarily target intracellular antigens (21). These antibodies themselves are not considered directly pathogenic to the neuron's surface but serve as highly specific diagnostic markers of an underlying cytotoxic T-cell-mediated immune response against neurons, typically associated with paraneoplastic syndromes (22, 23). The key distinction lies in the pathophysiology: surface antibodies are effectors of disease, making their associated conditions often more responsive to immunotherapies aimed at antibody removal, whereas intracellular antibodies are indicators of a more aggressive, T-cell-driven neuronal destruction, which is frequently less reversible and necessitates aggressive treatment alongside immunosuppression (10).

Anti-NMDAR encephalitis is the most prevalent form of autoimmune encephalitis (24, 25). It disproportionately affects women and is frequently associated with ovarian teratoma (26). The clinical presentation typically evolves from a prodrome of fever and headache to

epilepsy and severe psychiatric manifestations such as agitation, psychosis. This can progress to include complex movement disorders, autonomic dysfunction, and hypoventilation (25). An FDG-PET/CT imaging study for this condition, analyzed six patients in the acute phase (27). It revealed a characteristic metabolic signature: hypermetabolism in the frontal and temporal lobes coupled with relative hypometabolism in the occipital region - a pattern described as a distinct frontotemporal- to-occipital gradient (25, 27).

AE linked to what was initially termed "anti-VGKC (Voltage-gated Potassium Channels)" antibodies was first described in 2001, presenting conditions like neuromyotonia and limbic encephalitis (LE) (28, 29). The first FDG-PET/CT report in a patient with this condition, noted increased medial temporal lobe metabolism (30, 31). It was later discovered that the true pathogenic targets are not the potassium channel itself, but associated proteins: LGI1 and Caspr2 (Contactin-Associated Protein-Like 2) (32, 33). These define two distinct clinical syndromes. Anti-LGI1 encephalitis typically presents with LE and distinctive faciobrachial dystonic seizures (28, 34). In contrast, anti-Caspr2 encephalitis more often affects elderly men and manifests as LE, Morvan's syndrome, peripheral nerve hyperexcitability, and may include cerebellar symptoms (34).

In the scenery of intracellular targeting antibodies, GAD, a key enzyme for GABA synthesis, is classically associated with Stiff-Person Syndrome (SPS) and type 1 diabetes mellitus (35). Beyond SPS, they are also linked to LE, temporal lobe epilepsy, and dementia (15, 36). The first FDG-PET/CT study in anti-GAD LE was reported in 2005. A study of 53 LE patients, including 10 with anti-GAD antibodies, established a characteristic PET pattern: hippocampal hypermetabolism in the early disease phase (37). Broader imaging findings also frequently include diffuse cortical hypometabolism, and in some cases, hypermetabolism in the brainstem and basal ganglia (36).

It is also important to consider that AE is frequently presented as a paraneoplastic syndrome (PNS). In approximately 60% of cases, highly specific onconeural, intracellular antibodies (e.g., anti-Hu, anti-Yo, and anti-Ma/Ta) are detected, with neurological symptoms often preceding cancer diagnosis by several years (9, 38). In our previous literature review encompassing 1,462 AE patients, PET/CT identified malignancies in 18.2% (n = 266) of patients. The most common neoplasm was small cell lung cancer, followed by ovarian teratomas and other ovarian tumors. Less frequently detected malignancies include lymphomas, neuroendocrine tumors, and carcinomas of the breast, prostate, thyroid, and bronchi (7). The tables 1 and 2 below summarize the main characteristics of the AE related to specific surface

and intracellular antibodies, respectively.

Table 1: Characteristics of AE related to the surface antibodies commonly found in the literature (Anti-NMDA, Anti-LGI1, and Anti-Aquaporin-4).

Characteristic	Anti-NMDA	Anti-LGI1	Anti-Aquaporin-4
Target (Protein)	NMDA Receptor (GluN1 Subunit)	Leucine-rich Glioma-Inactivated 1 protein	Aquaporin-4 Water Channel
Target Location	Neuronal Surface	Neuronal Surface	Astrocyte Surface
Main Mechanism	Internalization and reversible receptor blockade	Blockade of LGI1, affecting potassium channels	Complement & *ADCC cytotoxicity, damaging astrocytes
Main Clinical Syndrome	Encephalitis with psychosis, dyskinesias, seizures	Limbic Encephalitis, amnesia, hyponatremia, faciobrachial seizures	Neuromyelitis Optica Spectrum Disorder (NMOSD)
Response to Immunotherapy	Very Good / Rapid	Good / Rapid	Good for attacks; requires chronic suppression
Cancer Association	Yes (Ovarian Teratoma)	Low (~5-10%, thymoma)	Rare
Antibody Nature	Surface (Better Prognosis)	Surface (Better Prognosis)	Surface (Good prognosis with treatment)

*ADCC: Antibody-Dependent Cellular Cytotoxicity.

Table 2: Characteristics of AE related to the intracellular antibodies reported in the literature (Anti-GAD, Anti-Amphiphysin, Anti-Hu, Anti-Yo).

Characteristic	Anti-GAD	Anti-Amphiphysin	Anti-Hu	Anti-Yo
Target (Protein)	Glutamic Acid Decarboxylase Enzyme	Synaptic Vesicle Protein	RNA-binding Nuclear Protein	Cytoplasmic Protein (CDR62)
Target Location	Intracellular (Cytoplasm)	Intracellular (Synaptic Terminal)	Intracellular (Nucleus)	Intracellular (Cytoplasm)
Main Mechanism	Cellular immune response (T-Cells)	Cellular immune response (T-Cells)	Cellular immune response (T-Cells)	Cellular immune response (T-Cells)
Main Clinical Syndrome	Cerebellar Ataxia, Epilepsy, Stiff-Person Syndrome	Stiff-Person Syndrome (paraneoplastic)	Paraneoplastic Encephalomyelitis, Sensory Neuropathy	Paraneoplastic Cerebellar Degeneration
Response to Immunotherapy	Limited / Slow	Very Limited (focus on cancer)	Very Limited / Poor (focus on cancer)	Very Limited / Poor (focus on cancer)
Cancer Association	Rare	Very Strong (Breast, Lung Cancer)	Very Strong (Small Cell Lung Cancer)	Very Strong (Ovarian, Breast Cancer)
Antibody Nature	Intracellular (Guarded Prognosis)	Intracellular (Paraneoplastic - Poor Prognosis)	Intracellular (Paraneoplastic - Poor Prognosis)	Intracellular (Paraneoplastic - Poor Prognosis)

In order to explore the state-of-art of the use of FDG-PET/CT in the diagnosis and follow-up of patients with AE, the first stage of the study consisted of a systematic review of the topic, improving knowledge in order to subsequently address clinical and imaging data from patients.

OBJECTIVES

The main objectives of the present study were:

- To analyze the clinical presentation and FDG-PET/CT findings in a group of patients clinically diagnosed with AE.
- To explore the visual and quantitative analysis of FDG-PET/CT for detection of brain metabolic changes in patients with AE related to different kinds of antibodies.

The secondary objectives were:

- To analyze the prevalence of brain alterations on brain-dedicated FDG-PET/CT for a group of patients clinically diagnosed with AE.
- To compare statistically the differences of brain-dedicated FDG-PET/CT in patients with intracellular and surface antibodies AE.
- Identify possible neoplasms on whole body FDG-PET/CT among the patients studied.

MATERIALS AND METHODS

Ethical Approval

This retrospective study was approved by the Ethics Committee of the School of Medical Sciences, University of Campinas (UNICAMP) (Research Ethics Committee Approval nº 4.878.196). Patients and parents informed consent for patients bellow 18 years-old, were collected by phone.

Participants

Physical and electronic medical records were reviewed by the researcher, and data collected, including: neurological symptoms and signs on presentation; diagnostic test results including serum and cerebral spine fluid (CSF) antibody assay results; diagnosis of neoplasia. The MRI findings, a diagnostic criterion for AE, were also reviewed, but not included in the present study.

The inclusion criteria were patients diagnosed as AE based on the Brazilian criteria

(13) and who had performed brain-dedicated and whole-body FDG-PET/CT, from 2013 to 2023. The exclusion criteria were patients with other neurological diseases and noisy PET/CT images. The antibody detection was made by CSF, serum or both, considering the standard methods and reference cutoffs established in the literature (39, 40). In case of anti-GAD AE, one of the most difficult to diagnose through in vitro analysis, the cutoff adopted was > 2000 U/mL (39).

PET/CT Imaging Acquisition and Reconstruction Protocol

The FDG-PET/CT images were acquired using a Siemens Biograph mCT 40 PET/CT scanner (Siemens, Erlangen, Germany) at the Nuclear Medicine Division of the Clinical Hospital, UNICAMP. The patients fasted for 6 hours before the intravenous administration of 3.7 MBq/kg of ^{18}F-FDG. After resting for 1 hour, images of the whole body and dedicated brain images have been performed. The dedicated brain images were obtained with the following acquisition and reconstruction parameters: CT: 80 kVp, 35 mAs, matrix 512 x 512, slice thickness 1.0 mm, brain window, convolution kernel H19s, Low Dose. FDG-PET: acquisition time: 10 minutes, 1 bed, matrix 400 x 400, zoom 2, reconstruction method TrueX+TOF (ultra- interactions, 21 subsets, Gaussian filter (FWHM = 2 mm).

FDG-PET/CT Visual Analysis

Visual analysis of PET/CT images was done by an expert board-certified nuclear medicine physician with 25 years' experience in brain and PET/CT images, looking for asymmetry and areas of hypermetabolism or hypometabolism. Results were organized in a datasheet to allow the correlation with the clinical manifestations, antibodies results, and statistical findings of the patients.

FDG-PET/CT Quantitative Analysis

For quantitative brain analysis, the Scenium® software (syngo.via., Siemens, Erlangen, Germany) was applied, providing powerful tools to quantify the FDG-PET/CT images, calculating statistical parameters of the patients compared to normal subjects. The software combines standardized anatomy, statistical analysis, and advanced imaging methods

to get the report of imaging quantification. It has reference databases of FDG-PET/CT images of the normal brains for different age ranges, allowing a statistical comparison of a specific patient against a group of normal reference images. The quantification results are demonstrated as standard deviation of the mean values from a normal database for each different brain region. Considering the robust fusion engine implemented in Scenium®, it is possible to register the image of the patient with the normal reference automatically, creating a color-coded statistical map that can highlight the patterns of unusual radiopharmaceutical uptake. Typically, minimum, maximum and mean intensity values are computed for each region together with statistical information. The software shows the results from -2 to +2 standard deviation (SD) as a normal result. Values higher than +2 are considered as hypermetabolism. Values below -2 are considered as hypometabolism.

We used the results from Scenium® named as combined regions, which is a composition of brain regions including the whole lobes. For all regions the software shows the right, left and bilateral values. There are 11 regions in the combined results: basal ganglia, central region, cingulate gyrus, striatum, cerebellum, frontal lobe, mesial temporal lobe, occipital lobe, parietal lobe, precuneus and temporal lobe.

Statistical Analysis Data

We also performed a group analysis of the quantitative results and we calculated a mean for these values in each antibody group which we called mean standard mean value (SMV). For the evaluation of the group of patients, heat maps of SD have been constructed, as well as the distribution of the standard deviation of the mean intensity. Figure 1 summarizes the main steps of the study.

In order to improve the characterization of the patients for quantification and statistical analysis, they were divided into 4 groups, according to CSF and blood tests: patients with positive tests for surface antibodies, intracellular antibodies, negative antibodies, and also untested subjects. A statistical analysis based on Student's T-Test, Analysis of Variance (ANOVA), as well as Spearman's Correlation has been conducted in order to characterize and compare specific groups of patients and search for relations in FDG uptake in different brain areas.

The Kruskal-Wallis test was applied to identify possible brain areas with statistically significant differences between the antibodies' groups in the first and in the second

scans, despite being distributed or not in the normal range of the numbers of the SD obtained from Scenium®. The Bonferroni's Correction was applied to the p-values. The corresponding analysis aimed to evaluate how the disease can change the metabolism of different brain regions according to the antibodies detected and the evolution of the disease.

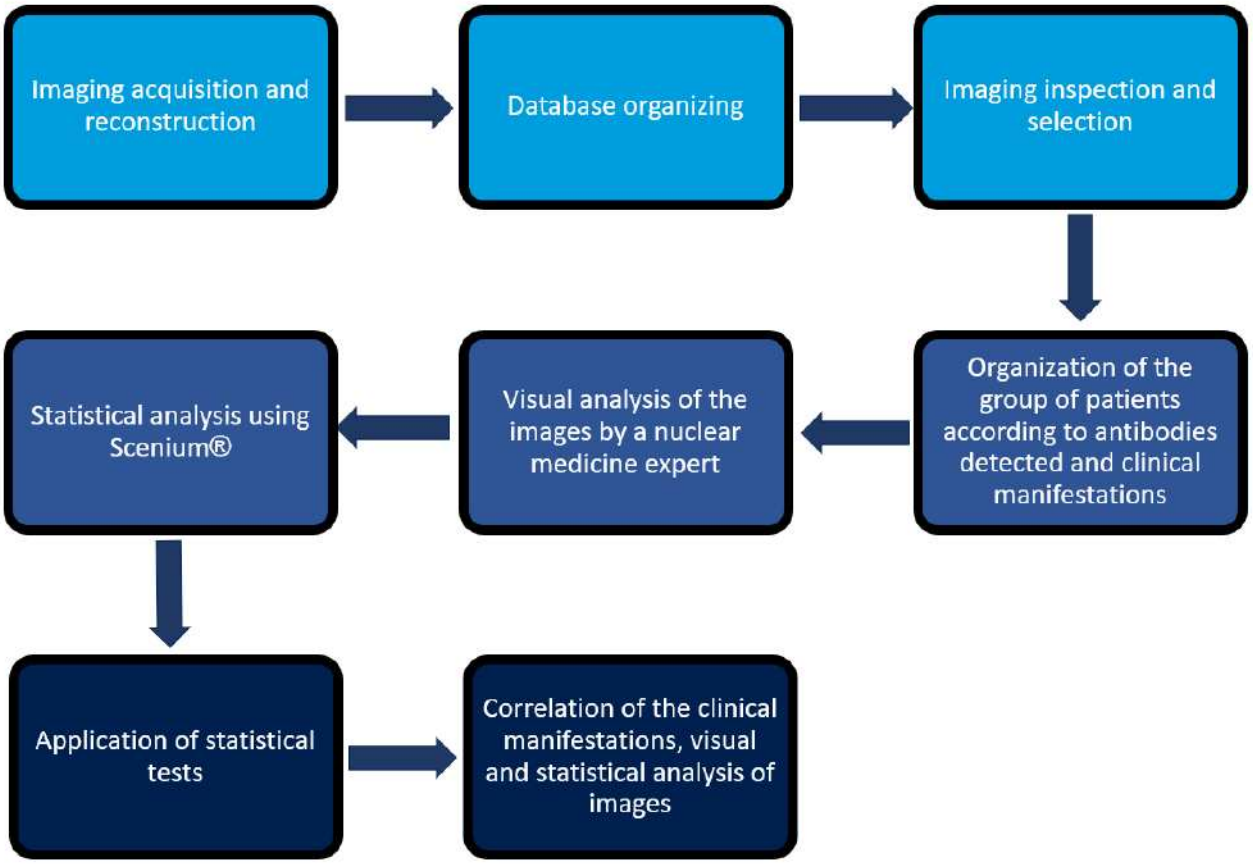

Figure 1. Block diagram summarizing the main steps of the study.

RESULTS

Systematic Review Published

A systematic literature review was published about the role and perspectives of the use of ^{18}F- FDG in the diagnosis and follow-up of patients with AE, which is presented in the Attachment I. The article was published in the journal *Clinical and Translational Imaging*, in 2023 (7). This chapter includes material previously published in Clinical and Translational Imaging: "Correction: FDG-PET in Patients with Autoimmune Encephalitis: A Review of

Findings and New Perspectives," by Maurício Martins Baldissin et al. (August 28, 2023). Reproduction authorized by Springer Nature via the Copyright Clearance Center (License No. 6247260898822).

In this paper we performed a wide review of the FDG-PET/CT findings in the different types of AE as well as the detection of neoplasm in these patients. We also performed a statistical analysis of the literature findings.

Clinical Data

From a database of 47 subjects who performed FDG-PET/CT, the study includes 37 patients who had clinical manifestation of the AE and were diagnosed with probable or definitive AE by antibodies test. The patients' ages ranges from 13 to 75 years old (median age 52, interquartile range 29-63).

Regarding the indication from the clinical physician to perform PET/CT study we had: 46% in order to identify brain metabolic changes related to the main clinical manifestations (epilepsy, ataxia, behavioral alterations); 32% to search for neoplasm of undetermined etiology; 22 % the exam justification was not found. Regardless of indication, all 37 patients enrolled in the study had whole-body and brain-dedicated images FDG-PET/CT.

The mean time between the symptom onset and the diagnosis by clinical and imaging findings, and/or antibodies test) was 285.65 ± 514.78 days (median 119, interquartile range 59 - 252). **Table 3** brings the sex and age distributions of the patients studied, as well as the percentage distribution of the antibodies detected. In outpatient settings, most patients are followed-up for an average period of 5 years (3.5 ± 2.7 years), which may vary depending on clinical conditions and findings.

The antibody detection was made by CSF (N =13), serum (N = 1), or both (N = 3). For 13 patients the detection method has not been described. Seven patients were not tested for antibodies. All 37 patients had at least one FDG-PET/CT while some patients had more than one study. Therefore, 17 patients performed a second FDG-PET/CT.

Table 3: Demographic characterization and the antibodies found in the group studied (n = 37). SD: Standard Deviation.

Antibodies	N(%)	Age (Range, (Mean + SD)) (years)	Sex	Mean Time From Symptoms Onset to Diagnosis (Mean + SD) (days)
Anti-NMDA	9 (24.32%)	13 to 74 (26.00 ± 20.89)	4 Female (44.44%)	63 ± 52.19
Anti-LGI1	1 (2.7%)	75	1 Male (100%)	92
Anti-Yo	3 (8.12%)	47 to 73 (58.33 ± 13.32)	3 Female (100%)	229.33 ± 271.84
Anti-GAD	2 (5.41%)	53 to 63 (58.00 ± 7.07)	1 Female (50%)	370.5 ± 309
Anti-Hu	1 (2.7%)	74	1 Female (100%)	73
Anti-Amphiphysin	1 (2.7%)	49	1 Female (100%)	30
Anti-Aquaporin-4	1 (2.7%)	47	1 Female (100%)	53
Negative	12 (32.43%)	15 to 75 (51.00 ± 18.87)	8 Female (66.67%)	211.33 ± 148.1
Untested	7 (18.91%)	13 to 65 (41.14 ± 20.60)	5 Female (71.43%)	415.57 ± 429.55
Total	**37 (100%)**	**13 to 75 (41.14 ± 20.60)**	**Female 24 (64.86%)**	**285.65 ± 514.78**

Among the antibodies detected, anti-NMDA had a higher prevalence (24.2%). From the 37 patients included in this study, 31 patients (83.80%) underwent some type of therapy before the first FDG-PET/CT scan. Only 6 patients had no report of therapy before the first PET/CT scan (1 for anti-aquaporin-4 and 5 from untested groups). The treatments included drugs to the inflammatory process (e.g. immunoglobulin, methylprednisolone, pulsotherapy, rituximab), as well as a variety of drugs to control specific symptoms. All the 17 patients who underwent the second PET/CT presented a recurrence of the disease, from which 88.23% followed their therapies between both scans.

FDG-PET/CT Visual Analysis

All 37 patients had at least one FDG-PET/CT while some patients had more than one study. Therefore, 17 patients performed a second FDG-PET/CT. Table 4 and Table 5 summarizes the most common manifestations reported for the patients studied, as well as the visual analysis findings of the first FDG-PET/CT and the second PET/CT respectively.

In visual analysis all patients presented some metabolic alteration on brain images totalizing 104 altered areas on first FDG-PET/CT: 65 areas of hypermetabolism in all patients (62.5%) and a total of 39 areas of hypometabolism (37.5%). In the second FDG-PET/CT it was detected a total of 58 areas of altered metabolism: 36 hypermetabolic areas (62%) and 22 hypometabolic areas (38%).

Table 4: Summary of the results of visual analysis of the first FDG-PET/CT images.

First PET/CT-FDG										
Antibodies	**N**	**Hypermetabolism**			**Hypometabolism**			**GAP**		**Clinical Manifestations**	
			N	**(%)**		**N**	**(%)**	**N**	**(%)**		**N**	**(%)**
Anti-LGI1	1	Basal Ganglia Temporal Mesial Lobe (left)	1 1	100 100	Frontal Lobe (right) Temporal Mesial Lobe (right)	1 1	100 100	1	100	behavioral alterations faciobrachial dystonic and convulsive seizures status epilepticus	1 1 1	100 100 100
Anti-Yo	3	Cingulate Gyri Basal Ganglia Thalamus (bilateral) Midbrain Precuneus (bilateral) Central region (bilateral)	2 1 1 1 1 1	66 33 33 33 33 33	Cerebellar Hemispheres (bilateral)	1	33	0	0	epilepsy cerebellar ataxia	2 1	66 33
Anti-GAD	2	Basal Ganglia Thalamus Midbrain Temporal Superior (bilateral)	2 1 1 2	100 50 50 100	Frontal Lobe (right, diffuse)	1	50	0	0	epilepsy long-term depression ataxia with aspects of stiff person syndrome	2 1 2	100 50 100
Anti-Hu	1	Cingulate Gyri	1	100	Cerebellar Hemispheres (bilateral)	1	100	0	0	epilepsy sensitive alterations	1 1	100 100
Anti-Amphiphysin	1	Precuneus (right) Cerebellar Vermis 1	1 1	100 100	Brain Hemisphere (left) Temporal Lobe (bilateral) Thalamus (left) Cerebellar Hemisphere (right)	1 1 1 1	100 100 100 100	0	0	epilepsy behavioral alterations	1 1	100 100
Anti-Aquaporin-4	1	Basal Ganglia Thalamus Midbrain Precuneus (bilateral) Cingulate Gyri	1 1 1 1 1	100 100 100 100 100	Occipital Lobes	1	100	0	0	tetraparesia facial, muscular disorders diplopia sensitivity syndromes	1 1 1 1	100 100 100 100
Anti-NMDA	9	Cingulate Gyri Precuneus Parietal Lobes Basal Ganglia	3 3 1 2	33 33 11 22	Parietal Lobes Cerebellar Hemispheres Temporoparietoccipital Temporal Lobe (bilateral) Temporoperietal	1 7 1 1 1	11 78 11 11 11	3	33	epilepsy status epilepticus aphasia dystonia behavioral alterations psychosis sensitive alterations movement disorders (in some cases leading to dysautonomia) diplopy agraphia and acalculia hypoventilation hand tremors decreased level of consciousness mutism	9 3 1 1 7 2 1 3 1 1 2 1 1 1	100 33 11 11 78 22 11 33 11 11 22 11 11 11
Untested	7	Cingulate Gyri Precuneus (bilateral) Parietal Lobes	4 3 1	57 43 14	Temporal Anterior (bilateral) Cerebellar Hemispheres Central Region (bilateral) Occipital Lobes	1 3 2 3	14 43 29 43	4	57	memory loss behavioral alterations depression psychosis visual hallucinations schizophrenia aggressiveness postural instability ataxia facial paresthesia	4 6 1 3 1 1 1 2 2 1	57 86 14 43 14 14 14 28 28 14
Negative	12	Basal Ganglia Cingulate Gyri Precuneus Temporal Mesial Lobe (bilateral) Central Region Thalamus Parietal Lobes	6 5 6 5 1 1 1	50 42 50 42 8 8 8	Basal Ganglia Cerebellar Hemispheres Parietal Lobes Temporal Lobes Frontal Lobes Temporoparietoccipital Thalamus	1 5 2 1 2 1 1	8 42 17 8 17 8 8	2	17	behavioral changes epilepsy headache dizziness vertigo postural instability confusional syndrome	7 8 1 2 2 5 2	58 67 8 17 17 42 17
Total (N)	**37**	**65**			**39**							

*GAP: anteroposterior gradient.

Table 5: Summary of the results of visual analysis of the second FDG-PET/CT images.

Second PET/CT-FDG										
Antibodies	**N**	**Hypermetabolism**			**Hypometabolism**			**GAP**		**Clinical Manifestations**		
			N	**(%)**		**N**	**(%)**	**N**	**(%)**		**N**	**(%)**
Anti-LGI1	1	Basal Ganglia Temporal Mesial Lobe (left)	1 1	100 100	Frontal Lobe (right) Temporal Mesial Lobe (right)	1 1	100 100	1	100	behavioral alterations faciobrachial dystonic and convulsive seizures status epilepticus	1 1 1	100 100 100
Anti-Yo	1		0	0	Cerebellar Hemispheres (bilateral)	1	100	0	0	cerebellar ataxia	1	100
Anti-GAD	1	Thalamus Midbrain	1 1	100 100	Frontal Lobe (right, diffuse)	1	100	0	0	epilepsy long-term depression ataxia with aspects of stiff person syndrome	1 1 1	100 100 100
Anti-Hu	1	Cingulate Gyri	1	100	Cerebellar Hemispheres (bilateral)	1	100	0	0	epilepsy sensitive alterations	1 1	100 100
Anti-Amphiphysin	1	Precuneus (right) Cerebellar Vermis 1	1 1	100 100	Brain Hemisphere (left) Temporal Lobe (bilateral) Thalamus (left) Cerebellar Hemisphere (right)	1 1 1 1	100 100 100 100	0	0	epilepsy behavioral alterations	1 1	100 100
Anti-NMDA	5	Temporal Superior (bilateral) Cingulate Gyri Precuneus Parietal Lobes	2 2 3 1	40 40 60 20	Parietal Lobes Cerebellar Hemispheres Temporoparietooccipital Temporoparietal	1 3 1 1	20 60 20 20	1	20	epilepsy behavioral alterations psychosis sensitive alterations movement disorders (in some cases leading to dysautonomia)	2 4 2 2 2	40 80 40 40 40
Negative	7	Basal Ganglia Cingulate Gyri Precuneus Temporal Mesial Lobe (bilateral) Central Region Thalamus Parietal Lobes	5 4 2 3 1 1 1	71 57 28 43 14 14 14	Precuneus Cerebellar Hemispheres Parietal Lobes	1 1 2	14 14 28	1	14	behavioral changes epilepsy movement disorders postural instability	4 3 2 3	57 43 28 43
Total (N)	**17**	**36**			**22**							

*GAP: anteroposterior gradient.

Surface Antibodies

Anti-NMDA Group (N = 9)

The antibody with higher number of patients was anti-NMDA (n = 9). Table 2 and Table 3 summarize the FDG-PET/CT visual analysis and clinical findings according to the antibody found. The first images acquired have shown higher uptake of ^{18}F-FDG in the following regions: cingulate gyrus (medium-posterior portion), precuneus, basal ganglia, and parietal lobe. Hypometabolism was observed in the cerebellar hemispheres, temporo-parieto-occipital areas. In addition, an anteroposterior gradient has been detected in 33% of patients of this group. The anteroposterior gradient was described as a hypometabolism in the posterior regions (parietal or parieto-occipital) in relation to the frontal lobes.

In the images of the second scan (n = 5), hypermetabolism was also observed in parietal lobes, cingulate gyrus and precuneus regions, but not in basal ganglia.

One subject, with three FDG-PET/CT scans in different stages of the disease, expressed a hypermetabolism in the basal ganglia in the earlier stage of the disease, when manifested epilepsy, ataxia, movement disorders, and behavioral alterations, evolving to mutism and decreased level of consciousness, needing intubation. The patient was submitted to immunotherapy, resulting in consciousness recovery and extubation, with the PET/CT

revealing a normal uptake pattern of the ^{18}F-FDG. The recurrence of the disease four months after the therapy led to a new cycle of treatment and a new imaging acquisition (three weeks after the end of the new cycle of immunotherapy). The PET/CT revealed a diffuse cortical hypometabolism in the left temporo-parieto-occipital region, as well as in the cerebellar hemispheres. At this stage, the number and types of clinical manifestations have also been reduced.

Figures 2 and 3 show some examples of ^{18}F-FDG PET/CT images in AE patients with anti-NMDA antibodies. Figure 2 highlights the hypermetabolism in temporal lobes of a patient with behavior alterations and status epilepticus. At the time of the first PET/CT, the patient has been treated with methylprednisolone, valproic acid and lacosamide (four months after the symptoms onset). A second scan was done four months later, due to recurrence of symptoms.

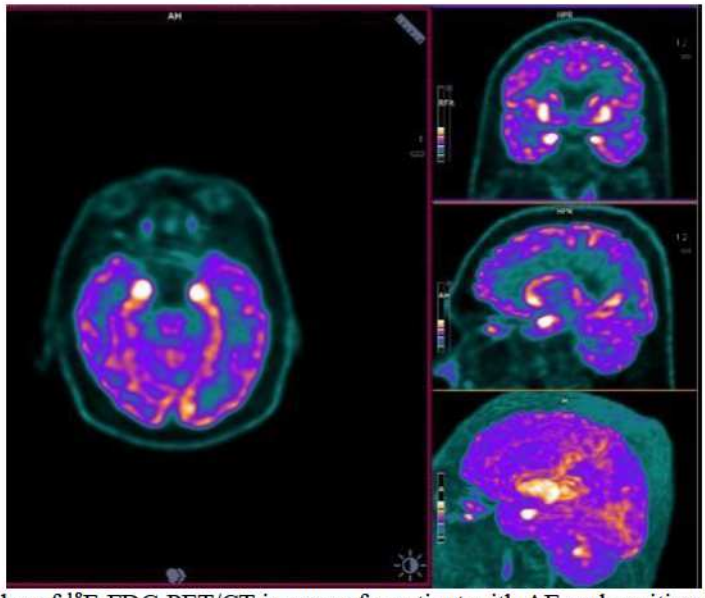

Figure 2. Examples of ^{18}F-FDG PET/CT images of a patient with AE and positive for anti-NMDA antibodies, presenting hypermetabolism in the mesial temporal lobes (more pronounced on the right).

On the other hand, Figure 3 brings the volumetric reconstruction of the PET for a patient with movement disorders, epileptic seizures, agraphia and acalculia. The patient started the therapy one month after the symptoms onset, being submitted to pulsotherapy three months before the first scan and two months after this one. A second PET/CT was required two years after the first one due to the worsening of epileptic seizures, suggesting recurrence of the disease.

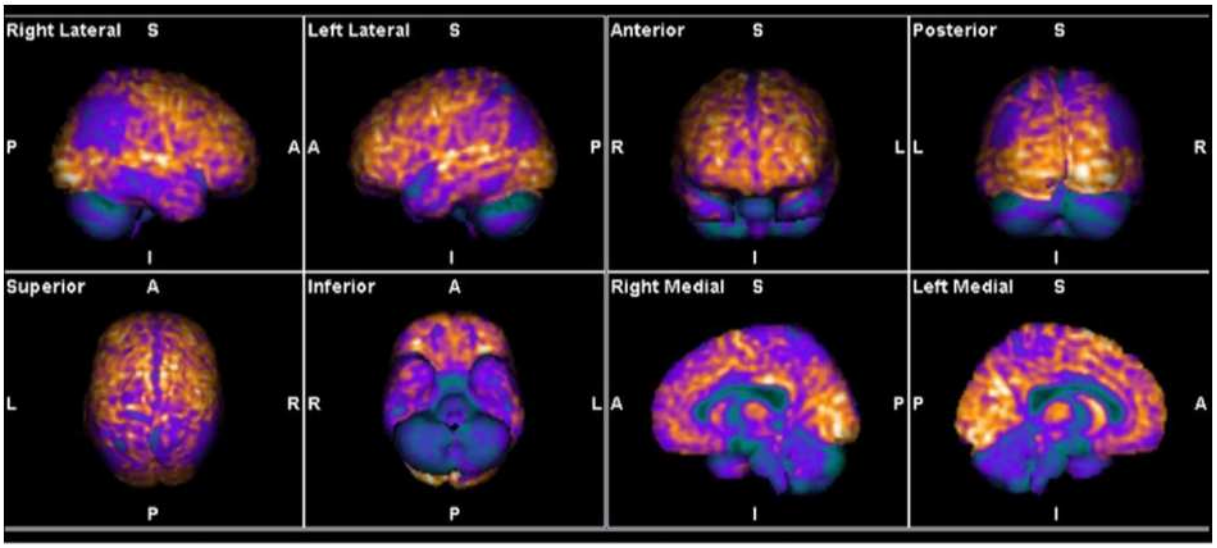

Figure 3. Examples of ^{18}F-FDG PET/CT images of a patient with AE and positive for anti-NMDA antibodies, presenting hypometabolism in the parietal lobes and cerebellum.

Anti-LGI1 (N = 1)

One patient presented anti-LGI1 antibodies and FDG-PET/CT showed: hypermetabolism in the left temporal mesial lobe and basal ganglia and hypometabolism in the right frontal lobe and right temporal mesial lobe. An anteroposterior uptake gradient has also been observed. Both symptoms and FDG patterns remained the same after therapy.

Anti-Aquaporin-4 (N = 1)

In one case of anti-aquaporin-4, a higher ^{18}F-FDG uptake in the basal nuclei, thalamus, midbrain, precuneus (bilaterally) and cingulate gyrus has been identified, added to hypometabolism in the occipital lobe (bilaterally).

Intracellular Antibodies

Anti-Yo (N = 3)

Patients with anti-Yo antibodies (N = 3) showed hypermetabolism in the basal ganglia, cingulate gyri, thalamus, midbrain, precuneus, and central region. All the areas with hypermetabolism had been resolved in the second PET/CT. One patient performed an FDG-PET after a four-year period showing hypometabolism in the cerebellar hemispheres in three different scans: in the earlier phase of the disease, two years after the treatment and 4 years after the first one, when the same symptoms recurred (epilepsy with memory loss and déjà-vu).

Figure 4 shows an example of PET/CT images of the patient with these antibodies. The patient manifested symptoms of cerebellar ataxia, being treated with pulsotherapy and immunoglobulin one month before the first PET/CT. After the image, remained under the care of the neurology team and died three years later (unknown cause).

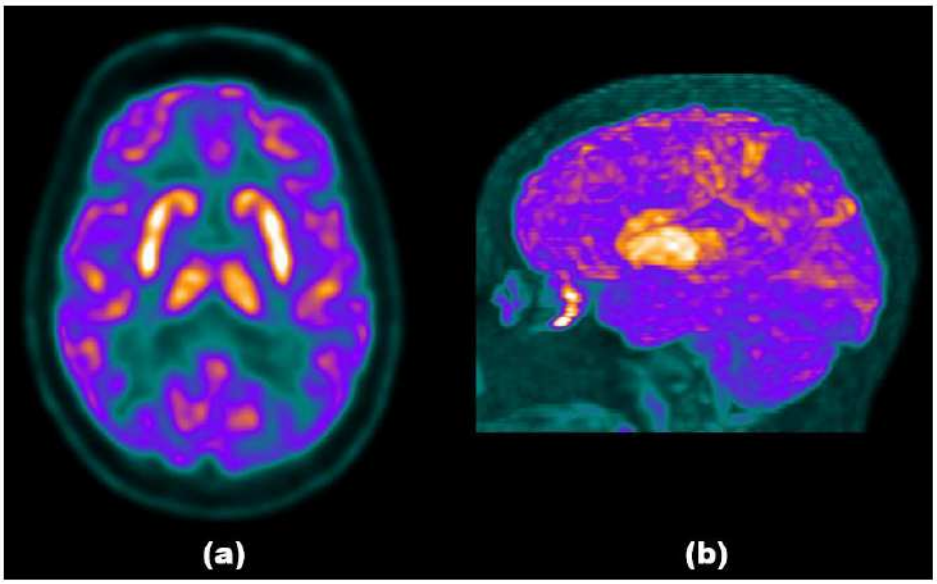

Figure 4. Examples of ^{18}F-FDG PET/CT images of a patient with AE and positive for anti-Yo antibodies, presenting hypermetabolism in the basal ganglia both in the transversal (a) and 3D (b) views.

Anti-Hu (N = 1)

For anti-Hu antibodies (N = 1), the first PET detected an increased uptake in the cingulate gyri (medium and posterior regions) and a decreased uptake was observed in

cerebellar hemispheres bilaterally. The second scan showed the same findings.

Anti-GAD (N = 2)

Considering the patients with anti-GAD antibodies (N = 2), FDG-PET/CT showed hypermetabolism in midbrain, temporal lobes, basal ganglia and thalamus, and a diffuse hypometabolism was observed in the right frontal lobe for one patient. Images and symptoms of one patient in the second scan revealed an analogous pattern.

Anti-Amphyphisin (N = 1)

One patient presented anti-amphiphysin antibodies and FDG-PET/CT showed hypermetabolism in cerebellar vermis and precuneus, with hypometabolism in the following areas: temporal lobes (bilaterally), left brain hemisphere (accentuated), left thalamus and right cerebellar hemisphere, this last one probably due to a cerebellar diaschisis. The second image revealed the same pattern of the first one, added to a hypermetabolism identified in the right central region.

Negative Antibodies (N = 12)

The group of patients with negative antibodies expressed clinical manifestations highly suggestive of AE. Among the clinical evidences reported, epilepsy, behavioral and psychiatric changes were the most common, followed by cerebellar ataxia and other motion disorders. Moreover, these patients presented ^{18}F-FDG uptake findings, and many of which were similar to those reported for positive antibodies patients. These patients presented FDG-PET with the following alterations: hypermetabolism on basal ganglia, thalamus, cingulate gyrus, precuneus, temporal mesial lobe, central region, and parietal lobes; hypometabolic areas on cerebellar hemisphere, temporal lobes, frontal lobes, parietal lobes, temporo-parieto-occipital region.

Seven of these patients had follow-up FDG-PET/CT images in different stages of the disease. The follow-up scans highlighted hypermetabolism in the same regions and also on pons, insula and cerebellar vermis. Hypometabolism was observed on temporal, parietal, and frontal lobes, as well as on cerebellar hemispheres. The GAP was present in 2 of patients (17%)

in the first FDG-PET/CT, and in one patient (14%) in the second scan. Tables 4 and 5 summarizes the results of the visual analysis for this group of patients.

Untested Patients (N = 7)

Different from other groups studied, for the untested patients, epilepsy was not the main manifestation reported, predominating behavioral, psychiatric, memory, and movement disorders. Three patients with prevalence of psychiatric alterations and memory loss had no hypermetabolism area. These three patients presented hypometabolism on cerebellar hemispheres, central regions, and occipital lobes in addition to a mild GAP.

Hypermetabolism in the cingulate gyrus and precuneus has been found for a patient with memory loss, behavior changes, and depression, in addition to the temporal anterior lobes hypometabolism.

Patients with motor disorders (e.g. postural instability, ataxia, facial paresthesia) presented hypermetabolism on cingulate gyrus, precuneus, and parietal lobes and hypometabolism on cerebellar hemisphere and temporal lobe. There was one case with a mild GAP.

MRI Findings

Despite not being the main focus of the study, MRI integrates the standard protocols for AE diagnosis. In the group studied, 33 patients (89.20 %) have at least one MRI scan, from which 6 (18.18 %) were normal (3 for anti-NMDA, 2 for negative and 1 for the untested group). The four patients without an MRI scan were anti-NMDA (N = 1), negative (N = 2), and untested group (N = 1).

The main MRI findings were:

- anti-NMDA group (N = 9): cortical thickening (N = 3), hippocampal atrophy (N = 2), and cerebellar atrophy (N = 1);
- anti-LGI1 (N = 1): cortical thickening;
- anti-aquaporin-4 (N = 1) antibodies: cortical thickening;
- anti-Yo antibodies (n = 2): cerebellar atrophy (2) and diffuse cortical volumetric

reduction;

- anti-Hu antibodies (n = 1): diffuse cortical volumetric reduction;
- anti-GAD antibodies (n = 2): presented thalamic thickening (n = 1) and left hippocampal atrophy (n = 1);
- anti-amphiphysin antibodies (n = 1): hippocampal and cortical T2 hypersignal (for the whole right hemisphere).

For the groups of negative antibodies and untested patients, a variety of alteration has been found from which the most prevalent are the cortical thickening, cerebellar atrophy, and diffuse cortical volumetric reduction, as such as found for cases of the antibodies previously mentioned.

Detection of Neoplasms of Undefined Origin

From the onset of symptoms to the start of therapies and patient follow-up, the search for neoplasms was conducted using different techniques. Figure 5 shows the types of methods and percentages of use for this purpose. Therefore, when performing PET/CT, most of patients had already some kind of investigation in search for neoplasms of unknown origin.

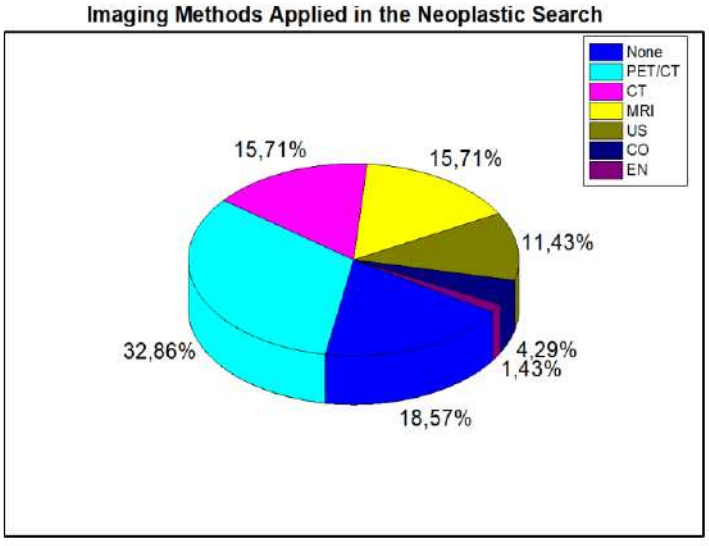

Figure 5. Imaging methods applied in the search for neoplasms, considering the whole group of patients (N = 37). PET/CT: Positron-Emission Computed Tomography with Computed Tomography; CT: Computed Tomography; MRI: Magnetic Resonance Imaging; US: Ultrasound; CO: Colonoscopy; EN: Endoscopy.

The present study detected 2 malignant neoplasms by PET/CT (2/37 – 5.4%). One female had a breast nodule with hypermetabolism and confirmed to be an in-situ ductal carcinoma (Figure 6) and a male patient had a focal hypermetabolism on prostate and a confirmed prostate adenocarcinoma by biopsy. None neoplasia was detected by the other imaging methods mentioned.

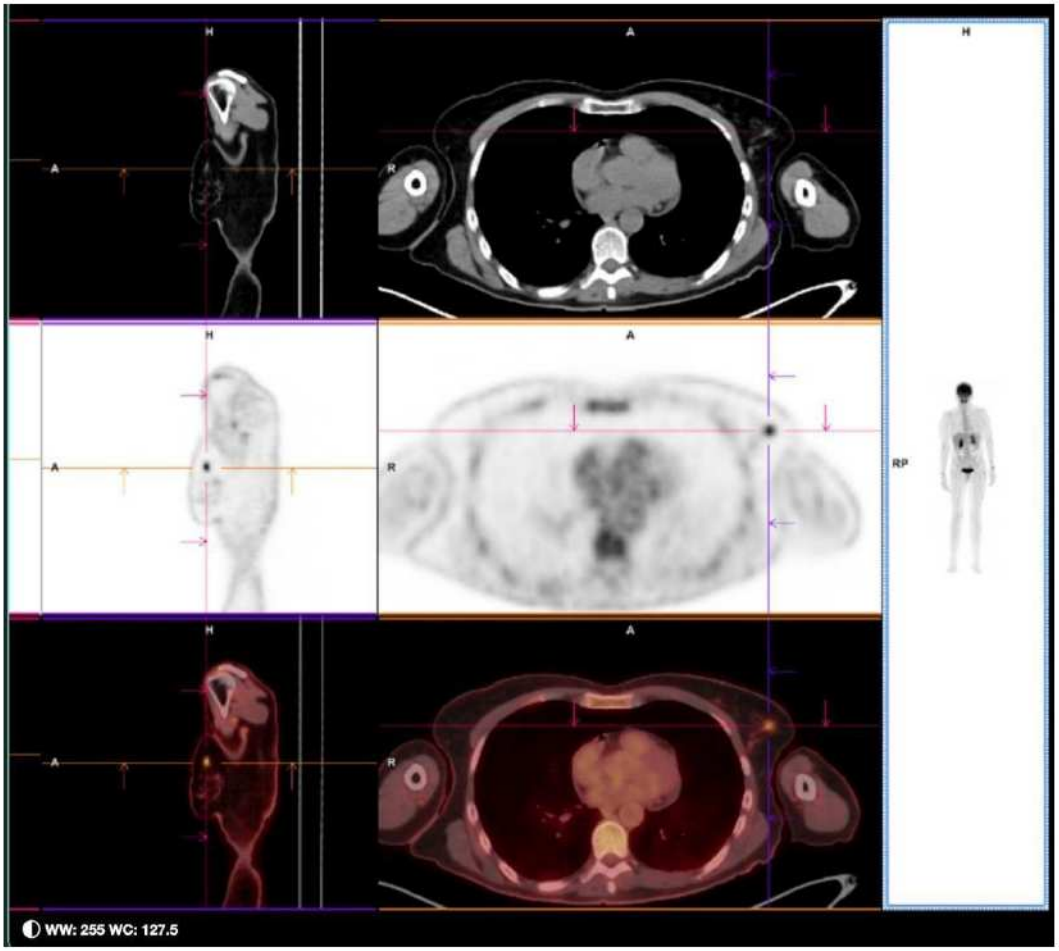

Figure 6. ^{18}F-FDG-PET/CT detection of breast nodule hypermetabolism in a patient with AE and negative antibodies.

Two patients had detection of thyroid nodules with hypermetabolism, which could be a neoplastic lesion. However, one patient did not perform follow-up and the other patient refused to perform biopsy and is in follow-up with ultrasound with TIRADS 4. Including these 2 patients we would have 4/37 neoplasm occurrence or 10.8%.

Other two patients had personal antecedents of neoplasm years before the AE diagnosis. One patient had breast cancer 5 years before the neurological symptoms and the other patient had thyroid cancer 12 years before. Table 6 summarizes the detection of neoplasms.

Table 6: Neoplasms detected in the whole group of patients.

Antibodies	Neoplasia	Detection	N	Percent (%)
Anti-NMDA	Thyroid	Personal Medical History	1	2.70 %
Untested Patients	Breast, Thyroid	Personal Medical History	1	2.70 %
Negative Antibodies	Prostate Adenocarcinoma	PET/CT	2	5.40 %
	Breast	PET/CT		

Quantitative FDG-PET/CT Analysis

Brain metabolism alteration

Table 7 highlights the number of hypometabolic and hypermetabolic areas found for the whole group of patients (N = 37) in the first PET/CT. In this case, 102 areas of hypermetabolism and 182 areas of hypometabolism have been found.

Table 7: Number of areas of FDG hypometabolism or hypermetabolism identified by quantitative analysis on the first PET/CT for all patients studied (N = 37).

Brain Area		All Patients - FDG Uptake - First PET/CT				
		Hypermetabolism	Hypometabolism	Normal uptake	% Hyper	% Hypo
Basal ganglia	Left	7	6	24	18,92	16,22
	Right	8	7	22	21,62	18,92
Central region	Left	2	8	27	5,41	21,62
	Right	2	7	28	5,41	18,92
Cerebellum	Left	3	9	25	8,11	24,32
	Right	2	10	25	5,41	27,03
Cingulate/paracingulate gyri	Left	1	8	28	2,70	21,62
	Right	2	6	29	5,41	16,22
Corpus striatum	Left	6	7	24	16,22	18,92
	Right	7	5	25	18,92	13,51
Frontal lobe	Left	3	22	12	8,11	59,46
	Right	0	21	16	0,00	56,76
Mesial temporal lobe	Left	10	4	23	27,03	10,81
	Right	8	4	25	21,62	10,81
Occipital lobe	Left	7	2	28	18,92	5,41
	Right	11	1	25	29,73	2,70
Parietal lobe	Left	3	16	18	8,11	43,24
	Right	4	14	19	10,81	37,84
Precuneus	Left	3	12	22	8,11	32,43
	Right	5	9	23	13,51	24,32
Temporal lobe	Left	4	3	30	10,81	8,11
	Right	4	1	32	10,81	2,70
Total		**102**	**182**	**530**	**12,53**	**22,35**

Table 8 brings these findings considering only the patients that had 2 scans (N = 17), in order to evaluate the behavior of the uptake standards between the first and the second PET/CT scan. We can observe 42 areas of hypermetabolism and 94 areas of hypometabolism in the first scan. On the second scan, these numbers reduced respectively to 37 and 86.

Table 8: Number of areas with hypometabolism or hypermetabolism identified by quantitative analysis for the patients that have 2 scans.

Brain Area		First PET/CT					Second PET/CT				
		Hypermetabolism	Hypometabolism	Normal Uptake	% Hyper	% Hypo	Hypermetabolism	Hypometabolism	Normal Uptake	% Hyper	% Hypo
Basal ganglia	Left	2	2	13	5,41	5,41	1	3	13	2,70	8,11
	Right	4	2	11	10,81	5,41	1	0	16	2,70	0,00
Central region	Left	1	5	11	2,70	13,51	1	6	10	2,70	16,22
	Right	2	3	12	5,41	8,11	4	4	9	10,81	10,81
Cerebellum	Left	1	3	13	2,70	8,11	1	5	11	2,70	13,51
	Right	1	4	12	2,70	10,81	1	5	11	2,70	13,51
Cingulate/paracingulate gyri	Left	0	5	12	0,00	13,51	0	4	13	0,00	10,81
	Right	0	4	13	0,00	10,81	1	3	13	2,70	8,11
Corpus striatum	Left	2	2	13	5,41	5,41	1	2	14	2,70	5,41
	Right	3	1	13	8,11	2,70	1	0	16	2,70	0,00
Frontal lobe	Left	1	12	4	2,70	32,43	0	12	5	0,00	32,43
	Right	0	11	6	0,00	29,73	0	13	4	0,00	35,14
Mesial temporal lobe	Left	4	3	10	10,81	8,11	3	3	11	8,11	8,11
	Right	3	2	12	8,11	5,41	4	1	12	10,81	2,70
Occipital lobe	Left	5	1	11	13,51	2,70	4	0	13	10,81	0,00
	Right	6	0	11	16,22	0,00	8	0	9	21,62	0,00
Parietal lobe	Left	0	10	7	0,00	27,03	1	10	6	2,70	27,03
	Right	0	9	8	0,00	24,32	0	7	10	0,00	18,92
Precuneus	Left	1	9	7	2,70	24,32	1	4	12	2,70	10,81
	Right	2	4	11	5,41	10,81	1	1	15	2,70	2,70
Temporal lobe	Left	2	2	13	5,41	5,41	1	3	13	2,70	8,11
	Right	2	0	15	5,41	0,00	2	0	15	5,41	0,00
Total		**42**	**94**	**238**	**11,23**	**25,13**	**37**	**86**	**251**	**9,89**	**22,99**

Figure 7 shows a graphic with hypermetabolic and hypometabolic areas of the first and second PET/CT images. It is observed that the most prevalent area of hypometabolism is the parietal lobe, followed by the frontal lobes. On the other hand, the higher prevalence of, hypermetabolism has been seen in the mesial temporal and the occipital lobes. In visual analysis it was observed a high prevalence of hypermetabolism on the primary visual area on occipital lobe. We did not document this finding on visual analysis since it is probably due to physiological stimulation during injection.

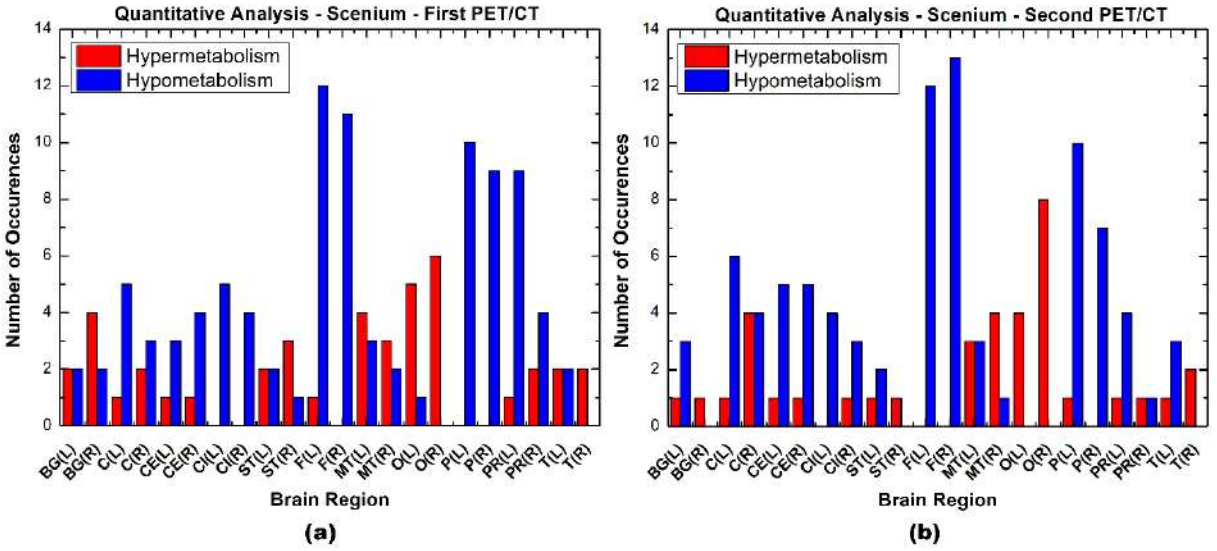

Figure 7. Histograms of the number of occurrences of hypermetabolism and hypometabolism in the first (a) and in the second PET/CT (b) (N = 17). BG(L): basal ganglia (left); BG(R): basal ganglia (right); C(L): central region (left); C(R): central region (right); CE(L): cerebellum (left); CE(R): cerebellum (right); CI(L): cingulate gyrus (left); CI(R): cingulate gyrus (right); ST(L): striatum (left); ST(R): striatum (right); F(L): frontal lobe (left); F(R):frontal lobe (right); MT(L): mesial temporal lobe (left); MT(R): mesial temporal lobe (right); O(L):occipital lobe (left); O(R): occipital lobe (right); P(L): parietal lobe (left); P(R): parietal lobe (right); PR(L): precuneus (left); PR(R): precuneus (right); T(L): temporal lobe (left); T(R): temporal lobe (right).

Surface Antibodies Group

Figure 8 presents a heat map with the results of the SD values obtained for patients with surface antibodies. Red color shows areas of significant hypermetabolism, and blue color shows areas of significant hypometabolism. We can observe that there are many regions with altered metabolism in the patient's brain with many areas of hypermetabolism and hypometabolism. In the second PET/CT, some regions changed from hypermetabolic to normal or hypometabolic. For example, we can observe patient P6, who expressed hypermetabolism in the basal ganglia and mesial temporal lobe which changed to normal or hypometabolism in the second scan. There was one patient (P2) who presented hypermetabolism in the mesial temporal lobe on second scan which was not observed in the initial study.

For one patient with LGI1 antibodies (P10), hypermetabolism was observed in the central region and hypometabolism in the frontal and mesial temporal lobes in the initial image. The second study showed a similar pattern of metabolism. The patient with aquaporin-4 antibody (P11) showed many hypermetabolic areas in the basal ganglia, cingulate gyrus, striatum, mesial temporal lobe, and precuneus.

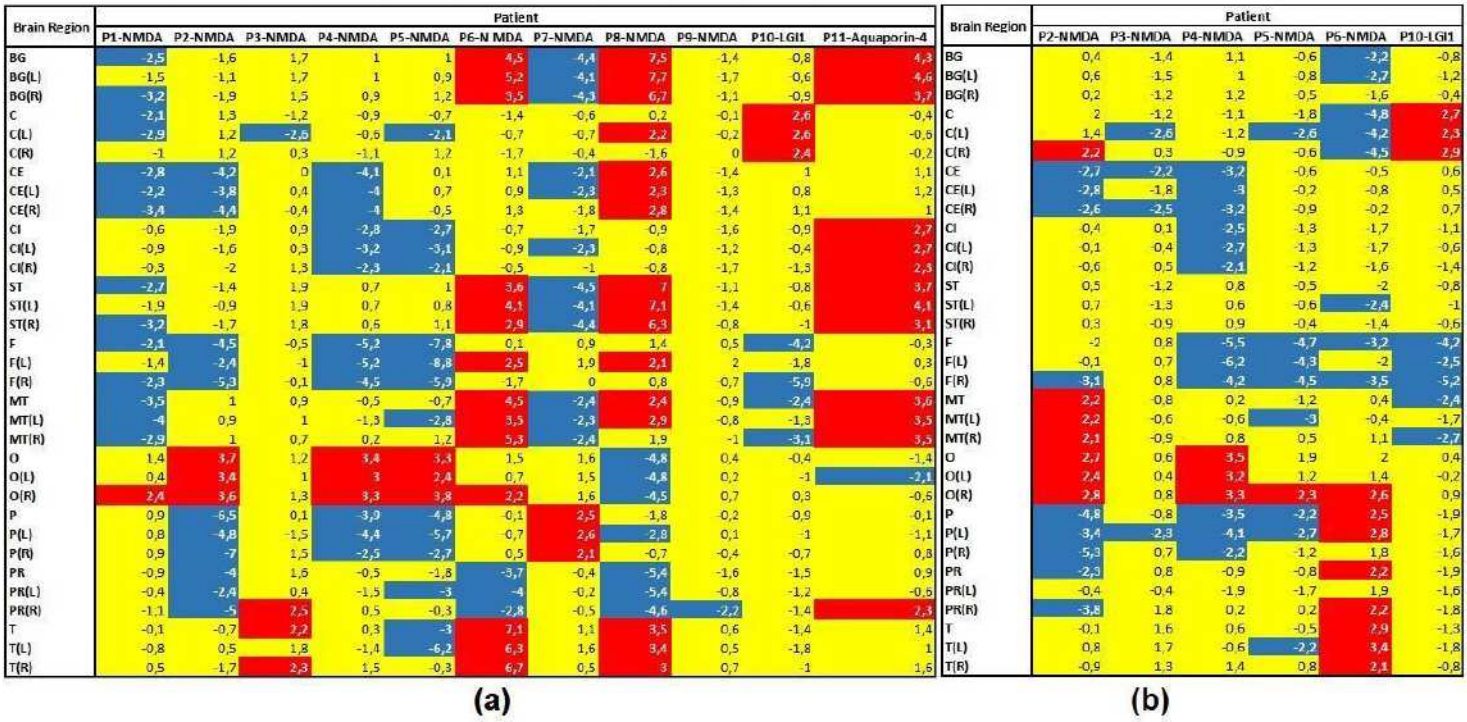

Brain Region	Patient										
	P1-NMDA	P2-NMDA	P3-NMDA	P4-NMDA	P5-NMDA	P6-N MDA	P7-NMDA	P8-NMDA	P9-NMDA	P10-LGI1	P11-Aquaporin-4
BG	-2,5	-1,6	1,7	1	1	4,5	-4,4	7,5	-1,4	0,8	4,3
BG(L)	-1,5	-1,1	1,7	1	0,9	5,2	-4,1	7,7	-1,7	-0,6	4,6
BG(R)	-3,2	-1,9	1,5	0,9	1,2	3,5	-4,3	6,7	-1,1	-0,9	3,7
C	-2,1	1,3	-1,2	-0,9	-0,7	-1,4	-0,6	0,2	-0,1	2,6	-0,4
C(L)	-2,9	1,2	-2,6	-0,6	-2,1	-0,7	-0,7	2,2	-0,2	2,6	-0,6
C(R)	-1	1,2	0,3	-1,1	1,2	-1,7	-0,4	-1,6	0	2,4	-0,2
CE	-2,8	-4,2	0	-4,1	0,1	1,1	-2,1	2,6	-1,4	1	1,1
CE(L)	-2,2	-3,8	0,4	-4	0,7	0,9	-2,3	2,3	-1,3	0,8	1,2
CE(R)	-3,4	-4,4	-0,4	-4	-0,5	1,3	-1,8	2,8	-1,4	1,1	1
CI	-0,6	-1,9	0,9	-2,8	-2,7	-0,7	-1,7	0,9	-1,6	-0,9	2,7
CI(L)	-0,9	-1,6	0,3	-3,2	-3,1	-0,9	-2,3	-0,8	-1,2	-0,4	2,7
CI(R)	-0,3	-2	1,3	-2,3	-2,1	-0,5	-1	-0,8	-1,7	-1,3	2,3
ST	-2,7	-1,4	1,9	0,7	1	3,6	-4,5	7	-1,1	-0,8	3,7
ST(L)	-1,9	-0,9	1,9	0,7	0,8	4,1	-4,1	7,1	-1,4	-0,6	4,1
ST(R)	-3,2	-1,7	1,8	0,6	1,1	2,9	-4,4	6,3	-0,8	-1	3,1
F	-2,1	-4,5	-0,5	-5,2	-7,8	0,1	0,9	1,4	0,5	-4,2	-0,3
F(L)	-1,4	-2,4	-1	-5,2	-8,8	2,5	1,9	2,1	2	-1,8	0,3
F(R)	-2,3	-5,3	-0,1	-4,5	-5,9	-1,7	0	0,8	-0,7	-5,9	-0,6
MT	-3,5	1	0,9	-0,5	-0,7	4,5	-2,4	2,4	-0,9	-2,4	3,6
MT(L)	-4	0,9	1	-1,3	-2,8	3,5	-2,3	2,9	-0,8	-1,3	3,5
MT(R)	-2,9	1	0,7	0,2	1,2	5,3	-2,4	1,9	-1	-3,1	3,5
O	1,4	3,7	1,2	3,4	3,4	1,5	1,6	-4,8	0,4	-0,4	-1,4
O(L)	0,4	3,4	1	3	2,4	0,7	1,5	-4,8	0,2	-1	-2,1
O(R)	2,4	3,6	1,3	3,3	3,8	2,2	1,6	-4,5	0,7	0,3	-0,6
P	0,9	-6,5	0,1	-3,9	-4,8	-0,1	2,5	-1,8	-0,2	-0,9	-0,1
P(L)	0,8	-4,8	-1,5	-4,4	-5,7	-0,7	2,6	-2,8	0,1	-1	-1,1
P(R)	0,9	-7	1,5	-2,5	-2,7	0,5	2,1	-0,7	-0,4	-0,7	0,8
PR	-0,9	-4	1,6	-0,5	-1,8	-3,7	-0,4	-5,4	-1,6	-1,5	0,9
PR(L)	-0,4	-2,4	0,4	-1,5	-3	-4	-0,2	-5,4	-0,8	-1,2	-0,6
PR(R)	-1,1	-5	2,5	0,5	-0,3	-2,8	-0,5	-4,6	-2,2	-1,4	2,3
T	-0,1	-0,7	2,2	0,3	-3	7,1	1,1	3,5	0,6	-1,4	1,4
T(L)	-0,8	0,5	1,8	-1,4	-6,2	6,3	1,6	3,4	0,5	-1,8	1
T(R)	0,5	-1,7	2,3	1,5	-0,3	6,7	0,5	3	0,7	-1	1,6

Brain Region	Patient					
	P2-NMDA	P3-NMDA	P4-NMDA	P5-NMDA	P6-NMDA	P10-LGI1
BG	0,4	-1,4	1,1	-0,6	-2,2	-0,8
BG(L)	0,6	-1,5	1	-0,8	-2,7	-1,2
BG(R)	0,2	-1,2	1,2	-0,5	-1,6	-0,4
C	2	-1,2	-1,1	-1,8	-4,8	2,7
C(L)	1,4	-2,6	-1,2	-2,6	-4,2	2,3
C(R)	2,2	0,3	-0,9	-0,6	-4,5	2,9
CE	-2,7	-2,2	-3,2	-0,6	-0,5	0,6
CE(L)	-2,8	-1,8	-3	-0,2	-0,8	0,5
CE(R)	-2,6	-2,5	-3,2	-0,9	-0,2	0,7
CI	-0,4	0,1	-2,5	-1,3	-1,7	-1,1
CI(L)	-0,1	-0,4	-2,7	-1,3	-1,7	-0,6
CI(R)	-0,6	0,5	-2,1	-1,2	-1,6	-1,4
ST	0,5	-1,2	0,8	-0,5	-2	-0,8
ST(L)	0,7	-1,3	0,6	-0,6	-2,4	-1
ST(R)	0,3	-0,9	0,9	-0,4	-1,4	-0,6
F	-2	0,8	-5,5	-4,7	-3,2	-4,2
F(L)	-0,1	0,7	-6,2	-4,3	-2	-2,5
F(R)	-3,1	0,8	-4,2	-4,5	-3,5	-5,2
MT	2,2	0,8	0,2	-1,2	0,4	-2,4
MT(L)	2,2	-0,6	-0,6	-3	-0,4	-1,7
MT(R)	2,1	-0,9	0,8	0,5	1,1	-2,7
O	2,7	0,6	3,5	1,9	2	0,4
O(L)	2,4	0,4	3,2	1,2	1,4	-0,2
O(R)	2,8	0,8	3,3	2,3	2,6	0,9
P	-4,8	-0,8	-3,5	-2,2	2,5	-1,9
P(L)	-3,4	-2,3	-4,1	-2,7	2,8	-1,7
P(R)	-5,3	0,7	-2,2	-1,2	1,8	-1,6
PR	-2,3	0,8	-0,9	-0,8	2,2	-1,9
PR(L)	-0,4	-0,4	-1,9	-1,7	1,9	-1,6
PR(R)	-3,8	1,8	0,2	0,2	2,2	-1,8
T	-0,1	1,6	0,6	-0,5	2,9	-1,3
T(L)	0,8	1,7	-0,6	-2,2	3,4	-1,8
T(R)	-0,9	1,3	1,4	0,8	2,1	-0,8

(a) (b)

Figure 8. Heat maps of the SD obtained for the group of patients with surface antibodies (NMDA, LGI1, and Aquaporin-4). (a) first PET/CT; (b) second PET/CT. Red: SD > 2.0 (hypermetabolism); blue: SD < 2.0 (hypometabolism); yellow -2.0 ≤ SD ≤ 2.0 (normal range). BG: basal ganglia (bilateral); BG(L): basal ganglia (left); BG(R): basal ganglia (right); C: central region (bilateral); C(L): central region (left); C(R): central region (right); CE: cerebellum (bilateral); CE(L): cerebellum (left); CE(R): cerebellum (right); CI: cingulate gyrus (bilateral); CI(L): cingulate gyrus (left); CI(R): cingulate gyrus (right); ST: striatum (bilateral); ST(L): striatum (left); ST(R): striatum (right); F: frontal lobe (bilateral); F(L): frontal lobe (left); F(R):frontal lobe (right); MT: mesial temporal lobe (bilateral) MT(L): mesial temporal lobe (left); MT(R): mesial temporal lobe (right); O: occipital lobe (bilateral); O(L):occipital lobe (left); O(R): occipital lobe (right); P: parietal lobe (bilateral); P(L): parietal lobe (left); P(R): parietal lobe (right); PR: precuneus (bilateral); PR(L): precuneus (left); PR(R): precuneus (right); T: temporal lobe (bilateral); T(L): temporal lobe (left); T(R): temporal lobe (right). The corresponding labeling of the brain regions is provided from Scenium software®.

Figure 9 presents the analysis of the standard mean value (SMV) for the group of NMDA patients in the first and in the second PET/CT. It is observed that basal ganglia, striatum, and temporal lobes changed from hypermetabolism to hypometabolism or normal metabolism in the second images. On the other hand, parietal lobes and precuneus changed from

hypometabolism to normal in the second PET/CT.

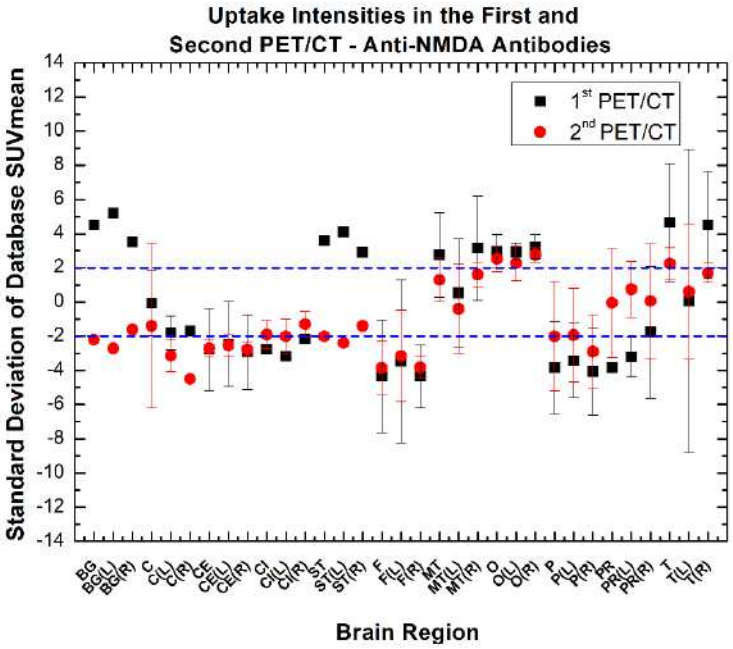

Figure 9. Scatter plots of the SMV for patients with anti-NMDA antibodies, in the first and second PET/CT.

Intracellular Antibodies Group

Regarding this group of patients, the Yo antibodies patients (n = 3) presented hypermetabolism in the basal ganglia, striatum, mesial temporal and temporal lobes, as well as a reduced FDG uptake in the frontal lobes and parietal lobes. In the second image of one patient (P12), some normal regions became hypometabolic (basal ganglia, striatum, and mesial temporal lobe), while the occipital and temporal lobes turned hypermetabolic.

One patient with Hu antibodies (P15) was characterized by FDG hypometabolism in most of the regions studied (basal ganglia, central region, cerebellum, striatum, frontal and parietal lobes). It was also observed hypermetabolism in the occipital lobe. In the second scan, a reduction of areas with hypometabolism in the basal ganglia, central region, and parietal lobe was detected.

In the first PET/CT image, patients with GAD antibodies (n = 2) presented hypermetabolism in the mesial temporal, basal ganglia, and occipital lobes. Hypometabolism was observed in the following regions: cingulate gyrus, frontal lobes, parietal lobes, and precuneus. Hypometabolism was observed in the frontal lobes, parietal lobes, and precuneus. The second scan of one patient (P16) showed mild change in metabolism such as a new hypometabolism in the left cerebellar hemisphere.

In one patient with amphiphysin (P18) there was hypermetabolism in the basal ganglia, striatum, and precuneus. Figure 10 presents the heat maps for this group of patients.

Brain Region	Patient						
	P12-Yo	P13-Yo	P14-Yo	P15-Hu	P16-GAD	P17-GAD	P18-Amphyphisin
BG	0,2	5,9	-1	-2,7	0,8	1,6	2
BG(L)	0,2	6,8	-1,1	-3,3	0,8	2,2	1,4
BG(R)	0,2	5	-0,7	-2,1	0,7	1	2,4
C	-1,2	-0,6	0,7	-3,5	0,4	-1,5	-3,9
C(L)	-0,8	-0,3	1,2	-3,1	0,5	-1	-6,1
C(R)	-1,6	-0,8	0,1	-3,6	0,2	-1,9	-0,8
CE	0,2	-0,8	-0,4	-2,4	-0,6	1,5	-4,8
CE(L)	-0,1	-1,2	-0,4	-1,8	-1	1,3	-2,1
CE(R)	0,5	-0,4	-0,3	-2,8	-0,1	1,6	-7,1
CI	-1,3	1	-0,1	-1,4	-0,4	-2	-1,2
CI(L)	-1	1	-0,7	-1,5	-0,2	-0,9	-1,9
CI(R)	-1,5	1	0,4	-1,2	-0,6	-2,9	-0,6
ST	0,2	5,5	-0,8	-2,5	0,8	1,3	2,1
ST(L)	0,2	6,3	-1,2	-3	0,9	1,8	1,4
ST(R)	0,1	4,6	-0,4	-2	0,6	0,7	2,5
F	-3,8	-4,2	0,4	-5,3	-5,3	-8,9	-5,7
F(L)	-2,4	-3,4	0,6	-6,3	-4,4	-7,1	-11,8
F(R)	-4,6	-4,4	0,2	-3,7	-5,4	-9,3	0,6
MT	-0,6	3,1	-1,4	-0,3	1,6	3,8	-1
MT(L)	-0,4	3,3	-2,3	-0,3	2,2	3,6	-0,6
MT(R)	-0,8	2,6	-0,5	-0,3	0,8	3,6	-1,2
O	-0,1	-1	0,7	2,4	1,7	2,2	-0,9
O(L)	0,1	-1,2	0,6	2,1	1,4	2	-1,9
O(R)	-0,4	-0,6	0,8	2,3	1,8	2,2	0,2
P	-1,5	-2,6	1,2	-3,6	-3,9	-5,5	-4,8
P(L)	-0,9	-2,5	1,1	-3,1	-4,2	-4,3	-9,2
P(R)	-1,7	-2,1	1,1	-3,3	-2,6	-5,5	0,8
PR	1	-0,3	0,6	-1,1	-0,4	-2,6	-0,5
PR(L)	0,9	-0,6	0	-1,8	-2,1	-2,1	-3,8
PR(R)	0,9	0	1,1	-0,3	1,2	-2,5	2,6
T	-1,4	-0,7	2,2	0	0,1	0	-2,3
T(L)	-1	-0,4	2	-0,4	1	0,4	-4,6
T(R)	-1,6	-0,9	2	0,3	-0,6	-0,3	-0,3

(a)

Brain Region	Patient			
	P14-Yo	P15-Hu	P16-GAD	P18-Amphyphisin
BG	-2,2	-1,5	0,9	1,2
BG(L)	-2,6	-2,2	1	0,8
BG(R)	-1,7	-0,9	0,8	1,5
C	-0,2	-2,5	1,3	-0,6
C(L)	0	-1,6	0,6	-2,8
C(R)	-0,4	-3,2	2	2,2
CE	-1,9	-1,1	-1,1	-6,9
CE(L)	-2	-0,5	-2,1	-4,7
CE(R)	-1,7	-1,6	-0,1	-8,6
CI	-1,1	-1	0,6	-1,2
CI(L)	-1,6	-0,9	0,6	-1,7
CI(R)	-0,4	-1,1	0,6	-0,7
ST	-2,1	-1,4	0,7	1,3
ST(L)	-2,7	-2	0,8	0,8
ST(R)	-1,4	-0,8	0,6	1,5
F	-1,7	-4,1	-5,1	-6,2
F(L)	-1,7	-4,4	-4,3	-10,5
F(R)	-1,4	-3,2	-5,2	-1,6
MT	-2,6	0,7	2,1	-2,6
MT(L)	-3,7	1	1,9	-3,2
MT(R)	-1,4	0,4	2,1	-1,8
O	2,2	1,7	1,6	0,3
O(L)	2	1,8	1,6	-0,1
O(R)	2,3	1,3	1,5	0,6
P	0,1	-2,7	-2	-4
P(L)	0,1	-1,7	-2,5	-6,8
P(R)	0,1	-3,2	-1,1	-0,1
PR	-0,4	-1,5	0,3	-1
PR(L)	-0,4	-1,9	-1,1	-3,8
PR(R)	-0,4	-0,8	1,6	1,8
T	2,2	1,1	-0,2	-1,8
T(L)	1,7	1,5	0	-3,4
T(R)	2,4	0,8	-0,3	-0,4

(b)

Figure 10. Heat maps of the SD obtained for patients with intracellular antibodies (Yo, Hu, GAD, and amphiphysin). (a) first PET/CT; (b) second PET/CT. Red: SD > 2.0 (hypermetabolism); blue: SD < 2.0 (hypometabolism); yellow -2.0 ≤ SD ≤ 2.0 (normal range). BG: basal ganglia (bilateral); BG(L): basal ganglia (left); BG(R): basal ganglia (right); C: central region (bilateral); C(L): central region (left); C(R): central region (right); CE: cerebellum (bilateral); CE(L): cerebellum (left); CE(R): cerebellum (right); CI: cingulate gyrus (bilateral); CI(L): cingulate gyrus (left); CI(R): cingulate gyrus (right); ST: striatum (bilateral); ST(L): striatum (left); ST(R): striatum (right); F: frontal lobe (bilateral); F(L): frontal lobe (left); F(R):frontal lobe (right); MT: mesial temporal lobe (bilateral) MT(L): mesial temporal lobe (left); MT(R): mesial temporal lobe (right); O: occipital lobe (bilateral); O(L): occipital lobe (left); O(R): occipital lobe (right); P: parietal lobe (bilateral); P(L): parietal lobe (left); P(R): parietal lobe (right); PR: precuneus (bilateral); PR(L): precuneus (left); PR(R): precuneus (right); T: temporal lobe (bilateral); T(L): temporal lobe (left); T(R): temporal lobe (right). The corresponding labeling of the brain regions is provided from Scenium software®.

Statistical Analysis

All patients

According to the Kruskall-Wallis test (Table 9), there were 15 regions with statistical difference in the first PET/CT. In the second PET/CT, there were 10 regions with statistical difference among patients. In the initial PET/CT, significant differences have been found for central region, cerebellum, cingulate gyrus, precuneus, frontal, parietal, mesial temporal and temporal lobes, pointing out the heterogeneity of the disease depending on the antibodies found. The p-values depicted were corrected according to the Bonferroni's Analysis.

Table 9: Kruskall-Wallis statistics applied to all patients clinically diagnosed with AE in the first and in the second PET/CT.

Brain Region	1st PET/CT			2nd PET/CT		
	χ^2	Freedom Degrees	p-value	χ^2	Freedom Degrees	p-value
Basal Ganglia (total)	12.59	8	0.13	9.00	6	0.17
Basal Ganglia (left)	12.63	8	0.12	8.66	6	0.19
Basal Ganglia (right)	13.08	8	0.11	9.10	6	0.17
Central Region (total)	17.32	8	*0.03	16.25	6	*0.04
Central Region (left)	20.49	8	*0.01	9.20	6	0.13
Central Region (right)	18.04	8	*0.02	15.24	6	0.06
Cerebellum (total)	14.88	8	0.07	16.18	6	*0.04
Cerebellum (left)	12.20	8	0.15	7.44	6	0.25
Cerebellum (right)	18.01	8	*0.02	17.21	6	*0.02
Cingulate and Paracingulate Gyri (total)	13.83	8	0.09	7.12	6	0.28
Cingulate and Paracingulate Gyri (left)	16.53	8	*0.04	16.15	6	*0.04
Cingulate and Paracingulate Gyri (right)	13.93	8	0.08	7.03	6	0.26
Corpus Striatum (total)	12.78	8	0.12	8.95	6	0.15
Corpus Striatum (left)	12.37	8	0.14	8.84	6	0.16
Corpus Striatum (right)	12.01	8	0.15	8.93	6	0.15
Frontal Lobe (total)	20.43	8	*0.01	16.98	6	*0.03
Frontal Lobe (left)	20.78	8	*0.01	15.21	6	0.06
Frontal Lobe (right)	21.25	8	*0.02	15.94	6	*0.05
Mesial Temporal Lobe (total)	14.73	8	0.07	16.31	6	*0.04
Mesial Temporal Lobe (left)	13.43	8	0.16	8.94	6	0.10
Mesial Temporal Lobe (right)	18.06	8	*0.04	16.95	6	*0.03
Occipital Lobe (total)	13.14	8	0.11	14.82	6	0.06
Occipital Lobe (left)	14.77	8	0.07	15.89	6	*0.05
Occipital Lobe (right)	12.97	8	0.10	8.79	6	0.17
Parietal Lobe (total)	17.53	8	*0.03	8.86	6	0.16
Parietal Lobe (left)	20.22	8	*0.01	15.91	6	*0.05
Parietal Lobe (right)	17.28	8	*0.03	6.95	6	0.29
Precuneus (total)	12.61	8	*0.13	8.80	6	0.14
Precuneus (left)	17.76	8	0.05	15.30	6	0.06
Precuneus (right)	16.62	8	*0.04	14.25	6	0.08
Temporal Lobe (total)	20.57	8	*0.01	13.97	6	0.09
Temporal Lobe (left)	18.54	8	*0.02	13.54	6	0.11
Temporal Lobe (right)	14.73	8	0.07	6.15	6	0.39

* Statistically significant values.

Surface x Intracellular Group

Regarding the comparison of these groups of patients, it was observed that in both scans the patients with intracellular antibodies tend to express a higher number of hypometabolic regions, being their hypometabolism more intense when compared to the surface group, especially in frontal and parietal lobes.

For the first scan, comparing the patients with surface and intracellular antibodies

using the Paired t-Test, given the Gaussian nature of data, it was found a p-value = 0.007 point out a significant difference between these groups (**Table 10**). The mean value of the SD considering all 33 regions evaluated (μ) also revealed the higher intensity of hypometabolism in the intracellular group (μ = -1.14, against μ = -0.35 for the surface group). Among the parameters with higher statistical differences, the frontal lobes showed the higher discrepancy and lower values in both groups, more accentuated in the intracellular antibodies. The cerebellum has an important difference between the groups, with values around 1.01 for surface and -2.05 for intracellular group. The occipital lobes are one of the few areas with positive values in both groups, that are still lower in the intracellular antibodies (around 2.11 in surface, and 0.97 in intracellular). Despite this area being treated with careful due to possibility of visual stimuli during the rest period, the values are still lower in intracellular group.

In the second scan, p = 0.0004 point out a more significant difference between intracellular and surface groups than in the first one (**Table 10**). The mean values of parameters were μ = -0.82 for surface and μ = -1.17 for the intracellular group. The brain areas with higher differences were: cerebellum (μ = -2.69 for intracellular and μ = -1.41 for the surface group); frontal lobes (μ = -5.22 for intracellular and μ = -2.40 for the surface group), being the group of higher discrepances. The cingulate gyri are regions where these characteristics invert, being the intracellular group less hypometabolic than the surface one (μ = -0.67 for intracellular and μ = -1.15 for the surface group). The occipital lobes keep the same pattern than in the first scan (μ = 1.45 for intracellular and μ = 1.85 for the surface group).

Table 10: P-values from the comparison between the groups of patients with surface and intracellular antibodies in the first and second PET/CT.

	P-Values	
Antibodies	**1st PET/CT**	**2nd PET/CT**
Surface x Intracellular	0,007	0,0004

Regarding these groups of patients, the Spearman's correlation analysis revealed very strong positive correlation between striatum and mesial temporal lobe, as well as between frontal lobe and central region both in first and second PET/CT. The central region had also a strong positive correlation with the cerebellum in the first exam, which became moderated in the second one. On the other hand, moderate negative correlations were identified between the striatum and cingulate gyri in the first PET/CT, and between this region and the cerebellum in

the second scan. Table 11 summarize the results described in this section.

Table 11: Summary of the Spearman's correlation analyses highlighting the significant results.

1st PET/CT				2nd PET/CT			
Brain Area	**ρ**	**p-value**	**Status**	**Brain Area**	**ρ**	**p-value**	**Status**
ST ↔ MT	+0.942	<0.001	Very Strong	ST ↔ MT	+0.928	0.0001	Very Strong
C ↔ F	+0.918	0.0002	Very Strong	C ↔ F	+0.885	0.0006	Strong
CE ↔ C	+0.812	0.0031	Strong	CE ↔ C	+0.742	0.0081	Moderate
CI ↔ ST	-0.421	0.1542	Moderate	CI ↔ CE	-0.621	0.031	Moderate

DISCUSSION

The present study demonstrated the important role of FDG-PET/CT to detect metabolism alterations on brain images in AE patients. All patients presented brain metabolism alterations on PET images. FDG-PET/CT showed many areas of hypermetabolism and hypometabolism, both in the visual analysis and in the quantitative analysis. In visual analysis, it was identified 65 areas of hypermetabolism and 39 areas of hypometabolism in the first scan. On the other hand, in quantitative analysis it was identified 102 areas of hypermetabolism and 182 areas of hypometabolism in the first FDG-PET/CT. It is interesting to observe that almost brain pathologies lead to hypometabolic areas in FDG-PET/CT (e.g. Alzheimer disease, a frontal-temporal neurodegeneration). Encephalitis is one of the few pathologies which leads to hypermetabolic areas in FDG-PET/CT, despite the also high incidence of hypometabolism.

We observed that the group with intracellular antibodies lead to higher magnitude of hypometabolism in different brain regions. Hypometabolism may be due to the aggressive reaction of lymphocytes (e.g. CD8+) to destroy fragments of intracellular antigens, leading to cellular death. The death of neurons tends to reduce the metabolism in different brain areas, which is also a reason why the immunotherapy is not so effective in these cases (10, 41). Hypometabolism may occurs locally due to the death of cells, reducing the activity of the tissue and also in areas for which the activity depends on the signaling from the tissues where cellular death occurred (21). On the other hand, the presence of surface antibodies leads to inflammatory process (e.g. astrocytosis and microgliosis), where the cellular activity increases to fight the antibodies. In addition, these antibodies may attack inhibitory neurons, leaving the excitatory cells out of control, which may result in epileptic seizures, for example (10). In this FDG-

PET/CT analysis, hypermetabolic areas were found mainly in case of surface antibodies, as such as NMDA.

The quantitative analysis highlights the prevalence of frontal and parietal hypometabolism both in the first and in the second image, mainly in patient with psychiatric disorders refractory to therapies. On the other hand, the basal ganglia, central region and temporal lobe hypermetabolism has been seen in patients with epileptic seizures. In case of patients with ataxia and other motor disorders, patterns of hypermetabolism or hypometabolism has been detected, depending on the stage of the disease and the therapies applied. Considering the patients that have two scans, both the number of hypometabolic and hypometabolic regions reduced in the second image, pointing out the possible positive effect of the therapies.

The group of patients with surface antibodies expressed in the first PET/CT hypermetabolism mainly in the basal ganglia, striatum, and temporal lobe, with hypometabolism in the frontal lobe. Some of these patients presented both epileptic seizures and behavior disorders, which may be correlated with the imaging findings. In the second scan, the hypermetabolic areas tend to normal, but the frontal hypometabolism remained, going towards the clinical manifestations of the patients (some of them with control of epileptic seizures, maintaining the psychiatric disorders). These findings show the potential of the FDG-PET/CT to characterize AE due with the presence of surface antibodies.

Regarding the patients with intracellular antibodies, there is a prevalence of hypometabolism in frontal and parietal lobes in both scans. In the second scan, the hypometabolism of these remained, added to the cerebellum. These findings were seen mainly in patients with cerebellar ataxia and movement disorders added to behavior changes. The fact of the hypometabolic pattern practically does not change in the second PET/CT is an important signature of intracellular antibodies, given that this presence is related to death of neuronal cells that do not recovery with therapies. In addition, when compared to surface antibodies, the metabolism of most of brain regions showed lower for intracellular antibodies, even in the normal range of SD. In the literature, there is no specific FDG-PET/CT studies focused on the characterization of the FDG metabolism in case of surface and intracellular antibodies. An exception is the article of Watanabe et. al. that brings some FDG-PET/CT findings (20).

The most robust group was the NMDA group with nine patients (24%). FDG-PET/CT showed many areas of hypermetabolism an hypometabolism. In the literature, the basal ganglia and temporal lobe hypermetabolism has been reported both for children and adults. The

findings of Turpin et. al. revealed the basal ganglia hypermetabolism in 26.5 % of the patients from visual analysis and in 82.3% from statistical ones (8); the studies of Yuan (42), Probasco (25), and Tripathi (43) corroborate with these findings. In the present study, the visual analysis revealed basal ganglia hypermetabolism in 22% of the patients in the first PET/CT image, similar to literature visual analysis. For these patients, temporal lobe hypermetabolism has also been highlighted in the work of Wegner (44), Probasco (25), Moreno-Estébanez (45), and Baumgartner (36). The superior temporal lobes and cingulate gyrus hypermetabolism is also described by Probasco et. al. (25).

Unlike the literature, the present study found a discretely higher occurrence of NMDA in men (55% of cases), while most articles mentioned women as a population of higher incidence of this antibody (8, 15, 36). The work of Kerik-Rotenberg et. al. is an exception, presenting a population distribution of cases analogous to this study (higher incidence of NMDA antibodies in men) (19).

Not all patients studied had an MRI scan. Nevertheless, the MRI findings corroborate to characterize the brain anatomical changes related to the disease, despite thickening and atrophy were found throughout the whole group of patients. The hippocampal atrophy is present in most of patients manifesting epilepsy and hippocampal hypermetabolism, while cerebellar atrophy is highlighted in patients with cerebellar ataxia and hypometabolism in this brain region. The diffuse cortical volumetric reduction goes against the hypometabolism observed in the FDG-PET/CT

AE is a condition oftentimes expressed as PNS, being highly specific antineuronal antibodies (e.g., anti-Hu, anti-Yo, anti-Ma/Ta) detected in about 60% of patients, according to the literature (46-48). The variety of metabolic patterns previously reported for NMDA antibodies has been attributed to cryptogenic, viral or paraneoplastic causes (15, 24, 49). The most commonly found tumor in literature is the small cell lung cancer (SCLC), followed by the ovarian teratoma and other ovarian tumors (46, 50, 51). Interestingly, the neurological signs can precede the tumor detection in some years (46, 51). In the review paper we published, the incidence of neoplasm detected by PET/CT in literature was 18.2% (7). In the present study, we detected just two cases of neoplasm found among the patients (5.4%). One case of breast cancer and one of prostate cancer. These two tumors were also presented in literature reviews (7). Besides, there were two occurrences of tumors many years before the beginning of the AE manifestations. One patient which had a breast cancer 5 years before the AE diagnosis may

have a relation with encephalitis, however, the other patient who had a thyroid cancer 12 years before, probably did not had a relation with AE. Most of author consider that the cancer is related to encephalitis if occurs up to 5 years after the symptoms onset (in this case, a PNS is active) (11, 52). Nevertheless, recent studies expand this window to 9 years (53, 54). One possible reason to the finding of a very low prevalence of neoplasm detected by PET/CT, could be that most patients were referred to perform PET/CT in order to find a neoplasm. But all patients had investigation of neoplasm with other images modalities before PET/CT such as computed tomography. This may introduce a bias in our sample.

Even when the antibodies test is negative or for untested patients, FDG-PET/CT images had a relevant role to characterize the brain areas most harmed by disease. According to Graus et al., the AE investigation is based on clinical examination associated or not with laboratory tests (including blood, urine, cerebrospinal fluid—CSF), and magnetic resonance imaging (MRI) (6, 13). Nowadays, many types of antibodies have been associated with the disease. Some standards of ^{18}F-FDG uptake have been related to negative antibodies (55) and a new radiopharmaceutical, ^{18}F-DPA714 has been studied as a marker for the AE without detection of antibodies (56). This tracer binds to the Translocator Protein 18 kDa (TSPO), a marker for microglia injury commonly identified in these patients.

The Kruskall-Wallis statistical test applied for all AE patients revealed that the group of patients clinically diagnosed with AE presents different patterns of FDG uptake in several brain areas. In a first approach, these findings go toward the variety of clinical manifestations reported among the group, in the first and in the second PET/CT. It is possible to consider that the reduction in the number of brain areas statistically distinct in the second scan (10 areas and were 16 areas on first PET/CT) may be due to the therapy effect, leading the patients from pathological to normal FDG uptake pattern.

The pairwise comparison between the groups results in significative differences between intracellular and surface antibodies, both in the first ($p = 0.007$) and in the second PET/CT ($p = 0.0004$). Comparing surface and intracellular antibodies, the correlation analysis of the FDG uptake in different brain regions identified very strong between striatum and mesial temporal lobes in both PET/CT scans, for which a strong correlation between central region and frontal lobes, and a moderate correlation between cerebellum and central region has also been found. In addition, moderate correlations between cingulate gyri and striatum, and cingulate gyri and cerebellum were found in the first and second image, respectively. The correlation between the

metabolic FDG uptake may suggest the pattern of brain connectivity expressed in the disease. The mean value of the SMV for each brain region (μ) revealed a higher intensity of hypometabolism in the intracellular group (μ = -1.14) against for the surface group (μ = -0.35). This may be explained by a more destructive mechanism for intracellular antibodies disease leading to neurons death and a poor prognosis than surface antibodies disease.

We cannot compare the number of altered metabolic areas on visual analysis and quantitative analysis since the division of number of areas analyzed were higher on quantitative analysis than visual analysis. The objective of the present study was not comparing these two analyses. Moreover, the present study found a bigger proportion of hypermetabolic areas on visual analysis than on quantitative analysis. We make the hypothesis that this occurred because the eyes are more sensible to detect hypermetabolism than hypometabolism which sometimes can be very mild and only detectable by quantitative analysis.

For clinical neurologists, the metabolic characterization of the disease with PET/CT, can help choosing the best therapeutic approach for each kind of the disease, which can reduce the occurrence of brain damages due to long-time exposition to the inflammatory response. Furthermore, the cost to the public and private health systems tends to be minimized with more effective drugs applied in the first moment, and could result in better clinical outcomes.

The present study has some limitations. The mean time between the symptoms onset and the first FDG-PET/CT image was relatively high due to be a retrospective study and PET/CT do not take part in diagnosis guidelines for EA. Another limitation is the fact that some groups of antibodies are composed by few patients, corresponding to the lower incidence of some types of them (e.g. Hu, amphiphysin, aquaporin-4), as also seen in the literature (16, 36, 43, 45, 57). This did not allow us to perform a statistical analysis of the PET/CT findings among different types of antibodies. Other limitations are related to the retrospective approach of the study, implying eventual bias related to clinical data recording. Another limitation is that antibodies were not tested for all patients because were not available for all patient. Our institution has limited access to antibody tests as well as other institutions around the world (5, 58-60). FDG-PET/CT should be performed with EEG monitorization ideally in order to detect subclinical epileptic seizures or frequently discharges which could lead to hypermetabolism, however this has a rare occurrence.

This research has many strengths considering the present aim, focused on the daily clinical practice. In short, AE is a complex systemic and rapidly debilitating disease, expressed

in different clinical manifestations depending on the antibodies involved. The results reached in this research pointed out the relevance of the FDG-PET/CT to improve the comprehension of the brain metabolism for different antibodies, in different stages of the disease.

CONCLUSION

This study characterized the groups of patients clinically diagnosed with AE. Depending on the type of antibodies, specific brain areas expressed hypermetabolism or hypometabolism, both in the first and in the second scan. The pattern of the FDG uptake in different brain areas is related to the main clinical manifestations of the patients (epilepsy, psychiatric alterations and movement disorders). All patients underwent FDG-PET/CT, with integrated systematization of the metabolic dimensions of the clinical, visual, quantitative, and statistical analyses, offering a proper connection with the main symptoms.

FDG-PET/CT has a high potential to detect brain metabolism alterations showing many areas of brain hypermetabolism and hypometabolism alterations. Alterations in FDG-PET/CT occurred throughout the studied population, supporting its relevance as a predictive functional marker in AE. Therefore, FDG-PET/CT could be used in clinical practice to confirm AE.

The finding of brain hypermetabolism was more prevalent than hypometabolism in visual analysis, and due to its unusual occurrence in other pathologies, AE hypothesis should be made. The hypermetabolic findings configure a relevant metabolic signature of the disease.

A significant distinction occurred between surface and intracellular antibodies, suggesting different pathophysiological impacts. Hypometabolism was more prevalent in intracellular antibodies group, which could be related to the greater severity of this antibody.

The whole-body FDG-PET/CT identified few cases of neoplasm of unknown origin throughout the study in the present group (N = 2, 5.4%). Nevertheless, this technique should still be considered as a relevant method to detection and follow-up of different types of neoplasia. Further prospective studies, with a larger number of patients, should contribute to establishing PET/CT as an effective tool to reveal different metabolic signatures of AE.

FUTURE PERSPECTIVES

When compared to MRI and other imaging techniques, FDG-PET/CT is a method that has allowed the identification of brain alterations related to AE, both visually and statistically. Depending on the etiology of the disease, presence of specific antibodies and other factors, the FDG uptake may change in different levels, leading to a precise metabolic characterization of the condition. Studies applying the radiopharmaceuticals developed, as such as ^{18}F-Flortaucipir and ^{18}F-DPA714 may lead to the detailed metabolic characterization of different manifestations of the disease.

REFERENCES

1. Oppenheim H. Über Hirnsymptome bei Carcinomatose ohne nachweisbare Veränderungen im Gehirn. Charité-Annalen (Berlin). 1888;13:335-44.
2. Brierley JB, Corsellis JAN, Hierons R, Nevin S. Subacute Encephalitis of Later Adult Life Mainly Affecting the Limbic Areas. Brain. 1960;83(3):357-68.
3. Corsellis JAN, Goldberg GJ, Norton AR. "Limbic Encephalitis" and its Association with Carcinoma. Brain. 1968;91(3):481-96.
4. Machado S, Pinto A, Irani S. What Should You Know About Limbic Encephalitis? Arquivos de neuro-psiquiatria. 2012;70(10):817-22.
5. Patel A, Meng Y, Najjar A, Lado F, Najjar S. Autoimmune Encephalitis: A Physician's Guide to the Clinical Spectrum Diagnosis and Management. Brain sciences. 2022;12(9).
6. Graus F, Titulaer M, Balu R, Benseler S, Bien C, Cellucci T, et al. A Clinical Approach to Diagnosis of Autoimmune Encephalitis. Lancet Neurol. 2016;15(4):391-404.
7. Baldissin M, de Souza E, Watanabe N, Etchebehere E, Cendes F, Amorim B. FDG–PET in patients with autoimmune encephalitis: a review of findings and new perspectives. Clinical and Translational Imaging. 2023;12:15-30.
8. Turpin S, Martineau P, Levasseur M-A, Meijer I, Décarie J-C, Barsalou J, et al. ^{18}F-Flurodeoxyglucose positron emission tomography with computed tomography (FDG PET/CT) findings in children with encephalitis and comparison to conventional imaging. European Journal of Nuclear Medicine and Molecular Imaging. 2019;46(6):1309-24.
9. Linke R, Schroeder M, Helmberger T, Voltz R. Antibody-positive paraneoplastic neurologic syndromes: value of CT and PET for tumor diagnosis. Neurology. 2004;63(2):282-6.
10. Dalmau J, Graus F. Antibody-Mediated Encephalitis. The New England journal of medicine. 2018;378(9).
11. Graus F, Delattre J, Antoine J, Dalmau J, Giometto B, Grisold W, et al. Recommended diagnostic criteria for paraneoplastic neurological syndromes. Journal of neurology, neurosurgery, and psychiatry. 2004;75(8).
12. Geis C, Planagumà J, Carreño M, Graus F, Dalmau J. Autoimmune seizures and epilepsy. 2019.
13. Dutra L, Silva P, Ferreira J, Marques A, Toso F, Vasconcelos C, et al. Brazilian consensus recommendations on the diagnosis and treatment of autoimmune encephalitis in the adult and pediatric populations. Arquivos de neuro-psiquiatria. 2024;82(7).
14. Solnes LB, Jones KM, Rowe SP, Pattanayak P, Nalluri A, Venkatesan A, et al. Diagnostic Value of ^{18}F-FDG PET/CT Versus MRI in the Setting of Antibody-Specific Autoimmune Encephalitis. 2017.
15. Probasco JC, Solnes L, Nalluri A, Cohen J, Jones KM, Zan E, et al. Abnormal brain metabolism on FDG-PET/CT is a common early finding in autoimmune encephalitis. 2017.
16. Moreno-Ajona D, Prieto E, Grisanti F, Esparragosa I, Orduz LS, Pérez-Larraya JG, et al. ^{18}F-FDG-PET Imaging Patterns in Autoimmune Encephalitis: Impact of Image Analysis on the Results. Diagnostics. 2020;10(6):356.
17. Gibson LL, McKeever A, Coutinho E, Finke C, Pollak TA. Cognitive impact of neuronal antibodies: encephalitis and beyond. Translational Psychiatry. 2020;10(1):1-17.
18. Dale R, Merheb V, Pillai S, Wang D, Cantrill L, Murphy T, et al. Antibodies to Surface Dopamine-2 Receptor in Autoimmune Movement and Psychiatric Disorders. Brain: a journal of neurology. 2012;135(Pt 11).
19. Kerik-Rotenberg N, Diaz-Meneses I, Hernandez-Ramirez R, Muñoz-Casillas R, Reynoso-Mejia C, Flores-Rivera J, et al. A Metabolic Brain Pattern Associated With Anti-N-Methyl-D-Aspartate Receptor Encephalitis. Psychosomatics. 2020;61(1).
20. Watanabe N, Lizcano A, Araujo T, Barbosa R, Alvim M, Vieira A, et al. Neuronal surface and intracellular antibody testing in patients with long-term epilepsy. Epilepsia Open. 2025;10(5):1373.
21. Morita A, Kamei S. Limbic encephalitis with antibodies against intracellular antigens. Brain and nerve = Shinkei kenkyu no shinpo. 2010;62(4).
22. Mahale RR, Rajeevan S, Sivaprakash S, Padmanabha H, Mailankody P, Mathuranath P. Anti-GAD antibodies associated autoimmunity presenting as isolated dementia: an expansion of GAD antibody-spectrum disorders. Acta Neurologica Belgica. 2022:1-3.

23. Graus F, Keime-Guibert F, Reñe R, Benyahia B, Ribalta T, Ascaso C, et al. Anti-Hu-associated paraneoplastic encephalomyelitis: analysis of 200 patients. Brain: a journal of neurology. 2001;124(Pt 6):1138-48.
24. Nissen M, Ørvik M, Nilsson A, Ryding M, Lydolph M, Blaabjerg M. NMDA-receptor encephalitis in Denmark from 2009 to 2019: a national cohort study. Journal of neurology. 2021.
25. Probasco J, Solnes L, Nalluri A, Cohen J, Jones K, Zan E, et al. Decreased occipital lobe metabolism by FDG-PET/CT: An anti-NMDA receptor encephalitis biomarker. Neurology(R) neuroimmunology & neuroinflammation. 2017;5(1).
26. Dalmau J, Tüzün E, Wu H, Masjuan J, Rossi J, Voloschin A, et al. Paraneoplastic Anti-N-Methyl-D-Aspartate Receptor Encephalitis Associated with Ovarian Teratoma. Annals of neurology. 2007;61(1).
27. Leypoldt F, Buchert R, Kleiter I, Marienhagen J, Gelderblom M, Magnus T, et al. Fluorodeoxyglucose positron emission tomography in anti-N-methyl-D-aspartate receptor encephalitis: distinct pattern of disease. Journal of neurology, neurosurgery, and psychiatry. 2012;83(7).
28. Liguori R, Vincent A, Clover L, Avoni P, Plazzi G, Cortelli P, et al. Morvan's Syndrome: Peripheral and Central Nervous System and Cardiac Involvement with Antibodies to Voltage-Gated Potassium Channels. Brain: a journal of neurology. 2001;124(Pt 12).
29. Buckley C, Oger J, Clover L, Tüzün E, Carpenter K, Jackson M, et al. Potassium channel antibodies in two patients with reversible limbic encephalitis. Annals of neurology. 2001;50(1).
30. Ances B, Vitaliani R, Taylor R, Liebeskind D, Voloschin A, Houghton D, et al. Treatment-responsive limbic encephalitis identified by neuropil antibodies: MRI and PET correlates. Brain: a journal of neurology. 2005;128(Pt 8).
31. Sadaghiani M, Roman S, Diaz-Arias L, Habis R, Venkatesan A, Probasco J, et al. Comparison of quantitative FDG-PET and MRI in anti-LGI1 autoimmune encephalitis. Neuroradiology. 2023;65(8).
32. Shen K, Xu Y, Guan H, Zhong W, Chen M, Zhao J, et al. Paraneoplastic limbic encephalitis associated with lung cancer. Scientific reports. 2018;8(1).
33. Steriade C, Moosa A, Hantus S, Prayson R, Alexopoulos A, Rae-Grant A. Electroclinical features of seizures associated with autoimmune encephalitis. Seizure. 2018;60.
34. Irani S, Pettingill P, Kleopa K, Schiza N, Waters P, Mazia C, et al. Morvan Syndrome: Clinical and Serological Observations in 29 Cases. Annals of neurology. 2012;72(2).
35. McKeon A, Martinez-Hernandez E, Lancaster E, Matsumoto J, Harvey R, McEvoy K, et al. Glycine Receptor Autoimmune Spectrum with Stiff-Man Syndrome Phenotype. JAMA neurology. 2013;70(1):44-50.
36. Baumgartner A, Rauer S, Mader I, Meyer P. Cerebral FDG-PET and MRI findings in autoimmune limbic encephalitis: correlation with autoantibody types. Journal of neurology. 2013;260(11).
37. Malter M, Helmstaedter C, Urbach H, Vincent A, Bien C. Antibodies to glutamic acid decarboxylase define a form of limbic encephalitis. Annals of neurology. 2010;67(4).
38. Darnell R, Posner J. Paraneoplastic syndromes affecting the nervous system. Seminars in oncology. 2006;33(3).
39. Ricken G, Schwaiger C, De Simoni D, Pichler V, Lang J, Glatter S, et al. Detection Methods for Autoantibodies in Suspected Autoimmune Encephalitis. Frontiers in neurology. 2018;9.
40. Abbatemarco J, Yan C, Kunchok A, Rae-Grant A. Antibody-mediated autoimmune encephalitis: A practical approach. Cleveland Clinic journal of medicine. 2021;88(8).
41. Lancaster E, Martinez-Hernandez E, Dalmau J. Encephalitis and antibodies to synaptic and neuronal cell surface proteins. 2011.
42. Yuan J, Guan H, Zhou X, Niu N, Li F, Cui L, et al. Changing Brain Metabolism Patterns in Patients With ANMDARE: Serial ^{18}F-FDG PET/CT Findings. Clinical nuclear medicine. 2016;41(5):366-70.
43. Tripathi M, Tripathi M, Roy S, Parida G, Ihtisham K, Dash D, et al. Metabolic topography of autoimmune non-paraneoplastic encephalitis. Neuroradiology. 2018;60(2).
44. Wegner F, Wilke F, Raab P, Tayeb SB, Boeck A-L, Haense C, et al. Anti-leucine rich glioma inactivated 1 protein and anti-N-methyl-D-aspartate receptor encephalitis show distinct patterns of brain glucose metabolism in ^{18}F-fluoro-2-deoxy-d-glucose positron emission tomography. BMC Neurology. 2014;14.

45. Moreno-Estébanez A, Durán SB, Bilbao MM, Díaz-Cuervo I, Agirre-Beitia G, Martínez LC, et al. Autoimmune encephalitis and related disorders: A retrospective study of 43 cases in a tertiary hospital. Neurology Perspectives. 2021;1(4):197-205.
46. Crimì F, Camporese G, Lacognata C, Fanelli G, Cecchin D, Zoccarato M. Ovarian Teratoma or Uterine Malformation? PET/MRI as a Novel Useful Tool in NMDAR Encephalitis. In vivo (Athens, Greece). 2018;32(5):1231-3.
47. Dalmau J, Gleichman A, Hughes E, Rossi J, Peng X, Lai M, et al. Anti-NMDA-receptor encephalitis: case series and analysis of the effects of antibodies. The Lancet Neurology. 2008;7(12).
48. F G, JY D, JC A, J D, B G, W G, et al. Recommended diagnostic criteria for paraneoplastic neurological syndromes. Journal of neurology, neurosurgery, and psychiatry. 2004;75(8).
49. Zhao X. The different metabolic patterns of brain ^{18}F-FDG PET in anti-NMDA, anti-LGi-1 and anti-GABAb encephalitis. Journal of Nuclear Medicine. 2019;60(supplement 1):1475-.
50. Zaborowski M, Spaczynski M, Nowak-Markwitz E, Michalak S. Paraneoplastic neurological syndromes associated with ovarian tumors. Journal of cancer research and clinical oncology. 2015;141(1).
51. Silsby M, Clarke CJ, Lee K, Sharpe D. Anti-Hu limbic encephalitis preceding the appearance of mediastinal germinoma by 9 years. 2020;7(3).
52. Rees J. Paraneoplastic syndromes: when to suspect, how to confirm, and how to manage. Journal of neurology, neurosurgery, and psychiatry. 2004;75 Suppl 2(Suppl 2).
53. Silsby M, Clarke C, Lee K, Sharpe D. Anti-Hu limbic encephalitis preceding the appearance of mediastinal germinoma by 9 years. Neurology(R) neuroimmunology & neuroinflammation. 2020;7(3).
54. Falso S, Spagni G, Iorio R, Evoli A. Cancer detection after a 9-year course of Lambert-Eaton myasthenic syndrome complicated by anti-Hu associated limbic encephalitis. Neuromuscular disorders: NMD. 2023;33(9).
55. Deuschl C, Rüber T, Ernst L, Fendler W, Kirchner J, Mönninghoff C, et al. ^{18}F-FDG-PET/MRI in the diagnostic work-up of limbic encephalitis. PloS one. 2020;15(1).
56. Meng H, He L, Chunyu H, Zhou Q, Wang J, Qu Q, et al. ^{18}F-DPA714 PET/MRI as a potential imaging tool for detecting possible antibody-negative autoimmune encephalitis: a prospective study. Journal of neurology. 2024;271(12).
57. Matsuhisa A, Toriihara A, Kubota K, Makino T, Mizusawa H, Shibuya H. Utility of F-18 FDG PET/CT in Screening for Paraneoplastic Neurological Syndromes. Clinical Nuclear Medicine. 2012;37(1):39-43.
58. Liu X, Shan W, Zhao X, Ren J, Ren G, Chen C, et al. The Clinical Value of 18 F-FDG-PET in Autoimmune Encephalitis Associated With LGI1 Antibody. Frontiers in neurology. 2020;11.
59. Abboud H, Probasco J, Irani S, Ances B, Benavides D, Bradshaw M, et al. Autoimmune encephalitis: proposed recommendations for symptomatic and long-term management. Journal of neurology, neurosurgery, and psychiatry. 2021;92(8).
60. Ge J, Deng B, Guan Y, Bao W, Wu P, Chen X, et al. Distinct cerebral 18 F-FDG PET metabolic patterns in anti-N-methyl-D-aspartate receptor encephalitis patients with different trigger factors. Therapeutic advances in neurological disorders. 2021;14.

ATTACHMENTS

ATTACHMENT 1: ETHICAL COMISSION APPROVAL

PARECER CONSUBSTANCIADO DO CEP

DADOS DO PROJETO DE PESQUISA

Título da Pesquisa: ENCEFALITE AUTOIMUNE: CORRELAÇÃO CLÍNICA DO PET/CT-18FDG
Pesquisador: Bárbara Juarez Amorim
Área Temática:
Versão: 1
CAAE: 48731621.0.0000.5404
Instituição Proponente: Hospital de Clínicas da UNICAMP
Patrocinador Principal: Financiamento Próprio

DADOS DO PARECER

Número do Parecer: 4.878.196

Apresentação do Projeto:
As informações contidas nos campos "Apresentação do Projeto", "Objetivo da Pesquisa" e "Avaliação dos Riscos e Benefícios" foram obtidas dos documentos apresentados para apreciação ética e das informações inseridas pelo Pesquisador Responsável do estudo na Plataforma Brasil.

Introdução: A encefalite é uma condição inflamatória do encéfalo com diversas etiologias. Encefalite de causa viral é a mais comum, entretanto na última década foi detectado um crescente número de casos de encefalite não-viral, principalmente a encefalite de causa autoimune. O PET/CT é um método com diversas aplicações em neurologia, seja no diagnóstico, no planejamento de terapias, na definição de prognósticos e segmento das respostas do paciente. Dentre estas aplicações, pode-se mencionar a avaliação metabólica de tumores, a localização e a avaliação pré-cirúrgica do foco epileptogênico, avaliação do tecido cerebral na ocorrência de acidente vascular cerebral ou a sua predição (23-25), diagnóstico e segmento da evolução de demências (26-28), bem como a avaliação das desordens do movimento (29-31). No caso dos tumores cerebrais, é possível também a diferenciação entre tecidos tumorais ativos e áreas de necrose. Recentemente, o PET/CT com 18FDG (PET/CT-FDG) vem sendo empregado na avaliação da EA. O PET/CT-FDG com imagens de corpo inteiro tem o potencial para a investigação paraneoplásica em pacientes com EA. A realização de imagens de corpo inteiro nesses pacientes pode contribuir com a detecção de uma neoplasia desconhecida. Esse uso potencial do PET/CT-

Endereço: Rua Tessália Vieira de Camargo, 126
Bairro: Barão Geraldo **CEP:** 13.083-887
UF: SP **Município:** CAMPINAS
Telefone: (19)3521-8936 **Fax:** (19)3521-7187 **E-mail:** cep@fcm.unicamp.br

FDG ainda não foi descrito na literatura, sendo então abordado neste trabalho. Além disso, a maioria dos estudos anteriores se limitou à descrição qualitativa dos achados do PET, não realizaram imagens dedicadas de cérebro que possuem melhor resolução, foram restritos a síndromes específicas ou fizeram comparações limitadas com outros resultados diagnósticos incorporados nos critérios clínicos atuais.
O objetivo do presente trabalho é correlacionar os achados do PET/CT-FDG com os dados clínicos dos pacientes com EA, utilizando métodos qualitativos e quantitativos. Além disso, pretende-se avaliar a acurácia do exame na detecção de neoplasias de origem desconhecida nesses pacientes.

Objetivo da Pesquisa:

Objetivo Primário:

O objetivo do presente trabalho é correlacionar os achados do PET/CT-FDG com os dados clínicos dos pacientes com EA.

Objetivos Secundários:

- Avaliar a acurácia do PET/CT-FDG de corpo inteiro na detecção de neoplasia de origem desconhecida nos pacientes com EA.
- Analisar quantitativamente as imagens dedicadas de cérebro do PET/CT-FDG.

Avaliação dos Riscos e Benefícios:

Riscos: De acordo com os pesquisadores, por se tratar de um estudo retrospectivo com o emprego de imagens já adquiridas na rotina clínica, este estudo não apresenta riscos. Será assegurado, em todas as etapas do estudo, publicações ou apresentações, o sigilo em relação à identidade dos participantes.

Em relação aos benefícios, o principal benefício dessa pesquisa será a possibilidade de identificar alterações no PET/CT-18FDG que contribuam para o diagnóstico da EA. Isso poderá permitir, no futuro, uma melhor abordagem dos pacientes com EA e possivelmente a obtenção de melhores resultados no diagnóstico e, consequentemente, no tratamento dos pacientes.

Comentários e Considerações sobre a Pesquisa:

Este protocolo se refere ao Projeto de Pesquisa intitulado "ENCEFALITE AUTOIMUNE: CORRELAÇÃO CLÍNICA DO PET/CT-18FDG", cuja pesquisadora responsável é a PROFA. DRA. Bárbara Juarez Amorim, Coordenadora do Serviço de Medicina Nuclear – Hospital de Clínicas – UNICAMP,

Professora Associada - Faculdade de Ciências Médicas – UNICAMP, Maurício Martins Baldissin, doutorando em Clínica Médica na Faculdade de Ciências Médicas – UNICAMP e Edna Marina de Souza, Supervisora de Radioproteção - Serviço de Medicina Nuclear – Hospital de Clínicas – UNICAMP. De acordo com os pesquisadores, trata-se de um estudo retrospectivo, que fará uso de imagens de pacientes adquiridos na rotina de atendimentos do hospital. Os pesquisadores asseguram a manutenção do sigilo em relação às identidades dos participantes. Em relação aos aspectos metodológicos, serão levantados retrospectivamente pacientes com critérios sorológicos e/ou clínicos para diagnóstico de EA que tenham realizado estudo de PET/CT-FDG com imagens dedicadas de cérebro e imagens de corpo inteiro. Serão utilizadas imagens de pacientes já adquiridas no Serviço de Medicina Nuclear do Hospital de Clínicas da UNICAMP. No total, serão estudados 40 pacientes com EA.

Entre os critérios de inclusão, foram definidos:

1. Pacientes com diagnóstico confirmado de EA por sorologia;
2. Pacientes com critérios clínicos de EA;
3. Pacientes que realizaram o PET/CT-FDG com imagens dedicadas do cérebro e imagens de corpo inteiro;
4. Pacientes que aceitem participar do estudo. Por tratar-se de um estudo retrospectivo em que vários dos pacientes residem fora da região de Campinas e devido à pandemia causada pelo novo coronavírus, o consentimento dos mesmos para a participação no estudo será obtido via ligação telefônica, e não via a assinatura do Termo de Consentimento Livre e Esclarecido (TCLE). Nesta condição, solicita-se ao Comitê de Ética em Pesquisa (CEP) a liberação da necessidade do TCLE assinado pelo paciente ou responsável.

Entre os critérios de exclusão:

1. Pacientes com imagens do PET/CT-FDG de baixa qualidade ou incompletos;
2. Pacientes que se recusem a participar do estudo.

As imagens de PET/CT foram todas adquiridas no scanner PET/CT Biograph mCT 40 (Siemens Medical Solutions, USA, Inc). A reconstrução das mesmas é feita em rotinas implementadas nas estações de trabalho do próprio fabricante do scanner. A análise visual das imagens será realizada por médico nuclear com mais de 20 anos de experiência observando-se a homogeneidade de distribuição do traçador no cérebro, comparando-se os dois hemisférios cerebrais e cerebelares na procura por assimetrias e comparando-se a intensidade de captação dos hemisférios cerebrais com a dos núcleos da base e dos hemisférios cerebelares. A análise quantitativa será realizada com o software Scenium®, parte do pacote Syngo.Via® Neurology (Siemens CTI Molecular Imaging,

Knoxville,TN, USA). Esse software compara a imagem cerebral do paciente com um banco de dados de indivíduos normais pareados pela mesma faixa etária. Após o processamento o software mostra as áreas que se encontram acima ou abaixo do esperado com valores de desvio padrão. Nele, é feita uma quantificação automática. O software realiza uma comparação estatística voxel por voxel na imagem de PET de cada paciente com EA em relação a sua base de dados de indivíduos controle. Por ser uma quantificação automática, a análise não depende do operador. A análise quantitativa delineia áreas de hipometabolismo significativo (> 2 DPs da média) e as descreve em imagens e também em uma tabela. As regiões de hipo e hipermetabolismo são apresentadas em cores diferentes, sendo definida a região com maior hipometabolismo. Os dados obtidos neste software são então coletados em uma tabela excel para posterior análise estatística e correlação de valores com os achados clínicos dos pacientes acometidos por EA. Além disso, também serão analisadas visualmente as imagens de corpo inteiro na procura por focos de hipermetabolismo que possam ser suspeitos para neoplasia de origem desconhecida. As imagens de CT de corpo inteiro serão analisadas por um médico radiologista também na procura por alterações anatômicas suspeitas para neoplasia. Por fim, as análises feitas serão confrontadas com os dados clínicos dos pacientes, de modo a inferir os tipos de alterações metabólicas que possivelmente estão associadas à EA. Todos os dados serão coletados em tabela Excel para posterior análise. Será realizada análise estatística dos resultados para cálculo de sensibilidade e especificidade.

De acordo com o documento Informações Básicas do Projeto, o orçamento prevê recursos para aquisição de computador, HD externo e material de impressão, totalizando o valor de sete mil e quinhentos reais (R$7.500,00). O cronograma de atividades prevê o início da coleta de dados para o projeto em setembro de 2021 e a conclusão da pesquisa em agosto de 2024 com a publicação do estudo.

Considerações sobre os Termos de apresentação obrigatória:

Foram analisados os seguintes documentos de apresentação obrigatória abaixo listados.

Conclusões ou Pendências e Lista de Inadequações:

Não há pendências por resolver.

Considerações Finais a critério do CEP:

Este parecer foi discutido e aprovado durante a 6a Reunião Ordinária de 2021 do CEP-UNICAMP em 27 de Julho de 2021.

- O participante da pesquisa deve receber uma via do Termo de Consentimento Livre e Esclarecido,

na íntegra, por ele assinado (quando aplicável).

- O participante da pesquisa tem a liberdade de recusar-se a participar ou de retirar seu consentimento em qualquer fase da pesquisa, sem penalização alguma e sem prejuízo ao seu cuidado (quando aplicável).

- O pesquisador deve desenvolver a pesquisa conforme delineada no protocolo aprovado. Se o pesquisador considerar a descontinuação do estudo, esta deve ser justificada e somente ser realizada após análise das razões da descontinuidade pelo CEP que o aprovou. O pesquisador deve aguardar o parecer do CEP quanto à descontinuação, exceto quando perceber risco ou dano não previsto ao participante ou quando constatar a superioridade de uma estratégia diagnóstica ou terapêutica oferecida a um dos grupos da pesquisa, isto é, somente em caso de necessidade de ação imediata com intuito de proteger os participantes.

- O CEP deve ser informado de todos os efeitos adversos ou fatos relevantes que alterem o curso normal do estudo. É papel do pesquisador assegurar medidas imediatas adequadas frente a evento adverso grave ocorrido (mesmo que tenha sido em outro centro) e enviar notificação ao CEP e à Agência Nacional de Vigilância Sanitária – ANVISA – junto com seu posicionamento.

- Eventuais modificações ou emendas ao protocolo devem ser apresentadas ao CEP de forma clara e sucinta, identificando a parte do protocolo a ser modificada e suas justificativas e aguardando a aprovação do CEP para continuidade da pesquisa. Em caso de projetos do Grupo I ou II apresentados anteriormente à ANVISA, o pesquisador ou patrocinador deve enviá-las também à mesma, junto com o parecer aprovatório do CEP, para serem juntadas ao protocolo inicial.

- Relatórios parciais e final devem ser apresentados ao CEP, inicialmente seis meses após a data deste parecer de aprovação e ao término do estudo.

-Lembramos que segundo a Resolução 466/2012 , item XI.2 letra e, “cabe ao pesquisador apresentar dados solicitados pelo CEP ou pela CONEP a qualquer momento”.

-O pesquisador deve manter os dados da pesquisa em arquivo, físico ou digital, sob sua guarda e responsabilidade, por um período de 5 anos após o término da pesquisa.

Este parecer foi elaborado baseado nos documentos abaixo relacionados:

Tipo Documento	Arquivo	Postagem	Autor	Situação
Declaração de concordância	of88.pdf	24/06/2021 12:50:25	Carlos Eduardo Cavalcante Barros	Aceito

Solicitação Assinada pelo Pesquisador Responsável	ALTERACAO_PESQUISADOR_RESPONSAVEL_DECLARACAO.pdf	22/06/2021 18:04:03	MAURÍCIO MARTINS BALDISSIN	Aceito
Outros	VINCULO_INSTITUCIONAL_BARBARA_JUAREZ_AMORIM.pdf	22/06/2021 18:04:03	MAURÍCIO MARTINS	Aceito
Informações Básicas do Projeto	PB_INFORMAÇÕES_BÁSICAS_DO_PROJETO_1760082.pdf	17/06/2021 02:22:07		Aceito
Outros	VINCULO_INSTITUCIONAL_BARBARA_JUAREZ_AMORIM.pdf	17/06/2021 02:21:18	MAURÍCIO MARTINS	Aceito
Outros	ALTERACAO_PESQUISADOR_RESPONSAVEL_DECLARACAO.pdf	17/06/2021 02:20:39	MAURÍCIO MARTINS	Aceito
Folha de Rosto	FOLHA_DE_ROSTO_ENCEFALITE_AUTOIMUNE_BARBARA.pdf	17/06/2021 02:19:36	MAURÍCIO MARTINS	Aceito
TCLE / Termos de Assentimento / Justificativa de Ausência	SOLICITACAO_DE_DISPENSA_TCLE.pdf	10/06/2021 23:36:34	MAURÍCIO MARTINS BALDISSIN	Aceito
Cronograma	CRONOGRAMA_DETALHADO.pdf	10/06/2021 23:03:48	MAURÍCIO MARTINS	Aceito
Declaração de Pesquisadores	DECLARACAO_DOS_PESQUISADORES_ASSINADA.pdf	10/06/2021 22:51:47	MAURÍCIO MARTINS	Aceito
Projeto Detalhado / Brochura Investigador	PROJETO_DOUTORADO_CEP_ENCEFALITE_FINAL.pdf	10/06/2021 22:48:33	MAURÍCIO MARTINS BALDISSIN	Aceito
Orçamento	ORCAMENTO_DO_PROJETO.pdf	24/05/2021 01:54:07	MAURÍCIO MARTINS	Aceito

Situação do Parecer:
Aprovado

Necessita Apreciação da CONEP:
Não

CAMPINAS, 01 de Agosto de 2021

Assinado por:
jacks jorge junior
(Coordenador(a))

ATTACHMENT 2: PUBLISHED ARTICLE: CLINICAL AND TRANSLATIONAL IMAGING

This thesis includes material previously published in the journal Clinical and Translational Imaging, entitled "Correction: FDG-PET in patients with autoimmune encephalitis: a review of findings and new perspectives," authored by Maurício Martins Baldissin et al., published on August 28, 2023.

SPRINGER NATURE LICENSE
TERMS AND CONDITIONS

Apr 14, 2026

This Agreement between University of Campinas (UNICAMP), Campinas, Brazil ("You") and Springer Nature ("Springer Nature") consists of your license details and the terms and conditions provided by Springer Nature and Copyright Clearance Center.

License Number	6247260898822
License date	Apr 13, 2026
Licensed Content Publisher	Springer Nature
Licensed Content Publication	Clinical and Translational Imaging
Licensed Content Title	Correction: FDG–PET in patients with autoimmune encephalitis: a review of findings and new perspectives
Licensed Content Author	Maurício Martins Baldissin et al
Licensed Content Date	Aug 28, 2023
Type of Use	Thesis/Dissertation
Requestor type	academic/university or research institute
Format	print and electronic
Portion	full article/chapter
Will you be translating?	no
Circulation/distribution	1 - 29
Author of this Springer Nature content	yes
Title of new work	Correction: FDG–PET in patients with autoimmune encephalitis: a review of findings and new perspectives
Institution name	University of Campinas (UNICAMP), Campinas, Brazil
Expected presentation date	Apr 2026
The Requesting Person / Organization to Appear on the License	University of Campinas (UNICAMP), Campinas, Brazil
Requestor Location	Rua Barão de Teffé, 160 - salas 408e 409 Jundiaí, São Paulo 13208760 Brazil
Customer Tax ID	06850582801
Payment Type	Invoice
Email Address	m036752@dac.unicamp.br
Billing Address	Dr. Maurício Baldissin Rua Barão de Teffé, 160 - salas 408e 409 Jundiaí, Brazil 13208760
Total	0.00 USD

Clinical and Translational Imaging
https://doi.org/10.1007/s40336-023-00581-5

EXPERT REVIEW

FDG–PET in patients with autoimmune encephalitis: a review of findings and new perspectives

Maurício Martins Baldissin[1,2,3,6] · Edna Marina de Souza[3,4,6] · Nancy Watanabe[5,6] · Elba C. S. C. Etchebehere[1,3] · Fernando Cendes[5,6] · Bárbara Juarez Amorim[1,3]

Received: 30 March 2023 / Accepted: 13 July 2023

Abstract

Purpose The present review aims to discuss the role of the brain ^{18}F-FDG–PET and ^{18}F-FDG–PET/CT (FDG–PET) in diagnosis and follow-up of the autoimmune encephalitis (AE) patients, highlighting the main findings and the new perspectives on use of these methods in the study of the disease.

Methods The literature search was performed in the following databases: PubMed/MEDLINE, Scopus, Web of Science, Embase, and Google Scholar, according to the PRISMA statement. The main terms of search were: "autoimmune encephalitis" AND "^{18}F-FDG–PET OR ^{18}F-FDG–PET/CT", or the combination between the term "^{18}F-FDG–PET" OR "^{18}F-FDG–PET/CT" AND the antibodies receptors abbreviations (e.g., "NMDA", "VGKC", etc.). The methodological quality of the publications was assessed according to the QUADAS-2 criteria.

Results The search of the articles found 56 main articles. These articles encompassed 1,462 patients with AE positive antibodies, from which 808 had brain FDG–PET images with 714 (88.67%) showing alterations. Furthermore, some AE antibodies have specific metabolic signatures, detected in the images, which are discussed in the text. Moreover, patients at different stages of the disease may present different brain metabolic patterns. The areas of more common hypermetabolism were basal ganglia, hippocampus, amygdala, and cerebellum. The areas of more common hypometabolism were the visual cortex and a diffuse cortical metabolism.

Conclusions This extensive literature review shows the high sensitivity of FDG–PET and FDG–PET/CT in patients with AE. FDG–PET detects findings of hyper and hypometabolism which are suggestive of AE. Besides, AE caused by the different antibodies may present specific alterations which may be suggestive of each one. However, more prospective studies are necessary for these images become a standard diagnostic method of AE.

Keywords FDG–PET · FDG–PET/CT · Autoimmune encephalitis · Brain metabolism · Perspectives

Introduction

Autoimmune encephalitis (AE) is a debilitating neurological disorder characterized by inflammation of brain tissue. It is the most common cause of non-infectious acute encephalitis. This disease was described for the first time in 1888, when patients with neurological symptoms but without brain pathology were reported [1]. The post mortem investigation of patients with behavioral alterations related to acute encephalitis date from 1960s, revealing inflammation mainly in limbic region (hippocampus and amygdala), being the condition named limbic encephalitis (LE) [2], later associated with malignancy [3] and specific antibodies targeting intracellular neuronal antigens [4–8]. These onconeural autoantibodies are also associated with other paraneoplastic syndromes, characterized by relentless progression and poor treatment response, as they result from rapid and permanent neuronal loss. Over the past 20 years, novel forms of encephalitis associated with antibodies to neuronal surface or synaptic proteins have been described, generally with favorable outcome and good response to immunotherapy, even when associated with tumor, as they result from reversible neuronal dysfunction. Depending on associated antibody, AE can produce different clinical presentation and imaging findings.

The diagnosis of AE is still challenger. The clinical manifestations of AE may include behavioral, metabolic, inflammatory, infectious, due to a diversity of neurological

Extended author information available on the last page of the article

Published online: 11 August 2023

damage. According to the publication of Graus et al., the background of investigation is based on guidelines already defined [9], contemplating clinical attention with laboratory tests (including blood, urine, cerebrospinal fluid—CSF), and magnetic resonance imaging (MRI) [10]. Nowadays, many types of antibodies have been associated with the disease.

Anti-NMDA receptor AE was first described in twelve women with ovarian teratomas presenting seizures, memory impairment, and behavioral alterations [11]. Antibody-mediated internalization of NMDAR affects neuronal plasticity and synaptic transmission [12]. Gamma-aminobutyric acid-A ($GABA_A$) receptor antibodies were found in the serum and CSF of patients with refractory seizures and status epilepticus associated with autoimmune comorbidities [10]. Similarly, antibodies against gamma-aminobutyric acid-B ($GABA_B$) receptor have been associated with AE patients, especially LE, with high prevalence of malignancy [13]. Antibodies against target proteins associated with voltage-gated potassium channels (VGKCs), and contactin-associated protein-like 2 (Caspr2), are associated with specific neurological manifestations: LE with faciobrachial dystonic seizures (FDS) in patients with leucine-rich glioma inactivated 1 (LGI1) antibodies [14, 15], and LE, neuromyotonia [16], and Morvan's Syndrome in patients with CASPR2 antibodies [17, 18]. Antibodies against the α-amino-3hydroxy-5-methyl-4-isoxazolepropionic acid (AMPA) receptor are detected in patients with LE and frequently associated with tumors [19].

Dopamine-D2 receptor antibodies have been found in children with parkinsonism, chorea and psychiatric manifestations characterizing basal ganglia encephalitis [20]. The presence of Dipeptidyl-peptidase-like protein 6 (DPPX) generates similar symptoms to Dopamine-D2 receptor antibodies in adults, preceded by severe diarrhea with sudden weight loss, amnesia, dysphagia, trunk stiffness, and bladder dysfunction [21–23]. High concentration of glutamate decarboxylase (GAD) antibodies is associated with many neurological syndromes, including cerebellar ataxia (CA), LE, and stiff-person syndrome (SPS) in adult and pediatric patients [24, 25]. Recently, the SPS has also been associated with the presence of antibodies against glycine receptor (GlyR) in patients that may manifest progressive encephalomyelitis, myoclonus, and rigidity [26–29]. Although many types of AE have been described over the past years, neuronal antibody testing is not widely available, making the diagnosis of this condition frequently based on clinical aspects [10].

Positron emission tomography (PET) performed with fluorodeoxyglucose labeled with fluorine-18 (^{18}F-FDG) is an imaging technique able to identify glucose metabolic changes in several pathological conditions. When combined with computed tomography (PET/CT) or even with magnetic resonance imaging (PET/MRI), it is possible to fuse the physiological images from PET to the anatomical images from CT or MRI. FDG–PET can be applied in the diagnosis and follow-up of cardiovascular [30], infectious and inflammatory diseases, including the COVID-19 [31]. In the neurological studies, this technique has shown diagnostic and follow-up potential in the degenerative diseases [32], and epilepsy [33], being recently more explored in the AE [34]. The first case reports about the use of the PET in patients with symptoms of AE date from the 90s [35–38], and the first case series was reported in 2001, with the application of brain PET–FDG in the study of 11 patients with Rasmussen Encephalitis [39]. Given this context, this review summarizes the role of the FDG–PET and FDG–PET/CT in the diagnosis and follow-up of the patients with AE, bringing a discussion of the new perspectives for the use of these methods as a decisive tool to improve the knowledge about this disease, changing its diagnostic paradigm. Figure 1 shows examples of FDG–PET/CT images of patients with AE and the following positive antibodies: anti-NMDAR, anti-GAD and anti-LGI1.

Materials and methods

Literature search

To find the articles to compose this review, a computational organized literature search was conducted in the following databases: PubMed/MEDLINE, Scopus, Web of Science, Embase, and Google Scholar, according to the PRISMA statement. The literature research was done using the following terms, as well as their combinations: "autoimmune encephalitis", "^{18}F-FDG–PET/CT", "^{18}F-FDG–PET", "brain inflammation". The combination between the terms "^{18}F-FDG–PET/CT" and "^{18}F-FDG–PET", and the antibodies receptors abbreviations (e.g., "NMDA", "VGKC", "Yo", and "DPPX") were also applied. The references of the articles retrieved were also checked to find another potentially relevant publications to expand the results. The search was updated until September 2021, without beginning date.

All the search and analysis of publications were performed according to the PRISMA statement [40]. The quality of the methodological approaches of the articles was assessed based on the Quality Assessment of Diagnostic Accuracy Studies version 2 (QUADAS-2) [41].

Inclusion criteria

The articles had to fill the following inclusion criteria: be an original article, include at least 4 patients (pediatric and/or adult) suspected or diagnosed with AE, submitted to FDG–PET or FDG–PET/CT. Therefore, reviews, case reports, commentaries, editorials, meeting procedures, letters to the editor, only abstracts, books, electronic

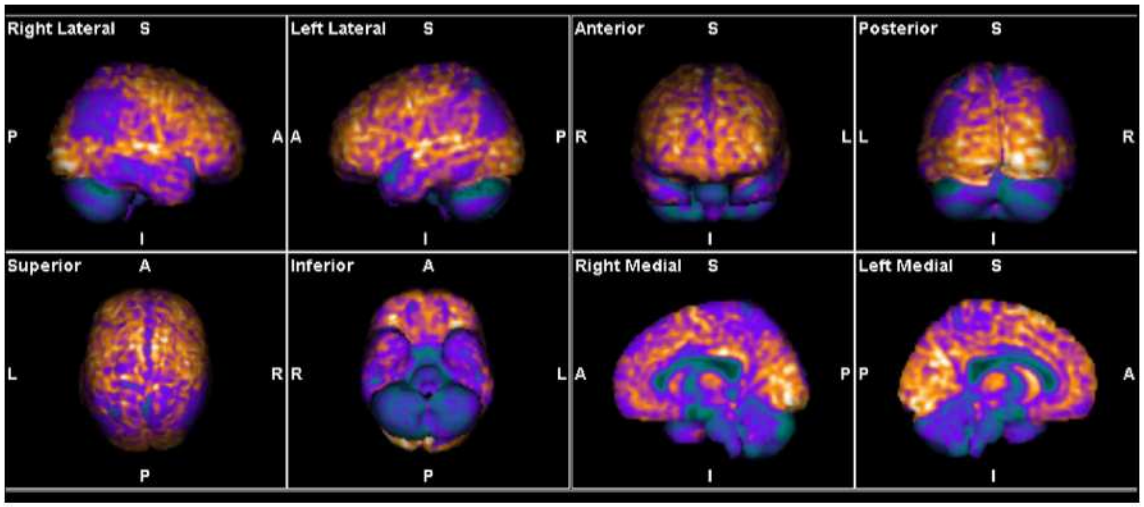

Fig. 1 Examples of ^{18}F-FDG–PET/CT images of a patient with AE and the positive NMDA antibodies. The 3D reconstructions of the ^{18}F-FDG–PET/CT show a hypometabolism in both parietal lobes and cerebellum

supplementary material, comments, preclinical studies, research reports, and other forms of scientific production were excluded.

Selection of articles

The articles which satisfied the inclusion criteria were also reviewed by our authors team, being included in this publication only after consensus. From 2,349 articles initially identified, 56 have been selected according to inclusion criteria.

Results

Literature findings and patients characterization

Figure 2 brings a diagram presenting the result of the literature search. From the literature explored, 1,462 patients

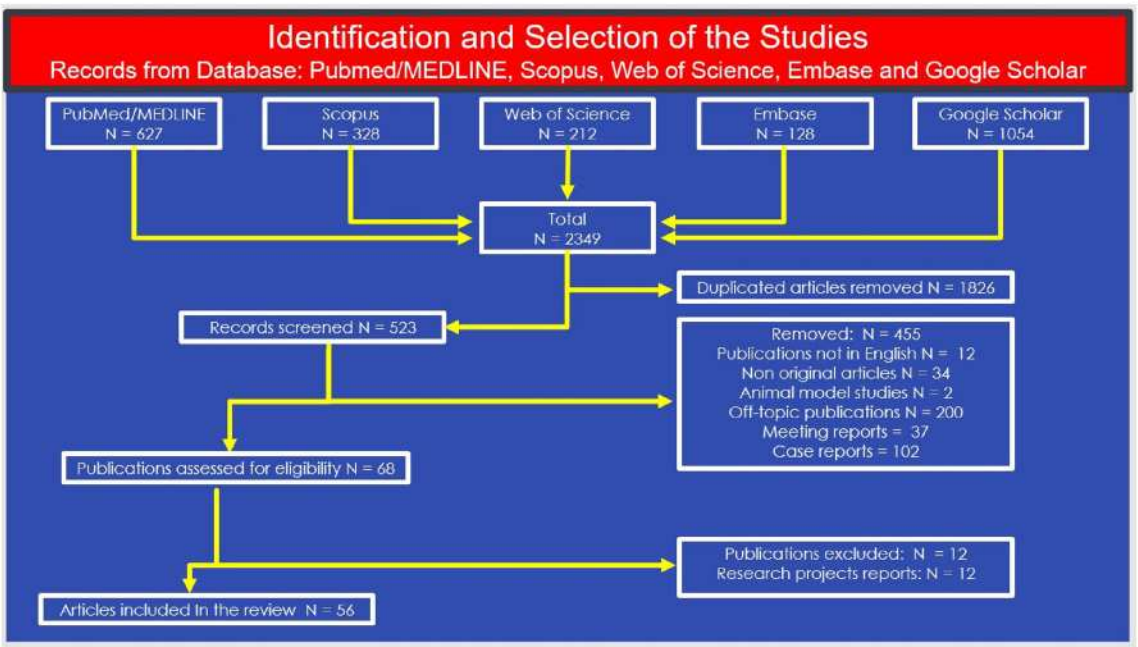

Fig. 2 PRISMA diagram outlining the identification and selection of the studies included in the review

were studied (699 male, 763 females), with age of symptoms onset 46.95 ± 17.63 years, median age 52 years. Some patients with AE presented more than one kind of antibody.

The articles encompassed 1,462 patients with AE positive antibodies, from which 808 had brain ^{18}FDG–PET (FDG–PET) images with 714 (88.67%) showing alterations. The percentage of each type of antibody is shown in Fig. 3.

The time between the PET imaging acquisition and the symptoms onset was very variable, ranging from 8 to 1,740 days (median = 87 days). Therefore, in most cases reported, FDG–PET imaging was not obtained in the acute phase of the disease.

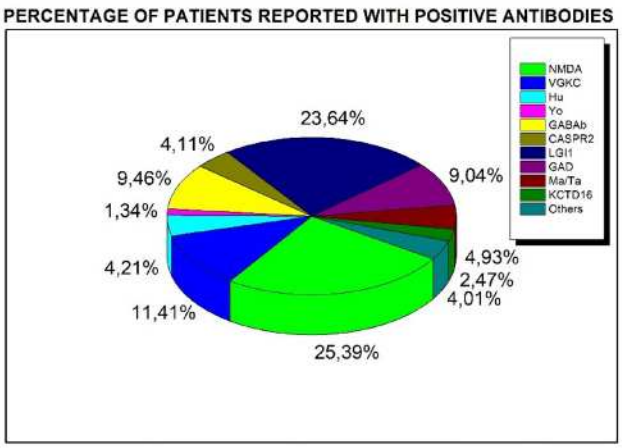

Fig. 3 Percentage of patients which present positive antibodies and brain FDG–PET alterations. In this figure, we included only patients with FDG–PET alterations and positive antibodies

General brain FDG–PET findings

Some authors analyzed the patient's data individually, whereas others worked with group statistical analysis. We compiled the results showing the brain regions with more common increased or decreased ^{18}F-FDG uptake due to AE. We analyzed the studies separating in individual or group statical analysis.

The studies analyzed patients individually or using imaging statistical tools for group evaluation. In the individual analysis, it is possible to note that basal ganglia are the brain regions more commonly affected within increased uptake of the radiotracer, followed by the hippocampus (Fig. 4A). On the other side, the visual cortex is the brain region with higher incidence of ^{18}F-FDG uptake reduction. Considering the group analysis, hypermetabolic findings were more frequently observed in cerebellum, hippocampus, basal ganglia (BG) and amygdala and hypometabolism was more frequently observed in the visual cortex, thalamus and striatum (Fig. 4B).

We also analyzed the studies which have explored the brain lobes as a whole to verify increasing or decreasing of ^{18}F-FDG uptake. In the individual analysis, for most of patients, increased uptake was more frequently observed in the temporal lobe, while decreased ^{18}F-FDG uptake was more frequent in the occipital lobe (Fig. 5A). In the group

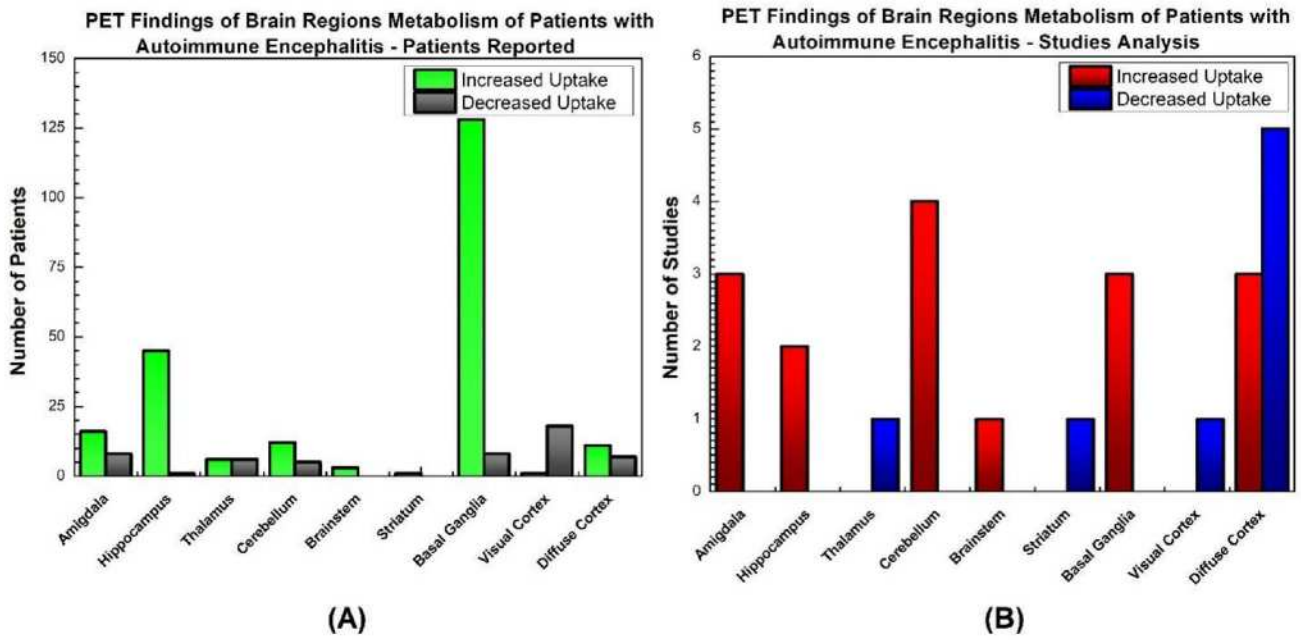

Fig. 4 Brain regions with hypermetabolism and hypometabolism on FDG–PET. Number of PET findings for brain areas of patients with AE for studies which considered individual subjects' analysis **A** and group analysis **B**

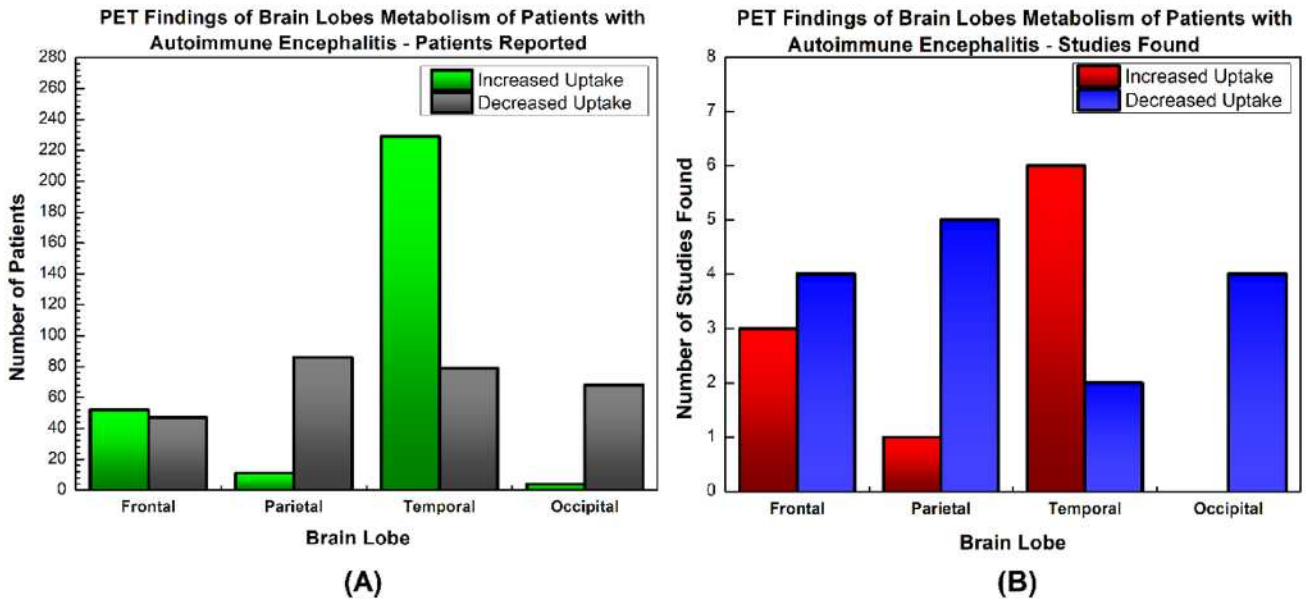

Fig. 5 Brain lobes with hypermetabolism and hypometabolism on FDG–PET. Number of PET findings for brain lobes of patients with AE for studies which considered individual subjects' analysis **A** and group analysis **B**

analysis, increased uptake was more common in the temporal lobe and decreased uptake was more common in the parietal lobe (Fig. 5B).

AE and brain FDG–PET Findings for specific antibodies

Based on subjects who presented just one type of neuronal antibody, it was possible to highlight some clinical manifestations of the specific-antibody syndrome and most common brain FDG–PET findings, which are displayed in Table 1. This table shows a correlation between antibody type, clinical manifestations of AE, and the main FDG–PET findings for patients with AE. Most studies report PET findings in patients with anti-NMDAR and anti-LGI1 encephalitis [42–45]. The following sections brings a literature overview of the clinical manifestations and the main FDG–PET findings in AE.

Anti-NMDAR encephalitis

Anti-NMDAR encephalitis is the most common type of AE [46], with higher incidence among women and frequent association with ovarian teratoma [11]. Clinically, in the early stage of the disease, the patients present fever, fatigue, and headache, followed by psychiatric alterations, such as psychosis, agitation and anxiety. Movement disorders, like choreoathetosis and orofacial dyskinesias altered consciousness, hypoventilation and dysautonomia may also occur throughout the disease course [47]. The first case series studying FDG–PET brain uptake in anti-NMDAR encephalitis, dates from 2012, when Leypoldt et al. conducted a retrospective statistical evaluation of 6 patients (mean age 21 years, 2 male), being the brain PET data extracted from the whole-body scan, acquired about 10 weeks after the symptoms started [48]. The results highlighted the increase of the ^{18}F-FDG uptake in the frontal and temporal regions in association with the occipital hypometabolism, described as a frontotemporal-to-occipital uptake gradient, in the acute phase. Some patients performed PET after the recovery phase of the disease, showing a decrease in the frontotemporal metabolism and an increase in the occipital metabolism. Probasco et al performed FDG–PET/CT in a group of 61 patients, from which 31 had antibodies detected (5 patients with anti-NMDAR) [34]. The images were acquired a median of 4 weeks after the symptom's onset, revealing an increased ^{18}F-FDG uptake in the basal ganglia, hippocampus, and in the temporal lobe as a whole, with a decreased uptake in the occipital lobe. The same antibodies were found in two patients with LE (aged 21–80 years), reported by Fisher et al. [49]. FDG–PET/CT were acquired between 4 and 60 days of disease and corroborated the previous results with increased metabolism in the temporal lobe and in the basal ganglia, and decreased metabolism in the occipital lobe.

Exploring the correlation between the ^{18}F-FDG–PET/CT findings and AE, Baumgartner et al. evaluated a series of 18 patients (mean age 45.6 years, 8 male), 3 of them having positive NMDAR antibodies [50]. An increased uptake in the striatum and cerebellum was found, as well

Table 1 Correlation between antibodies, clinical presentation and FDG–PET findings in AE

Antibodies	Patients reported	Typical clinical manifestations	FDG–PET main findings in early stage of the disease		References
			Hypermetabolism	Hypometabolism	
NMDA	185	Children: seizures, dyskinesias; adults: behavior changes	Frontal and pre-frontal areas; basal ganglia; temporal lobe	Occipital lobe	[34, 42, 43, 46–57, 66, 71, 78, 85, 94]
VGKC	230	Memory loss, faciobrachial dystonic seizures, hyponatremia	Mesial temporal lobe (hippocampus), basal ganglia, cerebellum	Diffuse	[13, 14, 34, 45, 47, 50, 51, 55, 57, 66, 71, 84–86]
$GABA_B$	90	Seizures, confusion, behavior changes, memory loss	Medial temporal lobe (amigdala and hipoccampus) and basal ganglia	Global hypometabolism	[46, 57, 60, 63–68, 81]
GAD	88	Seizures, muscle rigidity, CA, nausea, hallucinations	Hippocampus; cerebelar hemispheres,	Brain cortex (diffusely)	[13, 34, 47, 50, 55–57, 60, 66, 71, 72, 83, 84, 86]
Ma2/Ta2	46	Altered mental status; epilepsy; memory deficit;		Temporal, frontal, occipital and parietal lobes	[34, 47, 55, 60, 69, 71, 83]
Glycine	2	Muscle spasms, stiffness, rigidity, startle, eye movement disorders; sensory stimuli		Frontal lobe and midbrain	[72]
Ach	4	Memory loss, altered mental status without seizures		Mesial temporal lobe, diffuse cortical;	[34, 55]
Tr	1	Cerebellar syndrome		Cerebellum	[70]
KCTD16	24	Seizures, cognitive deficit, hallucinations, sleep disturbances	Mesial temporal lobe		[68]
Amphiphysin	3	Stiffness, disorientation, cognitive deficit		Temporal lobe	[46, 65, 72]
LGLON5	1	Sleep disorders, gait instability, peripheral symptoms	Primary sensorimotor cortices, basal ganglia and cerebellum		[60]
Aquaporin-4	2	Optical neuromyelitis, non-multiple sclerosis related		Occipital lobe	[34, 47]
CRMP5	3	Choreiform movements, ataxia, confusion, cognitive deficit		Caudate nucleus, putamen	[34, 47]
CV2	6	Parkinsonism, autonomic dysfunction	Hippocampus, amygdala		[34, 47, 60, 83]
Striational	3	Worsening balance, confusion	Cerebellum		[34, 47]
Ganglioside	1	Altered mental status, delirium, cranial nerve involvement		Generalized cortical	[65]
Contactin-2	2	Seizures, behavioral changes	Temporal lobe		[14]
Neuropil	7	Seizures, behavioral changes, peripheral manifestations	Frontal lobe	Temporal lobe	[86]
Ri	1	Ataxia, cognitive deficit, mild hemiparesis		Mesiotemporal area (severe)	[50]
AMPA	1	Ataxic gait, psychosis, agitation		Occipital	[63]

as a decreased uptake in the associative cortex, temporal and parietal lobes. Wegner et al. compared the uptake patterns of the ^{18}F-FDG in patients with anti-NMDAR and anti-LGI1 encephalitis [43]. For the first one, there was an increased uptake in the frontotemporal areas, while for LGI1, the hypermetabolism was observed in the basal ganglia, cerebellum, occipital and precentral areas.

Seizures outcomes of patients with LE associated with NMDA antibodies have been studied by Sarkis and colleagues, with the brain FDG–PET/CT obtained for 5 antibody positive patients [51], revealing increased uptake in the temporal lobes. Lagarde et al conducted a serial study with pediatric anti-NMDAR encephalitis patients that underwent FDG–PET/CT scans 3–4 weeks after the disease onset. Eleven patients were studied (mean age 10 years, 4 male), presenting behavioral troubles, movement disorders, and seizures. The brain ^{18}F-FDG uptake pattern was similar to that seen in adults (basal ganglia hypermetabolism), with the following particular features: extensive and symmetric cortical hypometabolism in the frontal lobe, and asymmetric anterior focus of hypermetabolism [42]. Other FDG–PET/CT study of children with AE was conducted by Turpin et al. From 34 subjects evaluated, six had NMDAR antibodies, and basal ganglia hypermetabolism was visually detect in 26.5% of the cases, and quantitatively in 82.3% [52].

The brain metabolism in different stages of anti-NMDAR encephalitis was reported by Yuan et al. in 2016, which acquired FDG–PET/CT images in the subacute, acute, early recovery, recovery, and relapsing phases [53]. Considering a group of 8 patients (aged 12–35 years, 3 male), there was a hypermetabolism in the basal ganglia, temporal and frontal lobes, and a severe hypometabolism in the bilateral occipital lobes in the subacute/acute phase (5–6 weeks from the disease onset high level of antibodies). In the early recovery phase (9–13 weeks from the onset), the previous pattern is almost preserved, but there is a discrete reduction in the basal ganglia metabolism. Concurrent antibody levels were weakly positive. Finally, in the recovery phase, the brain metabolism is almost normal (no antibodies detected). Three patients presented relapsing disease, each one with positive antibodies and different symptoms: seizures, unconsciousness and abnormal behavior. Although the occipital metabolism had returned to normal, new focus of hypermetabolism were found in the temporal lobe and in the basal ganglia.

Two patients with recurrence of the disease were reported by Quian et al, that characterized the abnormalities of the brain FDG–PET in a group of 11 patients (mean age 25.9 years, 6 male) with AE, 3 of them with NMDAR antibodies [54]. The mean time between the disease onset (with two or more symptoms) and the FDG–PET acquisition was 21 days. Increased uptake was observed in the prefrontal, frontal, parietal and temporal lobes, and in the basal ganglia, with decreased metabolism seen in the occipital lobe.

In a voxel-by-voxel semiquantitative analysis, Solnes et al have found statistical differences between brain uptake in patients presenting positive NMDA or other types of antibodies, as such as those related to rubella virus, herpes simplex virus and cytomegalovirus, with characteristic occipital hypometabolism in patient positive for this antibody [55]. Even with the application of different analysis methods, recent studies have corroborated these metabolic findings on FDG–PET in anti-NMDAR AE. The increased metabolism in basal ganglia with decreased metabolism in occipital lobe is also reported in the studies of Tripathi [56], Probasco [47], Strohm [57], Turpin [52], Ge [58], Nissen [59], and Moreno-Stébanez [60].

Tripathi et al. reported a series of 24 patients (mean age 52 years, 10 male), with 16 anti-NMDAR encephalitis patients [56]. The authors performed visual analysis and two distinct routines of semiquantitative analysis of the FDG–PET/CT brain images: GE Cortex ID and Siemens Scenium software. These computational routines were developed by the PET/CT scanners manufacturers and allow the statistical analysis of the patients' images, which are compared with an imaging database of the normal subjects to identify significant areas of hypometabolism or hypermetabolism. The visual analysis showed lower sensitivity than the semiquantitative approach. Both quantitative software led to analogous results: hypermetabolism in the basal ganglia and in the temporal lobes, with hypometabolism in the occipital region. Z-score values from both tools allowed to distinguish the FDG–PET uptake pattern of anti-NMDAR encephalitis from the AE associated with the anti-LGI1 or anti-GAD.

The GE Cortex ID software has also been used by Probasco et al. [34], which retrospectively explored a database of 61 patients (mean age 26 years), with 8 anti-NMDAR encephalitis patients. FDG–PET/CT imaging acquisitions were done about 8 weeks from symptoms start. They concluded that most of the patients have both hypo and hypermetabolic areas in the occipital and temporal lobes, respectively, from which the uptake magnitude can be evaluated statistically (e.g., Mann–Whitney *U* test with Bonferroni correction) to distinguish the brain uptake patterns in different types of AE.

Strohm et al. applied the FDG–PET to study 12 patients with new-onset status epilepticus, three of them anti-NMDAR positive. For these patients, a parietal and occipital hypometabolism that persists throughout the disease course was detected [57]. The work conducted by Ge et al. explored the acute phase of the disease in a group of 24 anti-NMDAR positive patients. The visual and the statistical analysis (comparing patients to the control group) revealed a significant occipital hypometabolism, as well as the basal ganglia and the frontal–temporal hypermetabolism [58]. In a populational study of the AE in Denmark, Nissen et al. analyzed the FDG–PET of 17 anti-NMDAR encephalitis patients, and found decreased occipital metabolism in 15 (88%) patients [59]. In the series of 43 patients reported by Moreno-Estébanez et al. (55.8% seropositive patients and 13% with NMDAR antibodies), patterns of hypermetabolism in limbic areas were identified [60].

In summary, the main alterations in the FDG–PET images are the hypermetabolism in the frontal, temporal

and striatum regions, with the occipital hypometabolism in the acute and sub-acute phases of the disease, sometimes described as a frontotemporal-to-occipital uptake gradient.

Anti-Caspr2 and anti-LGI1 encephalitis

The first reports of the AE associated initially with anti-VGKC date back to 2001, describing patients with neuromyotonia, Morvan's syndrome and LE [16, 63]. The investigation of this disease using the FDG–PET date from 2005, when Ances et al. reported 1 patient with LE and anti-VGKC antibodies with increased brain uptake in the medial temporal lobes [64]. While the clinical spectrum emerged, it became clear that the pathogenicity is associated with the antibodies against proteins complexed with the VGKC: leucine-rich-glioma-inactivaed1 (LGI1) and contactin-associated protein-like 2 (Caspr2) [65, 66]. Anti-LGI1 encephalitis is characterized by LE with faciobrachial dystonic seizures [67, 68]. Anti-Caspr2 encephalitis predominantly affects elderly men and can be associated with LE, with or without cerebellar dysfunction, Morvan syndrome and peripheral nerve hyperexcitability [66].

Irani et al. reported abnormal brain ^{18}F-FDG uptake in 8 patients (mean age 64 years) with LE and faciobrachial dystonic seizures related to VGKC antibodies, especially anti-LGI1 [12]. For most of the patients, the temporal lobe and basal ganglia hypermetabolism was found. Flanagan et al. studied 11 patients with faciobrachial dystonic seizures and LGI1 antibodies using FDG–PET, reporting basal ganglia hypermetabolism in 4 patients, basal ganglia hypometabolism in 2 patients, diffuse hypometabolism in 3, mesial temporal hypermetabolism in 3 and bifrontal hypometabolism in 2 patients [69]. LE have also been studied using FDG–PET by Baumgartner et al. [52]. From a group of the 18 patients (mean age 55.3 years, 8 male), 7 had VGKC antibodies, 2 in association with anti-CAspr2, one with anti-LGI1, and one with anti-NMDAR. A visual analysis associated with scores identified mesiotemporal hypermetabolism and hypometabolism in the association cortices in one anti-Caspr2 and anti-LGI1 patient. The patient with Caspr2 antibodies had striata hypermetabolism and the patient with anti-NMDAR had thalami hypometabolism. Similar results have been found in other study [70]. To compare the metabolic brain patterns of the anti-NMDA and anti-LGI1 AE, Wegner et al. evaluated statistically the FDG–PET/CT images of 10 patients (mean age 36.5 years, 4 males, 6 with anti-NMDAR encephalitis, and 4 with anti-LGI1 encephalitis [45]. The mean time between the symptoms onset and the imaging acquisition was 2.5 months. As a result, it was observed that the anti-LGI1 encephalitis was characterized by hypermetabolism in the basal ganglia, cerebellum, occipital and precentral areas, with hypometabolism in the frontomesial region. On the other side, images of patients with anti-NMDAR encephalitis demonstrated a regionally limited hypermetabolism in the frontotemporal areas, in addition to the occipital hypometabolism.

The outcome of the patients with anti-LGI1 AE was evaluated by Shin et al., that studied a group of 10 subjects (mean age 60.5 years, 8 male), some of them presenting faciobrachial dystonic seizures [71]. The statistical analysis of the FDG–PET/CT images acquired in the early phase of the disease and after treatment indicated a poor outcome for patients with medial temporal hypermetabolism, with greater chance of recurrence. Given the relevance of the temporal lobe metabolic alterations for the outcome of patients with anti-VGKC AE, Celicanin et al. focused on the analysis of the hippocampus using the FDG–PET/CT [47]. From a group of 9 patients (mean age 62 years), it was observed unilateral ($n = 3$) or bilateral ($n = 4$) hippocampal hypermetabolism, and unilateral hypometabolism ($n = 1$). One subject had a normal scan. Follow-up images of 3 patients were available, showing unilateral ($n = 2$) or bilateral ($n = 1$) hippocampal hypometabolism. Analogous results (bilateral hippocampal hypermetabolism) were found by Lv et al. in a study comparing the sensitivity of the visual and the semi-quantitative analysis of the FDG–PET/CT applied to the 23 patients with anti-LGI1 encephalitis [72]. In the semi-quantitative analysis, alterations in temporal lobe and basal ganglia were found, respectively, in 56% and 73% of the patients. These alterations were not detected in the visual analysis. It was concluded that the semiquantitative analysis of the images increases the sensitivity to identify brain metabolic alterations related to anti-LGI1 encephalitis.

A voxel-by-voxel statistical analysis of the FDG–PET/CT conducted by Dodich et al. revealed altered metabolic patterns in 2 patients with anti-LGI1: hypometabolism in the prefrontal cortex, cingulate, insula, pallidum, and in the medial temporal lobe, and hypermetabolism in the bilateral sensorimotor cortex, and in the lateral temporal lobe. They also reported an anti-Caspr2 with the FDG–PET showing hypometabolism in the bilateral orbitofrontal cortex, nucleus accumbens, cerebellum and insula, and hypermetabolism in the hippocampus and sensorimotor cortex [73].

The brain metabolic differences of the patients presenting anti-LGI1 antibodies with or without faciobrachial dystonic seizures were explore by Liu et al., for a group of 34 patients (mean age 61 years, 24 males, 50% manifesting the seizures) [74]. From the voxel-based statistical analysis of the brain FDG–PET/CT, it was verified that the basal ganglia hypermetabolism only occurs in patients with this type of seizures, reinforcing the potential of this imaging method to diagnose and to characterize the patients with AE.

Qin et al. reported 25 patients with Caspr2 antibodies and 5 patients underwent PET scan, with CNS altered metabolic findings in one patient: increased metabolism of the bilateral basal ganglia and the mesial temporal lobe [75].

Finally, Li et al. evaluated retrospectively the brain metabolism in the anti-LGI1 AE [76]. The authors divided the patients into four groups, according to the semiology of the disease: focal impaired awareness seizures (FIAS), faciobrachial dystonic seizures FBDS-only, faciobrachial dystonic seizures plus (FDBS-plus) and focal aware motor seizures. The number of subjects in each group was 17, 6, 8, and 2, respectively, totalizing a group of 33 patients (median age 60 years, 22 men). The average time from symptoms onset was 3.1 months. In the quantitative analysis comparing the patients to control group, it was highlighted that patients with FIAS displayed extensive hypermetabolism in the following areas: bilateral basal ganglia, cerebellum, mesial temporal lobe, insula, and precentral gyrus. In a similar way, patients with FBDS-plus also present a wide range of hypermetabolism (bilateral basal ganglia, mesial temporal lobe, precuneus, cerebellum, left postcentral gyrus, insula, and superior parietal lobule, right substantia nigra, middle occipital gyrus, and cuneus), contrasting with the findings of the patients with FBDS-only, in whom a limited hypermetabolism of cerebellum and left medial globus pallidus was found. Anti-LGI1 encephalitis may present different metabolic patterns on FDG–PET, being hypermetabolic changes more frequently observed in the medial temporal lobe, and in the basal ganglia, the latter especially in the patients with FBDS. Cerebellum hypermetabolism may also be observed. Hypometabolic changes are diverse and may be diffuse or include the basal ganglia, frontal regions, mesial temporal lobe, and thalamus.

Few data are available on anti-Caspr2 encephalitis brain metabolic patterns on FDG–PET, but the most frequent finding is the hypermetabolism in the mesial temporal lobes and basal ganglia. Areas of cortical and cerebellum hypometabolism may also be observed.

Anti-GABAB receptor encephalitis

Neurological manifestations associated with the GABA antibodies have been reported since the 1980s [61, 62]. Among these manifestations, seizures, confusion, memory loss, muscle stiffness, and sensory polyneuropathy may be highlighted. Anti-$GABA_B$ receptor AE was initially described by Lancaster et al. [13], and the first FDG–PET/CT series investigating the disease was reported by Kim et. al. in 2014, which studied a group of 5 patients with $GABA_B$ receptor antibodies (mean age 63 years, 4 male) [63]. The authors found the medial temporal lobe hypermetabolism in 2 patients, and the diffuse cortical hypometabolism in one patient. This pattern remained almost unchanged in the follow-up images of most of the patients. The time between the symptom's onset and the brain imaging acquisition was ranged from 20 days to 2 years (mean 30 days). Diffuse cortical decreased metabolism was observed in three patients.

FDG–PET/CT images was used by Zhu et al. to study a group of 14 patients with anti-$GABA_B$ receptor AE (mean age 52 years, 9 male) [64]. Increased uptake in the temporal lobe, hippocampus, and basal ganglia were observed in 6 patients. Shen et al. applied a semiquantitative analysis in a group of 15 patients with LE, 13 of them harboring $GABA_B$ receptor antibodies, and 2 patients had positive brain FDG–PET finding: the cortical hypometabolism. The authors mentioned that the cortical hypometabolism could be a characteristic of the synaptic dysfunction, while the mesial temporal hypermetabolism might be a consequence of the inflammatory process [65].

Strohm et al. verified medial temporal lobe hypermetabolism in one patient with anti-$GABA_B$ positive new-onset refractory status epilepticus [57], whereas the works of Steriade verified the mesial temporal lobe hypermetabolism in one patient with anti-$GABA_B$ receptor encephalitis [66].

The evolution of the $GABA_B$ AE, and its prognostic factors were also explored by Wen et al., which followed a group of 20 patients (mean age 59.4 years, 12 male) [67]. Three of them had an FDG–PET/CT scan, and one patient presented bilateral hippocampal hypermetabolism. Based on the follow-up of the group, it is seen that older patients had a poor outcome when compared to younger ones, which is reinforced when the hippocampal hypermetabolism remains, even after the treatment. Concluding, it was observed that in positive patients for $GABA_B$ antibodies the FDG–PET images have detected hypermetabolism mainly in the medial temporal lobe, including amygdala, hippocampus, and the basal ganglia, associated with the global cortical hypometabolism [68].

Anti-GAD encephalitis

Antibodies against the GAD, the rate limiting enzyme for the GABA synthesis, were first detected in the serum and CSF of patients with SPS, a rare CNS disease which produces rigidity, CA, and cramps commonly related to the other autoimmune conditions, usually the type I diabetes mellitus [74, 75]. These antibodies may also be associated with LE, CA, temporal lobe epilepsy and dementia [83]. Patients with LE and anti-GAD were studied with the FDG–PET/CT for the first time in 2005 [61].

In 2010, Malter et al. studied 53 LE patients (mean age 47 years), from which 10 presented anti-GAD, and brain FDG–PET/CT showing the hippocampal hypermetabolism in the earlier phase of the disease [84], which is also reported by other authors [50]. In addition to the temporal lobe hypermetabolism, some studies have described the diffuse cortical hypometabolism for this group of patients [48, 53, 58, 80, 85], as well as the brainstem and basal ganglia hypermetabolism [51]. Strohm et al. mentioned the presence of the diffuse cortical hypometabolism as a predictor of poor

outcome for patients presenting GAD antibodies alone or in combination with others [79].

Amygdala hypometabolism were related by Deuschl et al. in three patients expressing GAD antibodies, one of them with bitemporal and biparietal hypometabolism. From a sample of 20 patients (mean age 38 years, 5 male), 8 presented GAD antibodies. Combining visual and quantitative analysis, the authors also reported that patients with bitemporal and biparietal hypometabolism were the subjects with a worse outcome [86].

Wang et al. studied recently a sample of 170 subjects with SPS and CA [87]. From this sample, 50 patients (mean age 41.5 years, 16 male) had brain FDG–PET/CT images. The range time between the symptoms onset and imaging acquisition was 0–333 months, considering the follow-up exams. In a group of 30 patients with GAD65 antibodies, the visual and quantitative analysis of patients' images in the acute/subacute phase of the disease revealed different metabolic patterns depending on the clinical phenotype: SPS patients showed thalamus hypometabolism and brainstem hypermetabolism, while the brainstem, and the cerebellar hypermetabolism were observed in the patients with pure CA. Follow-up images acquired about 3 years after the symptom's onset have shown hypometabolism of the cerebellum in one patient.

From the studies reviewed, it was observed that each clinical phenotype associated with GAD antibodies presents different metabolic patterns in the FDG–PET: LE with increased or reduced uptake in the temporal lobe, including hippocampus and amygdala; SPS with thalamus hypometabolism and brainstem hypermetabolism; and CA with brainstem and cerebellar hypermetabolism. Some patients may also present diffuse cortical hypometabolism.

Other antibodies

AE associated with other antibodies may also present brain metabolic alterations showed in the FDG–PET/CT images. Ma2/Ta2, Hu and Yo are antibodies detected targeting intracellular neuronal antigens, typically associated with the paraneoplastic neurological syndromes [55]. Temporal lobe hypermetabolism has been reported in patients with anti-Ma2/Ta2 positive LE [34, 47, 69]. Patients with Hu antibodies often associated with LE, have presented hypermetabolism in the medial temporal lobes, and hypometabolism in the association cortices [34, 55]. Anti-Yo is associated with paraneoplastic cerebellar degeneration and FDG–PET studies reveal the cerebellar hypermetabolism [70, 71].

Antibodies against glycine receptors have been found in children and adult patients with SPS, or progressive encephalomyelitis, rigidity, and myoclonus [27]. There are few FDG–PET/CT images described in the literature about these patients, and they commonly presented the frontal lobe and midbrain hypometabolism [72].

Table 1 summarizes the main findings of the literature explored, and the number of patients reported. The table highlights the main brain areas of hypometabolism or hypermetabolism in the FDG–PET/CT studies, for the antibodies described in this session and others antibodies studied.

Paraneoplastic syndromes

The AE is a condition oftentimes expressed as a paraneoplastic syndrome. In about 60% of patients, highly specific antineuronal antibodies (e.g., Hu, Yo, Ma/Ta) can be detected. For about two-thirds of these patients, the neurological manifestation precedes the tumor diagnosis up to 4 years [70, 73].

Since the 90s, the literature has reported the findings of tumors in patients with symptoms of AE and positive antibodies, using whole-body images acquired with the PET or PET/CT techniques [37, 38]. Considering the articles revised in this work, from the 1,462 patients studied, 266 had tumors detected by ^{18}F-FDG–PET/CT, corresponding to 18,20% of the whole sample. The most commonly found tumor was the small cell lung cancer (SCLC) [8], followed by the ovarian teratoma [11, 74], and other ovarian tumors [75]. The number of the patients affected by each one of these tumors was 61, 40 and 61, respectively, corresponding to 4,17%, 2,73% and 4,17% of the whole sample.

Lymphomas and neuroendocrine tumors have also been detected in some of these patients, corresponding, respectively, to 2,32% and 0,82% of the patients reported [70]. Other less common, but also found tumors include the breast and prostate tumors, as well as seminoma, thyroid tumors, and the bronchial carcinoma [34, 50]. The graphic of Fig. 6 summarizes the distribution of the most commonly found tumors in the patients with symptoms of AE.

Meta-analysis for FDG–PET brain findings

The forest plot of Fig. 7 brings the meta-analysis results based on the odds ratio, and the random effect model [93]. From the articles explored, the detection sensitivity of the FDG–PET–CT in the AE is 87% (72 to 97%), with a heterogeneity index $I2 = 69\%$ ($p < 0.001$). The statistical analysis reveals that most articles point to the high capability of the FDG–PET–CT to diagnosis and follow-up of the patients with AE, which may include the potential to differentiate the pathology from other diseases [49, 53].

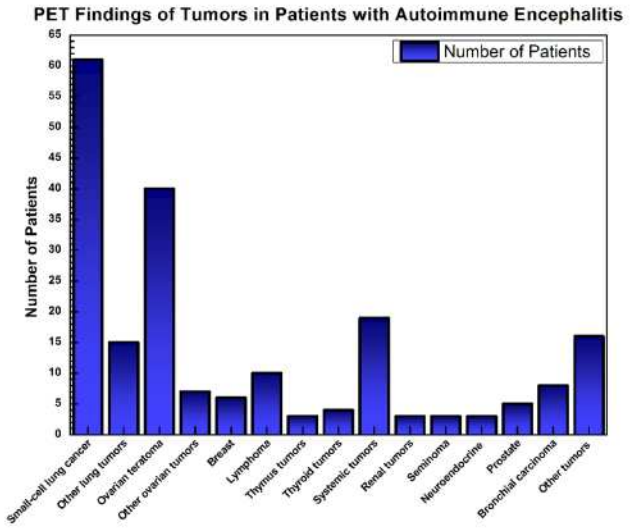

Fig. 6 Distribution of the main tumors found in the literature using PET in patients with symptoms of AE

Discussion

We presented an extensive literature review regarding the use of the FDG–PET or FDG–PET/CT in AE. One of the main findings of this review is the high sensitivity of FDG–PET (87%) to detect metabolic alterations in the large population of patients with AE ($n = 1{,}462$). FDG–PET can detect findings of hyper and hypometabolism, which may be suggestive of AE. Besides, depending on the neuronal antibody type and the clinical phenotype, different metabolic patterns are expected in the PET–FDG. These findings contribute to change the diagnostic paradigm of the AE.

This study brought a compilation of the main findings of FDG–PET for diagnosis and follow-up of patients with AE. The findings also highlight the importance of the method to discern metabolic brain patterns of AE identifying brain ^{18}F-FDG uptake suggestive of some types of antibodies, such as NMDA, $GABA_B$, GAD, and antibodies of the VGKC complex. FDG–PET can contribute to the diagnosis of the disease, especially when specific antibody tests are not available, which is the reality of many developing countries.

According to the most reported studies, patients with the anti-NMDAR encephalitis presented higher ^{18}F-FDG uptake in the temporal lobe and basal ganglia, and lower uptake in the occipital lobe [34, 47, 52, 54]. Hypermetabolism in frontal, prefrontal, and parietal areas have also been found. Some authors describe this pattern as a frontotemporal-to-occipital uptake gradient [54, 60]. Despite some differences between the common symptoms observed in children (seizures and dyskinesias), and adults (behavioral changes), the ^{18}F-FDG uptake patterns for both groups are similar [52, 76]. Few studies diverge from these findings, relating a decreased ^{18}F-FDG uptake

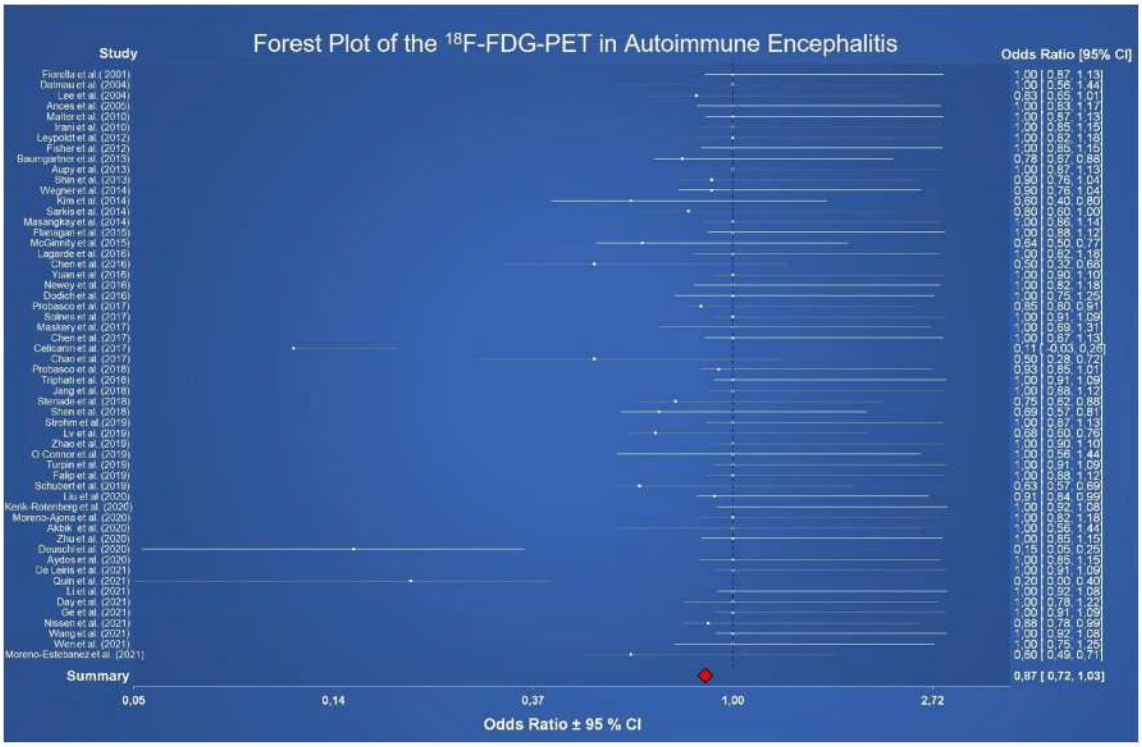

Fig. 7 Forest plot summarizing the meta-analysis of the FDG–PET for patients with AE (log scale)

in the associative cortex, temporal, and parietal lobes [49, 56, 58].

Only one prospective study explored the different stages of the anti-NMDAR AE using the ^{18}F-FDG–PET/CT, reporting different uptake characteristics among the disease phases: subacute and acute phase (basal ganglia, temporal and frontal lobe hypermetabolism, with severe occipital hypometabolism); early recovery phase (same pattern as the previous stages, with mild reduction in the basal ganglia metabolism); recovery phase (almost normal brain metabolism); and relapsing phase (new focus of hypermetabolism). Thereby, this study showed that the FDG–PET/CT findings depend on the disease stage [53].

During the disease, many patients have their brain metabolic alterations resolved throughout the treatment. Multiple FDG–PET acquisitions of the same patient in different phases of the AE revealed that some subjects manifested new brain alterations between different scans, and some of them have metabolic alterations which persisted throughout the disease course, pointing out a poor outcome [57, 77]. These findings reinforce the importance of the straight definition of the disease stage of each patient before the group statistical analysis.

A difference in the recovery has also been reported for the different age groups. Younger patients with anti-$GABA_BR$ have had a better outcome when compared to older ones, for whom the hippocampal hypermetabolism still remains after the treatment [67]. Even in other types of AE, younger patients' tend to have a better outcome [59].

Some uptake findings are common between different antibodies. Hypermetabolism in basal ganglia and mesial temporal lobe including the hippocampus can be observed in many cases of AE, with anti-LGI1 [44, 45, 78, 79], anti-Caspr2 [45, 80], anti-$GABA_B$ [13] and anti-Hu [70] antibodies. Another finding is the hypermetabolism in the cerebellar hemispheres which has been reported in AE related to anti-NMDAR, anti-GAD and anti-Yo antibodies. These hypermetabolic areas may be consequence of the inflammatory processes [60].

Another common finding among the patients with AE is the diffuse hypometabolism of the cerebral hemispheres, which can be observed in the anti-LGI1 [43, 81, 82] and anti-GAD AE [72, 83, 84]. Some researchers have noted that these findings of the ^{18}F-FDG uptake are hypothetically a characteristic of the synaptic dysfunction [24]. Besides, others authors consider this lower ^{18}F-FDG uptake as a predictor of poor outcome [48]. A worse outcome has also been highlighted for the patients with bitemporal and biparietal hypometabolism. Following these patients for 3 years, some authors verified that the hypermetabolic areas has become hypometabolic over time, which may also occur in other AE type [72].

It was observed a variety of different methods to analyze the brain images. Among the analysis methods applied to the PET data (visual, semi-quantitative, and quantitative), it is possible to notice that the visual analysis is complemented by semi-quantitative or quantitative analysis to evaluate the alterations due to AE. A variety of tools was applied in the imaging quantification, among which is possible to highlight the Statistical Parametric Mapping (SPM), GE CortexID®, and Siemens Scenium® as the main choices, being the SPM the most used software. Some brain metabolic changes due to the disease can be subtle, difficult to identify by visual analysis. From all articles included in this review, many of them have used quantitative analyses (43.75%), showing the importance of PET imaging quantification for an accurate evaluation of the brain metabolic changes due to AE [34, 48, 54, 55, 60, 78, 83, 85].

AE manifestations may represent paraneoplastic conditions and some authors have performed a whole-body FDG–PET for tumor screening. In the literature reviewed, from the 1,462 patients studied, 18.20% had some tumor. The most commonly found tumor was the SCLC [34, 65, 70], followed by ovarian teratoma [34, 58–60, 77], and other ovarian tumors [13, 34, 60, 70, 71, 77]. It was observed that AE has been rarely related to tumors in the pediatric population [52]. Other diseases detected were lymphomas [34, 59, 70, 71], neuroendocrine tumors [13, 65, 71], thyroid [77, 86], breast [34, 45, 50, 71] and prostate tumors [59, 87], as well as seminoma [34, 71] and bronchial carcinoma [50].

Although the studies explored in this review have brought many positive findings that corroborate for the use of FDG–PET as a tool for diagnostic, characterization, and follow-up of the patients with AE, there are some limitations to consider. First of all, there is not a standard protocol for the imaging acquisition, reconstruction, and processing of the FDG–PET data, leading to a risk of bias in the results, mainly in the quantitative analysis. In some cases, PET data were acquired and processed with different methods are compared in the same study [50, 59]. Other limitation is that most of the studies with the FDG–PET and FDG–PET/CT in AE are retrospective series [47, 50, 52, 59, 60, 67]. Unfortunately, prospective studies are still rare, despite the increase of access to PET/CT scanners [83, 88, 89]. Another important limitation is that the studies reviewed showed a large range of time between symptom's onset and PET acquisition (8–1,740 days, median = 87 days). This finding reveals that each study reflects a different phase of AE. Besides, sometimes data from patients in different stages of the disease have been analyzed in the same group [34, 45, 56, 72, 85].

Some studies explored in this review also present magnetic resonance imaging (MRI) findings for patients with AE, as well as the FDG–PET/MRI data. According to the authors, FDG–PET/CT has detected brain metabolic changes even when the MRI is normal [50, 55, 83]. It is pointing out

that FDG–PET/CT can be seen as the first choice for images of AE patients, not disregarding the importance of the MRI in these cases, especially considering the great versatility of the protocols provided by this method.

The development of new radiotracers tends to improve the specificity to detect the brain physiology alterations in AE. One of these is the ^{18}F-Flortaucipir, used in studies of the Alzheimer's disease (AD) [90]. It is a compound capable of binding paired-helical filaments that comprise neurofibrillary (tau) tangles, being the first radiotracer that allows the detection of the tau pathology, a distinctive characteristic of the AD in the brain, recently identified in the recovery phase of the anti-LGI1 AE. Considering four patients in the recovery phase of this disease, normal, and AD subjects, the authors observed an increase of the standard uptake value (SUV) in the amygdala, inferior temporal lobe, lateral occipital, and entorhinal cortex for the first group. In this case more specific radiopharmaceuticals are interesting, given that in general, young patients tend to present temporal and diffuse hypermetabolism in the early phases of the disease, while older ones have PET findings of hypometabolism that may be confused with degenerative diseases [91]. Other radiotracer applied to study AE patients is the [^{18}F] GE-179, a ligand that can selectively binds to the NMDA channels. For patients with refractory epilepsy related to NMDAR antibodies, there was an increased uptake of this marker in the frontal, parietal and temporal lobes. However, antidepressant drugs can lead to bias in the results [92]. Some others radiopharmaceuticals for brain imaging, as such as ^{18}F-SMBT-1 (a reactive gliosis marker) [93], and ^{11}C-BTFP (proliferation, migration, and survival of different nerve cells) [94], should also be explored to improve the knowledge about the disease.

The work of Graus et al., reference as a diagnostic algorithm of the AE, brings the main criteria for the diagnosis of this disease. The approach includes clinical and laboratorial exams, CSF analysis and analysis of the MRI findings. FDG–PET is just mentioned as an alternative to MRI when bilateral abnormalities on T2-weighted fluid-attenuated inversion recovery are highly restricted to the medial temporal lobes [10]. Given the vast evidences collected from the articles reviewed, there is a high potential of FDG–PET to change the diagnostic paradigm of the AE.

Conclusion

This extensive literature review shows the high sensitivity of FDG–PET and FDG–PET/CT to detect brain metabolic changes in patients with AE. FDG–PET detects findings of hyper and hypometabolism which are suggestive of AE. Some metabolic patterns may suggest association with specific neuronal antibodies and clinical phenotypes, which can change the diagnostic paradigm of the disease. However, more prospective studies are necessary for these images become a standard diagnostic method of AE.

Acknowledgements The authors would like to thank the whole team of the Nuclear Medicine Division of the Clinical Hospital—UNICAMP, the Brazilian Institute of Neuroscience and Neurotechnology (BRAINN), and the Department of Neurology—Campinas Medical School – UNICAMP.

Author contributions Literature search and review, manuscript writing, meta-analysis and content planning, manuscript writing and editing (journal suggestion): BS, AE. Study conception and design: BS, AW. Acquisition of data: BSW. Analysis and interpretation of data: BS. Drafting of manuscript: BS, AE. Critical revision: EAC. Approval of the final version: BS, AWE, Cendes.

Funding None.

Data availability Not applicable.

Declarations

Conflict of interest The authors declare no conflict of interest.

Ethical approval This article does not contain any studies with human participants or animals performed.

References

1. Oppenheim H (1888) Über Hirnsymptome bei Carcinomatose ohne nachweisbare Veränderungen im Gehirn. Charité-Annalen (Berlin) 13:335–344
2. Brierley JB, Corsellis JAN, Hierons R, Nevin S (1960) subacute encephalitis of later adult life mainly affecting the limbic areas. Brain 83(3):357–368
3. Corsellis JAN, Goldberg GJ, Norton AR (1968) "Limbic encephalitis" and its association with carcinoma. Brain 91(3):481–496
4. Machado S, Pinto A, Irani S (2012) What should you know about limbic encephalitis? Arq Neuropsiquiatr 70(10):817–822
5. Russel D (1961) Encephalomyelitis and carcinomatous neuropathy. In: van Bogaert LRJ, Hozay J, Lowenthal, (eds) The encephalitidies. Elsevier, Amsterdam
6. Wilkinson P (1964) Serological findings in carcinomatous neuromyophathy. Lancet London 1:7346
7. Trotter J, Hendin B, Osterland C (1976) Cerebellar degeneration with hodgkin disease an immunological study. Archives Neurol. 33(9):660
8. Graus F, Cordon-Cardo C, Posner J (1985) Neuronal antinuclear antibody in sensory neuronopathy from lung cancer. Neurology 35(4):22
9. Patel A, Meng Y, Najjar A, Lado F, Najjar S (2022) Autoimmune encephalitis: a Physician's guide to the clinical spectrum diagnosis and management. Brain Sci 12(9):1130
10. Graus F, Titulaer M, Balu R, Benseler S, Bien C, Cellucci T et al (2016) A clinical approach to diagnosis of autoimmune encephalitis. Lancet Neurol 15(4):391–404
11. Dalmau J, Tüzün E, Wu H, Masjuan J, Rossi J, Voloschin A et al (2007) Paraneoplastic anti-N-Methyl-D-aspartate receptor encephalitis associated with ovarian teratoma. Anna Neurol. 61(1):25

12. Hughes E, Peng X, Gleichman A, Lai M, Zhou L, Tsou R et al (2010) Cellular and synaptic mechanisms of anti-NMDA receptor encephalitis. J Neurosci off J Soci Neurosci. 30(17):5866
13. Lancaster E, Lai M, Peng X, Hughes E, Constantinescu R, Raizer J et al (2010) Antibodies to the GABA(B) receptor in limbic encephalitis with seizures: case series and characterisation of the antigen. Lancet Neurol 9(1):67
14. Irani S, Michell A, Lang B, Pettingill P, Waters P, Johnson M et al (2011) Faciobrachial dystonic seizures precede Lgi1 antibody limbic encephalitis. Ann Neurol 69(5):892–900
15. Lai M, Huijbers M, Lancaster E, Graus F, Bataller L, Balice-Gordon R et al (2010) Investigation of LGI1 as the antigen in limbic encephalitis previously attributed to potassium channels: a case series. Lancet Neurol 9(8):776
16. Vincent A, Buckley C, Schott J, Baker I, Dewar B, Detert N et al (2004) Potassium channel antibody-associated encephalopathy: a potentially immunotherapy-responsive form of limbic encephalitis. J Neurol 127(3):33
17. Irani S, Pettingill P, Kleopa K, Schiza N, Waters P, Mazia C et al (2012) Morvan syndrome: clinical and serological observations in 29 Cases. Anna Neurol. 72(2):214
18. Liguori R, Vincent A, Clover L, Avoni P, Plazzi G, Cortelli P et al (2001) Morvan's syndrome: peripheral and central nervous system and cardiac involvement with antibodies to voltage-gated potassium channels. Brain J Neurol. 124(12):2417
19. Lai M, Hughes E, Peng X, Zhou L, Gleichman A, Shu H et al (2009) AMPA receptor antibodies in limbic encephalitis alter synaptic receptor location. Annals Neurol. 65(4):424
20. Dale R, Merheb V, Pillai S, Wang D, Cantrill L, Murphy T et al (2012) Antibodies to surface dopamine-2 receptor in autoimmune movement and psychiatric disorders. Brain J Neurol. 135(11):3453
21. Boronat A, Gelfand J, Gresa-Arribas N, Jeong H, Walsh M, Roberts K et al (2013) Encephalitis and antibodies to dipeptidyl-Peptidase-Like protein-6, a Subunit of Kv42 potassium channels. Annals Neurol. 73(1):120–128
22. Tobin W, Lennon V, Komorowski L, Probst C, Clardy S, Aksamit A et al (2014) DPPX potassium channel antibody: frequency, clinical accompaniments, and outcomes in 20 patients. Neurology 83(20):1797–1803
23. Balint B, Jarius S, Nagel S, Haberkorn U, Probst C, Blöcker I et al (2014) progressive encephalomyelitis with rigidity and myoclonus: a new variant with DPPX antibodies. Neurology 82(17):1521–1528
24. Lancaster E, Dalmau J (2012) Neuronal autoantigens-pathogenesis, associated disorders and antibody testing. Nat Rev Neurol 8(7):380–390
25. Saiz A, Blanco Y, Sabater L, González F, Bataller L, Casamitjana R et al (2008) Spectrum of neurological syndromes associated with glutamic acid decarboxylase antibodies: diagnostic clues for this association. Brain Journal Neurol 131(Pt 10):2553–2663
26. Hutchinson M, Waters P, McHugh J, Gorman G, O'Riordan S, Connolly S et al (2008) Progressive encephalomyelitis, rigidity, and myoclonus: a novel glycine receptor antibody. Neurology 71(16):1291–1302
27. McKeon A, Martinez-Hernandez E, Lancaster E, Matsumoto J, Harvey R, McEvoy K et al (2013) Glycine receptor autoimmune spectrum with stiff-man syndrome phenotype. JAMA Neurol 70(1):44–50
28. Carvajal-González A, Leite M, Waters P, Woodhall M, Coutinho E, Balint B et al (2014) Glycine receptor antibodies in PERM and Related syndromes: characteristics, clinical features and outcomes. Brain J Neurol 137(Pt 8):2178–2192
29. Wuerfel E, Bien C, Vincent A, Woodhall M, Brockmann K (2014) Glycine receptor antibodies in a boy with focal epilepsy and episodic behavioral disorder. J Neurol Sci 343(1–2):180–182
30. Borges-Rosa J, Oliveira-Santos M, Silva R, Gomes A, de Almeida J, Costa G et al (2022) [18 F]FDG-PET in cardiac sarcoidosis: a single-centre study in a southern European population. Int J cardiol 347:22
31. Rodríguez-Alfonso B, Ruiz Solís S, Silva-Hernández L, Pintos Pascual I, Aguado Ibáñez S, Salas AC (2021) 18 F-FDG-PET/CT in SARS-CoV-2 Infection and its Sequelae. Revista Espanola de Med Nucl Imagen Mol. 40(5):299
32. Rosen R, Fayad L, Wahl R (2006) Increased 18F-FDG Uptake in degenerative disease of the spine: characterization with 18F-FDG PET/CT. J Nucl Med offi Publ Soc Nucl Med. 47(8):3
33. Tang Y, Liow JS, Zhang Z, Li J, Long T, Li Y et al (2018) the evaluation of dynamic FDG-PET for detecting epileptic foci and analyzing reduced glucose phosphorylation in refractory epilepsy. Front Neurosci 12:993
34. Probasco JC, Solnes L, Nalluri A, Cohen J, Jones KM, Zan E et al (2017) Abnormal brain metabolism on FDG-PET/CT is a common early finding in autoimmune encephalitis. Neurol Neuroimmunol Neuroinflamm. 4:352
35. Zupanc M, Handler E, Levine R, Jahn T, ZuRhein G, Rozental J et al (1990) Rasmussen encephalitis: epilepsia partialis continua secondary to chronic encephalitis. Pediat neurol. 6(6):397
36. Bernsen R, Jong B (1997) Limbic encephalitis, specifically depicted by PET - Bernsen 1997 European Journal of Neurology Wiley Online Library. Eur J Neurol 4:507–511
37. Provenzale J, Barboriak D, Coleman R (1998) Limbic encephalitis: comparison of FDG PET and MR imaging findings. AJR Amer J Roentgenol. 170(6):1659
38. Fakhoury T, Abou-Khalil B, Kesller RM (1999) Limbic encephalitis and hyperactive foci on PET scan. Seizure 8:427–430
39. Fiorella D, Provenzale J, Coleman R, Crain B, Al-Sugair A (2001) (18)F-fluorodeoxyglucose positron emission tomography and MR imaging findings in Rasmussen encephalitis. Amer J Neuroradiol. 22(7):2
40. McInnes M, Moher D, Thombs B, McGrath T, Bossuyt P, Clifford T et al (2018) Preferred Reporting Items for a Systematic Review and Meta-analysis of Diagnostic Test Accuracy Studies: The PRISMA-DTA Statement. JAMA 319(4):388–396
41. Whiting P, Rutjes A, Westwood M, Mallett S, Deeks J, Reitsma J et al (2011) QUADAS-2: a revised tool for the quality assessment of diagnostic accuracy studies. Ann Intern Med 155(8):529–536
42. Lagarde S, Lepine A, Caietta E, Pelletier F, Boucraut J, Chabrol B et al (2016) Cerebral (18)FluoroDeoxy-Glucose positron emission tomography in paediatric anti n-methyl-d-aspartate receptor encephalitis: a case series. Brain develop 38(5):461
43. Wegner F, Wilke F, Raab P, Tayeb SB, Boeck A-L, Haense C et al (2014) Anti-leucine rich glioma inactivated 1 protein and anti-N-methyl-D-aspartate receptor encephalitis show distinct patterns of brain glucose metabolism in 18F-fluoro-2-deoxy-d-glucose positron emission tomography. BMC Neurol. https://doi.org/10.1186/1471-2377-14-136
44. Park S, Choi H, Cheon G, Wook Kang K, Lee D (2015) 18F-FDG PET/CT in anti-LGI1 encephalitis: initial and follow-up findings. Clin Nucl Med 40(2):156
45. Celicanin M, Blaabjerg M, Maersk-Moller C, Beniczky S, Marner L, Thomsen C et al (2017) Autoimmune encephalitis associated with voltage-gated potassium channels-complex and leucine-rich glioma-inactivated 1 antibodies - a national cohort study. Eur J Neurol 24(8):999–1005
46. Zhao X (2019) The different metabolic patterns of brain 18F-FDG PET in anti-NMDA, anti-LGi-1 and anti-GABAb encephalitis. J Nucl Med 60(1):1475
47. Probasco J, Solnes L, Nalluri A, Cohen J, Jones K, Zan E et al (2017) Decreased occipital lobe metabolism by FDG-PET/CT: An anti-NMDA receptor encephalitis biomarker. Neurol Neuroimmunol Neuroinflam. 5(1):413

48. Leypoldt F, Buchert R, Kleiter I, Marienhagen J, Gelderblom M, Magnus T et al (2012) Fluorodeoxyglucose positron emission tomography in anti-N-methyl-D-aspartate receptor encephalitis: distinct pattern of disease. J Neurol, Neurosurgand psychiat. 83(7):681
49. Fisher R, Patel N, Lai E, Schulz P (2012) Two different 18F-FDG brain PET metabolic patterns in autoimmune limbic encephalitis. Clinical Nucl Med. 37(9):213
50. Baumgartner A, Rauer S, Mader I, Meyer P (2013) Cerebral FDG-PET and MRI findings in autoimmune limbic encephalitis: correlation with autoantibody types. J Neurol 260(11):2744
51. Sarkis R, Nehme R, Chemali Z (2014) Neuropsychiatric and seizure outcomes in nonparaneoplastic autoimmune limbic encephalitis. Epilepsy Behav 39:21–25
52. Turpin S, Martineau P, Levasseur M-A, Meijer I, Décarie J-C, Barsalou J et al (2019) 18F-Flurodeoxyglucose positron emission tomography with computed tomography (FDG PET/CT) findings in children with encephalitis and comparison to conventional imaging. Eur J Nucl Med Mol Imag 46(6):1309–1324
53. Yuan J, Guan H, Zhou X, Niu N, Li F, Cui L et al (2016) Changing Brain Metabolism Patterns in Patients With ANMDARE: Serial 18F-FDG PET/CT Findings. Clin Nucl Med 41(5):366–370
54. Qian C (2017) 18F FDG-PET features in anti-NMDA receptor encephalitis. J Nucl Med 58(1):223
55. Solnes LB, Jones KM, Rowe SP, Pattanayak P, Nalluri A, Venkatesan A et al (2017) Diagnostic Value of 18F-FDG PET/CT Versus MRI in the setting of antibody-specific autoimmune encephalitis. J Nucl Med 58:1307
56. Tripathi M, Tripathi M, Roy S, Parida G, Ihtisham K, Dash D et al (2018) Metabolic topography of autoimmune non-paraneoplastic encephalitis. Neuroradiology 60(2):1307
57. Strohm T, Steriade C, Wu G, Hantus S, Rae-Grant A, Larvie M (2019) FDG-PET and MRI in the evolution of new-onset refractory status epilepticus. Am J Neuroradiol 40(2):238–244
58. Ge J, Deng B, Guan Y, Bao W, Wu P, Chen X et al (2021) Distinct cerebral 18 F-FDG PET metabolic patterns in anti-N-methyl-D-aspartate receptor encephalitis patients with different trigger factors. Therap Adv Neurol Dis. 14:1756
59. Nissen M, Ørvik M, Nilsson A, Ryding M, Lydolph M, Blaabjerg M (2021) NMDA-receptor encephalitis in Denmark from 2009 to 2019: a national cohort study. J Neurol 269:1618
60. Moreno-Estébanez A, Durán SB, Bilbao MM, Díaz-Cuervo I, Agirre-Beitia G, Martínez LC et al (2021) Autoimmune encephalitis and related disorders: a retrospective study of 43 cases in a tertiary hospital. Neurol Perspect 1(4):197–205
61. Solimena M, Folli F, Denis-Donini S, Comi G, Pozza G, De Camilli P et al (1988) Autoantibodies to glutamic acid decarboxylase in a patient with stiff-man syndrome, epilepsy, and type I diabetes mellitus. New Engl J Med. 318(16):1012
62. Solimena M, Folli F (1988) Stiff-man syndrome and type I diabetes mellitus: a common autoimmune pathogenesis? Annali dell'Istituto superiore di sanita. 24(4):583
63. Kim T, Lee S, Shin J, Moon J, Lim J, Byun J et al (2014) Clinical manifestations and outcomes of the treatment of patients with GABAB encephalitis. J Neuroimmunol 270(1–2):45–50
64. Zhu F, Shan W, Lv R, Li Z, Wang Q (2020) Clinical characteristics of Anti-GABA-B receptor encephalitis. Frontiers Neurol. https://doi.org/10.3389/fneur.2020.00403
65. Shen K, Xu Y, Guan H, Zhong W, Chen M, Zhao J et al (2018) Paraneoplastic limbic encephalitis associated with lung cancer. Sci Rep 8(1):2
66. Steriade C, Moosa A, Hantus S, Prayson R, Alexopoulos A, Rae-Grant A (2018) Electroclinical features of seizures associated with autoimmune encephalitis. Seizure. 60:22
67. Wen X, Wang B, Wang C, Han C, Guo S (2021) A retrospective study of patients with GABA B R encephalitis: therapy, disease activity and prognostic factors. Neuropsychiatr Dis Treat 17:99–110
68. van Coevorden-Hameete MH, de Bruijn MA, de Graaff E, Bastiaansen DA, Schreurs MW, Demmers JA et al (2019) The expanded clinical spectrum of anti-GABABR encephalitis and added value of KCTD16 autoantibodies. Brain 142(6):1631–1643
69. Dalmau J, Graus F, Villarejo A, Posner JB, Blumenthal D, Thiessen B et al (2004) Clinical analysis of anti-Ma2-associated encephalitis. Brain 127(8):1831–1844
70. Linke R, Schroeder M, Helmberger T, Voltz R (2004) Antibody-positive paraneoplastic neurologic syndromes: value of CT and PET for tumor diagnosis. Neurology 63(2):282–286
71. De Leiris N, Ruel B, Vervandier J, Boucraut J, Grimaldi S, Horowitz T et al (2021) Decrease in the cortex/striatum metabolic ratio on [18 F]-FDG PET: a biomarker of autoimmune encephalitis. Europ J Nucl Med Mol Imag. 221:223
72. Wang Y, Sadaghiani M, Tian F, Fitzgerald K, Solnes L, Newsome S (2021) Brain and muscle metabolic changes by FDG-PET in stiff person syndrome spectrum disorders. Front Neurol. https://doi.org/10.3389/fneur.2021.692240
73. Darnell R, Posner J (2006) Paraneoplastic syndromes affecting the nervous system. Semi Oncol. 33(3):270
74. Crimì F, Camporese G, Lacognata C, Fanelli G, Cecchin D, Zoccarato M (2018) Ovarian Teratoma or Uterine Malformation? PET/MRI as a Novel Useful Tool in NMDAR Encephalitis. In vivo (Athens, Greece) 32(5):1231–1233
75. Zaborowski M, Spaczynski M, Nowak-Markwitz E, Michalak S (2015) Paraneoplastic neurological syndromes associated with ovarian tumors. J Cancer Res Clin Oncol 141(1):99
76. Aydos U, Arhan E, Akdemir Ü, Akbaş Y, Aydin K, Atay L et al (2020) Utility of brain fluorodeoxyglucose PET in children with possible autoimmune encephalitis. Nucl Med Commun 41(8):800
77. Kerik-Rotenberg N, Diaz-Meneses I, Hernandez-Ramirez R, Muñoz-Casillas R, Reynoso-Mejia C, Flores-Rivera J et al (2020) A metabolic brain pattern associated with Anti-N-Methyl-D-aspartate receptor encephalitis. Psychosomatics 61(1):39
78. Moreno-Ajona D, Prieto E, Grisanti F, Esparragosa I, Orduz LS, Pérez-Larraya JG et al (2020) 18F-FDG-PET imaging patterns in autoimmune encephalitis: impact of image analysis on the results. Diagnostics 10(6):356
79. Chen C, Wang X, Zhang C, Cui T, Shi W, Guan H et al (2017) Seizure semiology in leucine-rich glioma-inactivated protein 1 antibody-associated limbic encephalitis. Epilepsy Behav 77:90
80. Dodich A, Cerami C, Iannaccone S, Marcone A, Alongi P, Crespi C et al (2016) Neuropsychological and FDG-PET profiles in VGKC autoimmune limbic encephalitis. Brain Cogn 108:81
81. Lv R, Pan J, Zhou G, Wang Q, Shao X, Zhao X et al (2019) Semi-quantitative FDG-PET analysis increases the sensitivity compared with visual analysis in the diagnosis of autoimmune encephalitis. Front Neurol. https://doi.org/10.3389/fneur.2019.00576
82. Liu X, Shan W, Zhao X, Ren J, Ren G, Chen C et al (2020) The clinical value of 18 F-FDG-PET in autoimmune encephalitis associated with LGI1 antibody. Front Neurol. https://doi.org/10.3389/fneur.2020.00418
83. Deuschl C, Rüber T, Ernst L, Fendler W, Kirchner J, Mönninghoff C et al (2020) 18F-FDG-PET/MRI in the diagnostic work-up of limbic encephalitis. PLoS ONE 15(1):2279
84. Malter M, Helmstaedter C, Urbach H, Vincent A, Bien C (2010) Antibodies to glutamic acid decarboxylase define a form of limbic encephalitis. Anna Neurol. 67(4):470
85. Newey C, Sarwal A, Hantus S (2016) [(18)F]-Fluoro-Deoxy-glucose positron emission tomography scan should be obtained early in cases of autoimmune encephalitis. Auto Dis. 2016:1
86. Ances B, Vitaliani R, Taylor R, Liebeskind D, Voloschin A, Houghton D et al (2005) Treatment-responsive limbic encephalitis

identified by neuropil antibodies: MRI and PET correlates. Brain J Neurol. 128(8):1764
87. Flanagan EP, Kotsenas AL, Britton W et al (2015) Basal ganglia T1 hyperintensity in LGI1-autoantibody faciobrachial dystonic seizures. Neurol-Neuroimmunol Neuroinflam. 2:6
88. Yin Y, Wu J, Wu S, Chen S, Cheng W, Li L, et al. 2021 Usefulness of brain FDG PET/CT imaging in pediatric patients with suspected autoimmune encephalitis from a prospective study. European Journal of nuclear medicine and molecular imaging.
89. Jang Y, Lee S, Bae J, Kim T, Jun J, Moon J et al (2018) LGI1 expression and human brain asymmetry: insights from patients with LGI1-antibody encephalitis. J Neuroinfl. https://doi.org/10.1186/s12974-018-1314-2
90. Day GS, Gordon BA, Jackson K, Christensen JJ, Rosana Ponisio M, Su Y et al (2017) Tau-PET binding distinguishes patients with early-stage posterior cortical atrophy from amnestic alzheimer disease dementia. Alzheimer Dis Assoc Disord 31(2):87–93
91. Day G, Gordon B, McCullough A, Bucelli R, Perrin R, Bezinger T et al (2021) Flortaucipir (tau) PET in LGI1 antibody encephalitis-Day-2021-annals of clinical and translational neurology - wiley online library. Anna Clin Translat Neurol 8:491–497
92. McGinnity C, Koepp M, Hammers A, Riaño Barros D, Pressler R, Luthra S et al (2015) NMDA receptor binding in focal epilepsies. J Neurol Neurosurg Psychiatry 86:1150–1157
93. Harada R, Hayakawa Y, Ezura M, Lerdsirisuk P, Du Y, Ishikawa Y et al (2021) 18F-SMBT-1: A selective and reversible PET tracer for monoamine oxidase-B imaging. J Nucl Med 62:253
94. Neelamegam R, Kumar D (2021) Automated radiosynthesis and in vivo PET evaluation of VEGFR2 ligand [11C]BTFP. J Nucl Med 62:1205

Authors and Affiliations

Maurício Martins Baldissin[1,2,3,6] · Edna Marina de Souza[3,4,6] · Nancy Watanabe[5,6] · Elba C. S. C. Etchebehere[1,3] · Fernando Cendes[5,6] · Bárbara Juarez Amorim[1,3]

✉ Maurício Martins Baldissin
m036752@dac.unicamp.br

Edna Marina de Souza
emsouza@unicamp.br

Nancy Watanabe
n151463@dac.unicamp.br

Elba C. S. C. Etchebehere
elbehere@unicamp.br

Fernando Cendes
fcendes@unicamp.br

Bárbara Juarez Amorim
barbju@unicamp.br

1 Division of Nuclear Medicine, Department of Anesthesiology, Oncology and Radiology (DAOR), School of Medical Sciences, State University of Campinas (UNICAMP), Avenue Zeferino Vaz, S/N, PO Box 6149, Campinas, SP 13080 000, Brazil

2 Surgery Department, Jundiaí Medical School, Neurodiagnosis and Neurotherapy Clinic, Barão de Teffé St, 160, Office 405, 4th Floor, Jundiaí, SP 13208 760, Brazil

3 Cancer Theranostics Innovation Center (CancerThera), University of Campinas (UNICAMP), Campinas, Brazil

4 Nuclear Medicine Group, Biomedical Engineering Center, Nuclear Medicine Division, State University of Campinas (UNICAMP), 163 Alexander Fleming St, University City, Campinas, SP 13083 881, Brazil

5 Department of Neurology, School of Medical Sciences, University of Campinas (UNICAMP), Campinas, Brazil

6 Brazilian Institute of Neuroscience and Neurotechnology (BRAINN), University of Campinas (UNICAMP), Campinas, Brazil

ATTACHMENT 3: ABSTRACT BOOK - NMN SYMPOSIUM: PRECISION MEDICINE

DIAGNOSTIC AND THERAPEUTIC INNOVATIONS IN THE ERA OF PRECISION MEDICINE – NUCLEAR MEDICINE MEETS NEURO-ONCOLOGY

ABSTRACTBOOK

NMN Symposium: Precision Medicine

09.-10. May 2025 /Vienna, Austria
Palais Ferstel

www.nmn-society.org

Nuclear Medicine and Neurooncology (NMN)

Only the conflict of interests of individuals with a disclosure are included in the respective abstracts.

Nuclear Medicine and Neurooncology (NMN)
NMN Symposium:
Precision Medicine
09 - 10. May 2025 / Vienna, Austria
Palais Ferstel

Abstract Number: 15

Abstract Title: Paraneoplastic Syndromes and Autoimmune Encephalitis: Medical Records Review and FDG-PET/CT Outcomes

Authors:
Baldissin M[1,3,4,5], de Souza E[4,5,7], Watanabe N[5,6], Etchebehere E[2,4], Cendes F[5,6], Amorim B[2,4]

[1]Neurodiagnosis and Neurotherapy Clinic, Jundiai, Brazil, [2]Division of Nuclear Medicine, Department of Oncology and Radiology, University of Campinas (UNICAMP), Campinas, Brazil, [3]Surgery Department, Jundiaí Medical School (FMJ), Jundiaí, Brazil, [4]Cancer Theranostics Innovation Center (CancerThera), University of Campinas (UNICAMP), Campinas, Brazil, [5]Brazilian Institute of Neuroscience and Neurotechnology (BRAINN), University of Campinas (UNICAMP), Campinas, Brazil, [6]Department of Neurology, School of Medical Sciences, University of Campinas (UNICAMP), Campinas, Brazil, [7]Nuclear Medicine Group, Biomedical Engineering Center, Nuclear Medicine Division, State University of Campinas (UNICAMP), Campinas, Brazil

Background
Paraneoplastic syndromes (PNS) are conditions oftentimes expressed as encephalitis. In about 60% of patients with autoimmune encephalitis (AE) , highly specific antineuronal antibodies (e.g., Hu, Yo, NMDA) can be detected. In two-thirds of these patients, the neurological manifestation precedes the tumor diagnosis up to 4 years. The purpose of this study was to evaluated the clinical presentation and FDG-PET/CT findings in a group of patients clinically diagnosed with AE.

Materials and Methods
This study includes 37 patients, aged from 13 to 75 (47.08 ± 20,00 years), 65% female, who had been presented neurological manifestations of AE. Retrospectively, clinical records were analyzed by the neurology staff, being the clinical manifestations and the results of antibodies tests correlated with FDG-PET/CT brain images, analyzed by an expert in nuclear medicine.

Results
Among the patients studied, 24.3% had suspicion or confirmed neoplasia (most of them breast or thyroid lesions). Almost half of patients (49%) had positive antibodies. Some patients had negative antibodies (n = 12) and some were untested (n = 7). For most of the groups of patients, epilepsy was a common manifestation, followed by behavior and sensitive alterations.The exception is the aquaporin-4 antibody, for which muscular disorders are the main symptom, also highlighted in GAD patients. Considering the whole group, the areas of more common hypermetabolism are basal ganglia, temporal lobe, cingulate gyri, and precuneus. The main hypometabolic regions were the cerebellar hemispheres, and diffuse cortical areas (Fig.1).

Discussion
Patients with different neurological manifestations and antibodies may have different uptake patterns in brain FDG images. Independent of detection or suspicion of neoplasia, these findings can be a signal of PNS, contributing to the earlier diagnosis and definition of therapeutical approach.

Conclusion
Neurological manifestations and FDG-PET/CT findings showed specific signatures on the presence of symptoms of AE with or without PNS.

ATTACHMENT 4: ABSTRACT: HEMATOLOGY

TRANSFUSION CELL THERAPY

18TH EDWALDO CAMARGO SYMPOSIUM AND THE 2ND CANCERTHERA CONGRESS

AUTOIMMUNE ENCEPHALITIS AND PARANEOPLASTIC SYNDROMES: A CLINICAL AND FDG-PET/CT STUDY

DOI: 10.1016/j.htct.2025.103791

Maurício Martins Baldissin[a], Edna Marina de Souza[b], Nancy Watanabe[c], Elba Cristina Sá de Camargo Etchebehere[a], Fernando Cendes[c], Bárbara Juarez Amorim[a]

[a] Division of Nuclear Medicine, Department of Oncology and Radiology, Faculdade de Ciências Médicas, Universidade Estadual de Campinas (UNICAMP), Campinas, SP, Brazil

[b] Nuclear Medicine Group, Biomedical Engineering Center, Nuclear Medicine Division, Faculdade de Ciências Médicas, Universidade Estadual de Campinas (UNICAMP), Campinas, SP, Brazil

[c] Department of Neurology, Faculdade de Ciências Médicas, Universidade Estadual de Campinas (UNICAMP), Campinas, SP, Brazil

Introduction/Justification

Autoimmune encephalitis (AE) is a debilitating neurological disorder characterized by inflammation of brain tissue. Frequently, it is associated with the detection of highly specific antibodies, as such as NMDA, Yo, GAD, Hu, among others. Oftentimes, this condition is expressed as a paraneoplastic syndrome (PNS), for which the neurological manifestation precedes the tumor diagnosis up to 4 years in about two-thirds of the patients.

Objectives

This work applied the review of clinical findings and FDG-PET/CT images analysis to characterize and explore the outcomes of patients diagnosed with AE, both clinically and by antibodies test.

Materials and Methods

The study includes 37 patients, aged from 13 to 75 (47.08 ± 20,00 years), 65% female, who had been presented neurological manifestations of encephalitis and PNS. The group of patients was divided according to the antibodies detected (NMDA, Yo, Hu, LGI1, GAD, Amphiphysin, Aquaporin-4), being also studied a group of patients with negative antibodies and untested. Retrospectively, the clinical records were analyzed by the neurology staff, being the clinical manifestations and the results of antibodies tests correlated with FDG-PET/CT brain images, analyzed by an expert in nuclear medicine.

Results

Among the groups studied, 24.3% had suspicion or confirmed neoplasia (most of them breast or thyroid lesions), being 49% of the patients positive for antibodies related autoimmune encephalitis (AE). In the pretreatment phase, patients with Yo antibodies, manifested epilepsy and cerebellar ataxia, with FDG-PET/CT revealing hypermetabolism in the basal ganglia, cingulate gyri, thalamus, and midbrain, with hypometabolism in the cerebellar hemispheres. Hu antibodies has been associated with epilepsy, sensitive and behavior alterations, being the hypermetabolism in the cingulate gyrus and hypometabolism in the cerebellar hemispheres identified in the PET/CT images; on the other side, GAD antibodies resulted in higher FDG uptake in the thalamus and midbrain, with hypometabolism in the frontal lobes. In this case, the neurological manifestations include epilepsy, ataxia with aspects of stiff-person syndrome, behavior and sensitive alterations. Most of the clinical manifestations mentioned has also been observed in patients with NMDA antibodies, who expressed cingulate gyri, precuneus, parietal lobes and basal ganglia hypermetabolism, and cingulate hypermetabolism, with cerebellar hemispheres hypometabolism, characterizing an anteroposterior gradient of FDG uptake. LGI1 antibodies resulted in hypermetabolism in the basal ganglia and temporal mesial lobe, with frontal hypometabolism. For most of the groups of patients, epilepsy was a common manifestation, followed by behavior and sensitive alterations. The exception is the aquaporin-4 antibody for which muscular disorders are the main symptom, also highlighted in GAD patients.

Conclusion

PET/CT FDG is able to detect metabolic alterations in brain images with a high sensitivity. Different antibodies can show different patterns of hypermetabolism and hypometabolism. More studies with higher casuistic are necessary to better identify each pattern. Moreover, PET/CT FDG with whole body studies is able to detect neoplasm or suspicious neoplasm lesions.

Keywords:

Autoimmune encephalitis | FDG-PET/CT images | Paraneoplastic syndromes